Dlc-1 and *Dlc-2*, Studies of Two RhoGAP Genes in Etoposide Resistance and Apoptosis

By SHAUNA LOEWEN

A Thesis Submitted to
The Faculty of Graduate Studies
in Partial Fulfillment of the Requirements for the Degree of

MASTER'S OF SCIENCE

Department of Biochemistry and Medical Genetics
University of Manitoba
Winnipeg, Manitoba, Canada
October, 2007

THE UNIVERSITY OF MANITOBA

FACULTY OF GRADUATE STUDIES

*****

COPYRIGHT PERMISSION

Dlc-1 and *Dlc-2*, Studies of Two RhoGAP Genes in Etoposide Resistance and Apoptosis

BY

SHAUNA LOEWEN

A Thesis/Practicum submitted to the Faculty of Graduate Studies of The University of Manitoba in partial fulfillment of the requirement of the degree

MASTER OF SCIENCE

TABLE OF CONTENTS

CHAPTER 2 – EXPERIMENTAL PROCEDURES

CHAPTER 3 – RESULTS

LIST OF FIGURES

LIST OF ABBREVIATIONS

7AAD – 7 amino-actinomycin-D
AIF – apoptosis inducing factor
AMD – age-related macular degeneration
AML – acute myeloid leukemia
Amp – ampicillin
AP-2 – activator protein-2
APAF-1 – apoptotic protease activating factor-1
Autographa californica multiple nucleopolyhedrovirus – AcMNPV
Bcl-2 – B-cell lymphoma gene 2
Bcr – breakpoint cluster region
β-gal – β-galactosidase
BSA – bovine serum albumin
CARD – caspase recruitment domain
caspases – aspartate-specific cysteine proteases
cDNA – complementary DNA
CGH – comparative genomic hybridiazation
CHO – Chinese hamster ovary
CNV – choroidal neovascularization
cten – C- terminal tensin like
cyt c – cytochrome c
DD – death domain
DED – death effector domain
DEPBG – 4'-demethylepipodophyllin benzylidene glucoside
DISC – death-inducing signaling complex
Dlc – deleted in liver cancer
DMSO – dimethyl sulfoxide
EDTA – ethylene diamine tetra-acetic acid
ES – embryonic stem
FACS – fluorescence activated cell sorter
FADD – Fas-associated death domain
FITC – fluorescein isothiocyanate
GCF – GC factor
GDI – guanine dissociation inhibitor
GEF – guanine nucleotide exchange factor
GLM – generalized linear method
HCC – hepatocellular carcinoma
HEK – human embryonic kidney
HLV – hydrodynamic limb vein
HTV – hydrodynamic tail vein
HSV TK – herpes simplex virus thymidine kinase
IAP – inhibitors of apoptosis proteins
ICAD – inhibitor of caspase-activated DNAse
IL-2 – interleukin-2

JNK – c-Jun N-terminal kinase
KIP – kinase inhibitor protein
LIP1 – lysosomal acid lipase 1
LOH – loss of heterozygosity
LPS – lipopolysaccharide
LTR – long terminal repeat
MAPK – mitogen-activated protein kinase
MOMP – mitochondrial outer membrane permeabilization
MRNA – messenger RNA
MTT – 1-(4,5-dimethylthiazol-2-yl)-3,5-diphenylformazan
Neo – neomycin
NFκB – nuclear factor kappa B
NMR – nuclear magnetic resonance
NSCLC – non-small cell lung carcinoma
N-SMase – neutral sphingomyelinase
PARP – poly-(ADP-ribose) polymerase
PBS – phosphate buffered saline
PFA – paraformaldehyde
PGP – phosphatidylglycerolphosphate
PH – pleckstrin homology
PI – propidium iodide
PI3 – phosphatidyl inositol 3
PKC – protein kinase C
PRV – pseudorabies virus
PS - phosphatidylserine
PST – promoter-proximal sequence tag
PT – permeability transition
Rb – retinoblastoma
RhoGAP – Rho GTPase activating protein
RIP – receptor interacting protein
RNAi – RNA interference
ROS – Reactive oxygen species
SAM – sterile alpha motif
SH2 – src homology 2
shRNAi – short hairpin RNA interference
Smac – second mitochondria-derived activator of caspase
SMase – sphingomyelinase
SNP – single nucleotide polymorphisms
SP1 – specificity protein 1
SRE – serum response element
SRF – serum response factor
START – steroidogenic acute regulatory related lipid transfer
TAE – tris-acetate EDTA
TNF – tumor necrosis factor-α
TNF-R – tumor necrosis factor-receptor
TRAF2 – TNF-R associated factor 2

TRAIL – TNF related apoptosis inducing ligand
TRITC – tetramethylrhodamine B isothiocyanate
TUNEL – terminal transferase dUTP nick-end labeling
VEGF – vascular endothelial growth factor

ACKNOWLEDGEMENTS

Dear reader:

This thesis marks the end of a seemingly endless journey as a post-secondary student. I never expected to be attending University at this stage of my life, nor would I ever have guessed that science would be my calling. Sometimes life's experiences lead us in directions that we would not normally choose to go.

There are many people whom I credit with any success that I have had in this program. I must first mention the unwavering support of my family, especially my children Brianne, Ryan and Jordan, who I fear have had to make as many sacrifices for me to achieve this goal as I have had to make myself. They were a constant source of inspiration on this journey without ever realizing it. They will be happy not to have to attend University classes with their mother. It is my hope that one day, while pursuing their own academic careers, they may wander into the library, dust off a copy of this manuscript, and realize how important they were to its completion.

There are several friends I would also like to mention, Shannon Neumann, a wealth of information, laughter and chocolate, Cielo Monterrosa, Antonietta Senkow and Nicole Agnew for their friendship and support, Megan Schwabiuk, without whom I would probably still be struggling to complete my Table of Contents, thanks for motivating me to stay on track over countless beers and bottles of wine. There are also several people within the MICB that deserve special thanks. Dr. Sabine Mai for all her advice and

support, whom I'm certain was instrumental in having my funding extended as long as it was. Dr. Barb Triggs-Raine, who was much more than a member of my committee, for providing much needed direction and support. Dr. Asher Begleiter and Dr. Marek Los for serving on my committee and for their suggestions and feedback regarding this project. Dr. Jane Evans for allowing me the privilege of learning a little about the clinical side of things and for all her encouragement and support. Nichola Wigle… where would I be without you? Thanks for sharing all your knowledge, insight and patience (can I see that one more time?). If nothing else, I know how to handle mice! Ludger (Hey Punk) Klewes for the countless hours spent teaching me to use the FACS machine and then make sense of the results, answering the endless string of questions, and always making me laugh while doing it. Special thanks to all the Mowat lab members, past and present, for making work an enjoyable place to be, and especially to Heather for all her help with the mice. There are countless others who have shared their wisdom and expertise over the years, I'd love to thank you all personally but there are just too many to mention.

Last but not least, thanks to Dr. Michael Mowat for providing me the opportunity to contribute to this project. He allowed me the freedom to develop the project in my own way, yet managed to keep me on track, and was always willing to provide direction and support. I am grateful for all of the experience and knowledge I have gained at this Institute and for the many friendships that I hope will continue to flourish in the future.

Sincerely yours,

Shauna Loewen

ABSTRACT

The purpose of this project was to determine the effects of *Dlc-1* or *Dlc-2* gene disruption on the induction of programmed cell death in response to treatment with the chemotherapeutic drug, etoposide.

The role of these genes in apoptosis induction was studied using FACS analysis; cell survival was studied using crystal violet colony and MTT assays. These experiments were performed on cells that had a down-regulation of either the *Dlc-1* or *Dlc-2* gene transcript. Tissue expression and phenotype were studied using *Dlc-1* knock out mice.

We have demonstrated that the *Dlc-2* disrupted clone, E91, shows a statistically significant increase in cell survival relative to control after treatment with etoposide. While RNAi expressing cell lines also showed some increased survival as compared to controls, in most cases the differences did not reach significance. *Dlc-1* null embryos showed developmental defects. Therefore, these RhoGAP genes play an important role in development, cell survival and apoptosis.

CHAPTER 1 – LITERATURE REVIEW AND BACKGROUND INFORMATION

1.1 Introduction

This thesis discusses the role of Deleted in Liver Cancer (Dlc) genes 1 and 2 in oncogenic transformation and in resistance to etoposide induced apoptosis. These genes are homologous Rho GTPase Activating Proteins (RhoGAPs) found deleted in several types of cancer, and are bonafide tumor suppressor genes. What follows is a description of RhoGAP proteins, their role in cellular homeostasis and why the aberrant regulation of these genes may be important in oncogenesis. Some important features of apoptosis are illustrated, as well as the mode of action of the chemotherapeutic drug, etoposide. The experimental procedures undertaken during the course of this project to elucidate the function of these particular genes in resistance to programmed cell death induced by etoposide will be described. This will include an explanation of the creation of CHO K1 and H460 cell lines that have a disruption or knockdown of either *Dlc-1* or *Dlc-2*, as well as a description of the generation of a *Dlc-1* deficient mouse colony. The gene disruptions are either due to the insertion of a promoter trap retrovirus or RNA interference, and these techniques and their importance in functional studies are also depicted. Finally, the advances made in the project thus far, as well as its future directions are presented.

1.2 RhoGAP Proteins

Rho GTPase Activating Proteins (RhoGAPs) serve to stimulate the intrinsic GTPase ability of cells to return Rho GTPase proteins from the active, GTP-bound state, to the inactive, GDP-bound state. These proteins are identified by the presence of a RhoGAP domain that allows the protein to function as a molecular switch for the regulation of RhoGTPases (Moon and Zheng, 2003; Jaffe and Hall, 2005). This domain consists of a sequence of 150 amino acids that shows a minimum of 20% identity with other members of the family. It is comprised of nine α-helices and has a highly conserved arginine residue in the active site which functions to stabilize the conformation required for hydrolysis (Moon and Zheng, 2003; Brandao et al, 2006). RhoGAPs are often multidomain proteins, occurring with other functional domains, such as pleckstrin homology (PH), Src homology 2 and 3 (SH2 and SH3), and the serine/threonine kinase. Interaction with these motifs may link these proteins to various pathways, and contribute to their regulation (Moon and Zheng, 2003).

Rho GTPases are part of the Ras superfamily of small GTP-binding proteins. Members of the RhoGTPase family include RhoA, B and C, Rac1, 2 and 3, and Cdc42 and over twenty family members have been identified to date (Jaffe and Hall, 2005). The first RhoGAP identified was the Breakpoint cluster region (Bcr) by Diekmann *et al.* in 1991, and it is now predicted that the human genome contains about eighty RhoGAP genes. Given that there are only twenty substrates regulated by RhoGAPs, it would appear that

each of these proteins must have a very specific regulatory function (Moon and Zheng, 2003).

The GTPase cycle works in the following way. Upon stimulation, guanine nucleotide exchange factors (GEFs) catalyze the exchange of GDP for GTP, thus activating the protein. Active Rho proteins can then exert their effects on cells by binding with specific target (effector) proteins. Several effector proteins have been identified, including serine/threonine, tyrosine and lipid kinases, lipases, oxidases and scaffold proteins. RhoGAPs then serve to return the proteins to their inactive form, where they can interact with guanine dissociation inhibitors (GDIs), which stabilize the inactive form until the cycle begins again (Jaffe and Hall, 2002; Moon and Zheng, 2003; Boettner and van Aelst, 2002) (Figure 1).

Rho GTPases have many important effects on cellular processes that, should these proteins remain activated, can have severe consequences for cells. Therefore, regulation by RhoGAPs is critical for the maintenance of cellular homeostasis. Rho proteins have been reported to activate nuclear factor κB (NFκB) through positive regulation of NFκB-dependent promoters (Jaffe and Hall, 2005). This may prevent transformed cells from undergoing apoptosis. They also affect gene expression by acting on the serum response element (SRE) via regulation of the serum response factor (SRF) (Jaffe and Hall, 2005). In addition, they have effects on gene transcription through activation of the JNK and p38 MAP kinase (MAPK) pathways (Jaffe and Hall, 2005). Rho proteins promote the cell

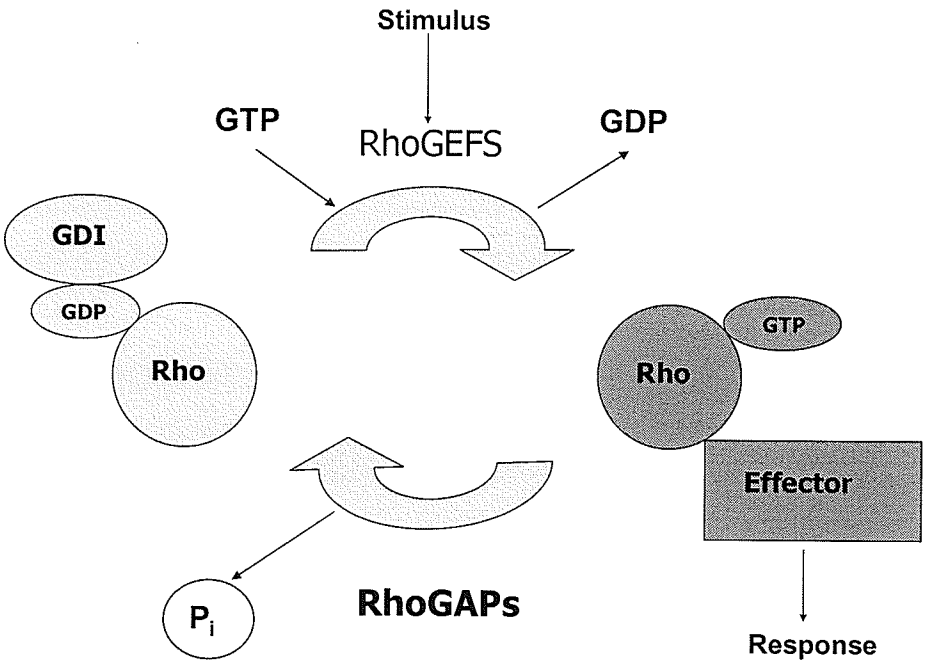

Figure 1. The Rho GTPase cycle.
RhoGEFs, Rho guanine nucleotide exchange factors; RhoGAPs, Rho GTPase activating proteins; GDI, guanine nucleotide dissociation inhibitor.

Adapted from: Jaffe, A.B. and Hall, A. 2005. RhoGTPases: biochemistry and biology, *Annu Rev Cell Dev Biol.* **21**: 247-69.

cycle progression from G1 to S phase in several ways. They inhibit $p21^{WAF1}$ expression and aid the degradation of $p27^{Kip1}$, either of which promotes the interaction of cyclin D1 with cdk4/cdk6 (Boettner and van Aelst, 2002). They also promote the interaction of cyclin E with cdk2. These pathways result in the phosphorylation of the retinoblastoma (Rb) gene, which allows G1 to S transition. Active Rho also leads to the formation of contractile actin:myosin filaments, which is thought to be the predominant mechanism of cellular motility in animal cells (Jaffe and Hall, 2005). In addition, they stimulate the formation of stress fibres, which enhances the ability of cells to move and to aggregate together. Stress fibres extend across the length of the cell and promote motility by pushing against the cell membrane on one side, while pulling in at the other (Jaffe and Hall, 2005).

Due to these effects, an absence of RhoGAP activity in cells and the resultant increase in active Rho proteins, could be expected to lead to oncogenic transformation, tumor formation and metastasis. In fact, several carcinomas have been found to contain mutations or deletions in RhoGAP genes, including hepatocellular carcinoma (HCC) (Yuan *et al.*, 1998), gliomas (Tikoo *et al.*, 2000) and acute myeloid leukemia (AML) (Kourlas *et al.*, 2000).

1.3 *Dlc-1* and *Dlc-2*

Dlc-1 and *Dlc-2* are homologous RhoGAP genes which have been found to be deleted in several different types of cancer, including liver, breast, prostate, colon, and more

recently, renal, uterine and rectal carcinomas (Ullmannova and Popescu, 2006). They share three conserved domains: the sterile alpha motif (SAM2) domain, the RhoGAP domain (previously described), and the steroidogenic acute regulatory related lipid transfer (START) domain. The SAM domain is common in signaling and nuclear proteins, and is thought to mediate cell-cell initiated signal transduction and in some cases homodimerization. Many SAM domain-containing proteins have an established role in development (Schultz *et al.*, 1997). Others, such as LIP1, appear to have a role in the disassembly of focal adhesions, which would affect such processes as migration and cellular differentiation (Schultz *et al.*, 1997). A recent paper by Li *et al.* indicates that although the *DLC-2* SAM domain is highly homologous with the *DLC-1* and p122 SAM domains, it actually shares little sequence similarity with other domains of its kind. Together, these form a new subfamily (DLC family) of SAM domains. While most SAM domains consist of five α-helices, this one contains only four. In addition, it appears that the *DLC-2* SAM does not dimerize as its counterparts do, but rather exists as a monomer. START is a lipid-binding StAR-related lipid-transfer domain often found in signaling proteins. It has been found to exert regulatory effects on other domains that occur with it in multidomain proteins, such as the RhoGAP domain (Ponting and Aravind, 1999) (Figure 2). The RhoGAP action of both the *Dlc-1* and *Dlc-2* proteins is specific for RhoA and Cdc42 (Wong *et al.*, 2003). Durkin *et al.* recently identified a third Dlc gene, *Dlc-3*, at chromosome Xq13. It shares homology with *Dlc-1* and *-2*, and also contains the same three conserved domains (Durkin *et al.*, 2006).

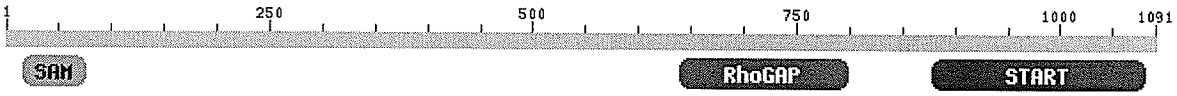

Dlc-1

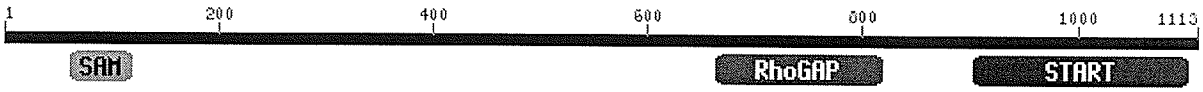

Dlc-2

Figure 2. *Dlc-1* and *Dlc-2* conserved domains.

Yuan *et al.* first identified *DLC-1* as a putative tumor suppressor gene in 1998. They noted loss of heterozygosity (LOH) of this gene in primary HCCs, as well as in several HCC cell lines. It is homologous to the rat $p122^{RhoGAP}$ gene. The human *DLC-1* cDNA contains 3850 base pairs that code for 1091 amino acids to give a molecular weight of ~125 kD. It is located at chromosome 8p21.3-22, which is an area frequently deleted in HCC, non-small cell lung carcinoma (NSCLC), colorectal and prostate carcinomas (Yuan *et al.*, 1998). According to Durkin *et al.* there are two different cDNA transcripts, one 3.7 kb and the other 7.4 kb. In the mouse, the *Dlc-1* gene codes for 1084 amino acids, contains 14 exons and is ~47 kb in length (Figure 3). The gene is widely expressed in mouse organs and tissues with highest expression in the heart, liver, ovary and lung. There are potential binding sites for several transcription factors in the promoter region, including SP1, GCF and AP-2, as well as a CpG island (Durkin *et al.*, 2002).

The human *DLC-1* protein has been found to localize to the cytoplasm in some HCC cell lines (Zhou *et al.*, 2004). This group found that restoring *DLC-1* function in two HCC tumor cell lines activated caspase-3-mediated apoptosis, and FACS analysis revealed an approximately two-fold increase in the proportion of apoptotic cells. These cell lines also exhibited a marked reduction in migration and tumor growth upon reactivation of *DLC-1* expression. Kim *et al.* recently reported their studies using HCC cell lines infected with recombinant adenovirus expressing *DLC-1* or LacZ. They found that cells overexpressing *DLC-1* showed a decrease in growth that correlated with an increase in apoptosis determined by flow cytometric analysis of the sub-G1 population. Yam *et al.*

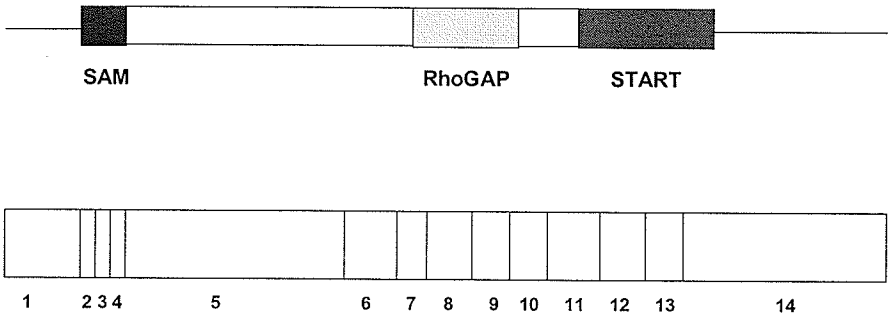

Figure 3. Structure of the Dlc-1 mouse gene. Alignment of the coding features of the mouse Dlc-1 cDNA with the exon boundaries of the gene. On top, the 5' and 3' UTRs of the cDNA are indicated by lines, while the open reading frame is represented by boxes. The segments of the cDNA encoding the SAM, RhoGAP, and START domains of the polypeptide are depicted as colored boxes. Below, the positions of the exon/intron boundaries in the cDNA are indicated, and the exons are numbered.

Adapted from: Durkin, M.E., Yuan, B-Z., Thorgeirsson, S.S. and Popescu, N.C. 2002. Gene structure, tissue expression, and linkage mapping of the mouse DLC-1 gene (Arhgap7). Gene 288: 119-27.

have demonstrated that *DLC-1* contains a caveolin-1 binding motif and acts in conjunction with tensin2 in caveolae to cause cytoskeletal rearrangements. Another tensin family member, cten (C-terminal tensin like), interacts with *DLC-1* via binding to the cten SH2 domain. *DLC-1*-cten proteins are localized to focal adhesions, whose turnover can then be mediated by the *DLC-1* RhoGAP domain through negative regulation of Rho proteins. This, in turn, has an impact on cell motility and proliferation (Liao *et al.*, 2007).

Four different isoforms of *DLC-2* have been identified in humans and are localized to chromosome 13q. They are referred to as *DLC-2α*, *DLC-2β*, *DLC-2γ* and *DLC-2δ*, three of which (*DLC-2α*, *DLC-2β* and *DLC-2γ*) contain a RhoGAP domain (Leung *et al.*, 2005). When transiently transfected into mouse fibroblasts, these three isoforms were found to localize to the cytoplasm. Cells showed a rounded morphology with numerous protrusions, in contrast to the spindle morphology of untransfected cells. TRITC-labeled phalloidin staining showed a reduction of stress fibre formation, indicating that the morphological changes may be due to alterations of the actin cytoskeleton. Pull down assays determined that there was a significant reduction in RhoA protein activity in HEK 293 cells transfected with *Dlc-2*. This group was able to conclude that the RhoGAP activity of *Dlc-2* was responsible for the changes in cellular morphology, and had effects on cell proliferation and motility as well (Leung *et al.*, 2005).

There is evidence of genetic and epigenetic modifications in the dysregulation of these genes (Wong *et al.*, 2003; Kim *et al.*, 2003; Yuan *et al.*, 2003). Comparative genomic

hybridization (CGH) analysis has shown that 8p and 13q deletions are common in tumors with reduced expression of *Dlc-1* and *Dlc-2*, especially lung, ovary, breast, kidney (Ullmannova and Popescu, 2006) and prostate (Guan *et al.*, 2006) tumors, and these loci are commonly found in regions of LOH in breast, lung and liver carcinomas (Ullmannova and Popescu, 2006). The major mechanisms for silencing of these genes are promoter hypermethylation, histone deacetylation and genomic deletion (Ullmannova and Popescu, 2006; Guan *et al.*, 2006; Park *et al.*, 2003). Yuan *et al.* found that several tumor cell lines showed methylation of the 5' CpG island in the human *DLC-1* gene, and that these lines lacked mRNA expression. In 2006, Guan *et al.* reported that *DLC-1* expression could be increased in some prostate carcinoma cell lines by treating them with DNA methyltransferase or histone deacetylase inhibitors. Kim *et al.* noted similar results in 2003, in their studies of gastric cancer cell lines. *Dlc-1* and *-2* are also implicated as metastasis suppressors (Goodison *et al.*, 2005). Down-regulation of both genes has been correlated with increased tumor invasiveness (Ullmannova and Popescu, 2006). This is not surprising given that the metastatic process involves changes to the actin cytoskeleton and disruption in cellular adhesion, two processes that are also affected by Rho proteins.

Single nucleotide polymorphisms (SNP) analysis and gene expression profiling have identified *Dlc-1* as a candidate gene for breast cancer susceptibility, and as the gene is highly methylated in several cancers, it may serve as a useful marker for early detection (Ullmannova and Popescu, 2006). Reactivation of *Dlc-1* function has shown promising results in cells from various carcinomas, such as breast, lung and liver, thus reinstating

the gene in tumors shows potential for novel therapeutics (Ullmannova and Popescu, 2006).

1.4 Basics of Apoptosis

Programmed cell death is an evolutionarily conserved process that is essential to the development of organisms. It can occur as a physiologic process in embryogenesis, tissue homeostasis and protection from viral infection or mutation, or pathologically as the result of injury (Buja, 1993). Aberrant apoptosis can result in disease; excessive apoptosis is associated with heart disease, stroke and neurodegenerative disorders, while a deficiency in apoptosis is implicated in immune disorders and cancer (Kam and Ferch, 2000).

The term 'apoptosis' was first proposed in 1972 by Kerr *et al.* in a crucial paper that described the morphological features of this type of cell death. Apoptosis is a form of programmed cell death that occurs in response to a variety of physiological conditions, and in which the cell itself actively participates. This energy-dependent process is characterized by distinct morphology, and incorporates changes in the mitochondria, nucleus and cytoplasmic membrane. Initially, the cell detaches from surrounding cells and the mitochondria lose their transmembrane potential. Shortly thereafter, the chromatin condenses, endonucleases cleave DNA resulting in fragmentation, and although the nuclear membrane remains intact, nuclear proteins are degraded resulting in changes to the positioning of nuclear pores (Chamond *et al.*, 1999; Kerr and Ferch,

2000). The cytoplasmic membrane also remains intact, however, it undergoes changes that result in the externalization of phospholipids such as phosphatidylserine (PS). Eventually, in the late stages of apoptosis, fragmentation of the cellular membrane occurs, resulting in the generation of apoptotic bodies which are membrane-bound vesicles containing cytoplasmic contents (Chamond *et al.*, 1999). In these final stages of apoptosis the cell becomes permeable to vital dyes such as propidium iodide (PI) and 7 amino-actinomycin-D (7AAD). Because there is no rupture of the membrane, an immune response is not generated by the apoptotic process; cellular debris is removed by phagocytosis.

The characteristic features of this process provide an opportunity to detect apoptosis and distinguish it from other forms of cellular death, primarily necrosis. For instance, agarose gel electrophoresis yields a characteristic 'ladder' pattern of fragmented DNA in apoptotic cells, while necrotic cells show only a smear on the gel. The terminal transferase dUTP nick-end labeling (TUNEL) assay can be used to preferentially label apoptotic cells by incorporating fluorescently labeled dUTPs into nucleotide polymers. The assay labels the 3'-OH ends of DNA strands generated by breakage that occurs during the apoptotic process (Gavrieli *et al.*, 1992). Analysis by flow cytometry uses dyes specific for apoptotic cells to distinguish them from necrotic and live cell populations (Kam and Ferch, 2000; Chamond *et al.*, 1999). This technique capitalizes on the fact that the calcium-dependent phospholipid binding protein, Annexin V, has a high affinity for PS. When it is conjugated to a fluorochrome, such as fluorescein isothiocyanate (FITC), it can be used to detect cells undergoing apoptosis. This is usually

used in conjunction with a DNA specific dye, such as PI or 7AAD, that is excluded from live cells with intact membranes. 7AAD intercalates DNA, is specific for G-C base pairs and has an emission spectrum in the far red range, therefore has little overlap with FITC (Schmid *et al.*, 1992). Cells staining positive for Annexin V-FITC are apoptotic, those positive for PI or 7AAD are undergoing necrosis, or are late stage apoptotic. The cells that are negative for both represent the live cell population (Darzynkiewicz *et al.*, 1997).

There are two stages of apoptosis: the 'initiation phase' and the 'execution phase'. The initiation phase is under the genetic control of several regulatory genes, including pro- and anti-apoptotic members of the *Bcl-2* family, tumor suppressors such as *p53*, and proto-oncogenes such as c-*myc* (Kam and Ferch, 2000). There are two major pathways leading to apoptosis: an intrinsic pathway that relies on mitochondrial involvement, and an extrinsic pathway involving interaction between a death receptor and a ligand. A family of aspartate-specific cysteine proteases, known as caspases, are responsible for carrying out the execution phase and are activated regardless of which of these pathways is pursued. They are evolutionarily conserved proenzymes consisting of two subfamilies, one of which, the ced-3 subfamily, is important in apoptosis. These effectors perform a variety of functions, from DNA and cytoskeletal protein cleavage to loss of adhesion, and there is evidence suggesting that apoptosis is reduced through caspase inhibition (Kam and Ferch, 2000; Chamond *et al.*, 1999). There are two categories of caspases important for apoptosis, initiators and effectors. The initiator caspases (caspases-2, -8, -9 and -10) contain a long prodomain and are responsible for activating the downstream effector caspases (caspases-3, -6 and -7) by proteolytic cleavage (Vermeulen *et al.*, 2005). The

prodomains of the initiator caspases contain domains that allow them to interact with adaptor proteins. Caspases-8 and -10 contain a death effector domain (DED), while caspases-2 and -9 contain a caspase recruitment domain (CARD). Once activated, the effector caspases act on their substrates to cause apoptosis. One of the first substrates to be cleaved is the DNA repair protein, poly-(ADP-ribose) polymerase (PARP) (Duriez and Shah, 1997). DNA fragmentation results from caspase cleavage of the inhibitor of caspase-activated DNAse (ICAD) (Sakahira *et al.*, 1998), while cleavage of lamins causes the nucleus to shrink (Orth *et al.*, 1996). Other important proteins that are cleaved by caspases during the induction of apoptosis include the retinoblastoma protein (pRb), NF-κB, Bcl-2 and Bid (Vermeulen *et al.*, 2005).

The key event in the mitochondrial cell death pathway is mitochondrial outer membrane permeabilization (MOMP) (Green and Kroemer, 2004). This leads to the release of inter-membrane proteins such as apoptosis-inducing factor (AIF) and cytochrome c (cyt c) (Susin *et al.* 1999). MOMP can initiate apoptosis in several ways: through the release of caspase-activating molecules, by releasing molecules responsible for caspase-independent death, or by inducing the loss of vital mitochondrial functions. Two mechanisms for initiating MOMP have been proposed, one involving the opening of the permeability transition (PT) pore of the inner mitochondrial membrane, the second mediated by Bcl-2 family members acting on the outer mitochondrial membrane (Green and Kroemer, 2004).

AIF is a mitochondrial flavoprotein that translocates to the nucleus upon induction of apoptosis. Once there, it initiates nuclear changes characteristic of apoptosis, such as chromatin condensation and fragmentation. It can act in a caspase-independent manner, and provides an association between the permeabilization of the mitochondrial membrane and nuclear apoptosis (Susin *et al.*, 1999). AIF contains three domains, one of which, the oxidoreductase domain, appears to be important for the apoptotic function of the protein (Daugas *et al.*, 2000).

Cytochrome c (cyt c) is also released from damaged mitochondria, along with apoptotic protease activating factor-1 (APAF-1) and ATP, to activate caspase-9 and initiate the caspase cascade triggering apoptosis (Green and Kroemer, 2004; Vermeulen *et al.*, 2005). This pathway is regulated by a family of proteins known as the inhibitors of apoptosis proteins, or IAPs. IAPs can suppress apoptosis by binding to procaspase-9 thereby blocking its activation, or by directly inhibiting active caspases (Du *et al.*, 2000; Deveraux *et al.*, 1998). In 2000, Du *et al.* identified a new mitochondrial protein, the second mitochondria-derived activator of caspase, Smac, which binds to IAPs counteracting their effects thus restoring the cyt c/Apaf-1 activation of caspase-9. In addition, it has been shown that the serine protease Omi is released from the mitochondria, along with cyt c and Smac, during the induction of apoptosis. This protein also binds IAPs and may aid Smac in countering the effects of IAPs to promote apoptosis (Hegde *et al.*, 2002).

Several biochemical pathways participate in the transmission of apoptotic signals. The death receptor family is characterized by the presence of a death domain (DD) and can initiate apoptosis upon binding to their specific ligands. Examples include the tumor necrosis factor receptor TNF-R1, TNF related apoptosis inducing ligand (TRAIL) and APO-1/Fas (CD95) (Scaffidi *et al.*, 1998). Activation of these receptors leads to the recruitment of proteins that form the death-inducing signaling complex (DISC). The DDs of these receptors bind to the DED of the Fas-associated death domain protein (FADD), which recruits caspase-8 and initiates the mitochondrial events leading to apoptosis (Hu *et al.*, 1997; Scaffidi *et al.*, 1998). On the other hand, binding of TNF to TNF receptor 2 (TNF-R2) can lead to activation of a pro-survival pathway. The interaction of TNF with TNF-R2 stimulates TNF-R associated factor 2 (TRAF2) and subsequent phosphorylation of receptor interacting protein (RIP). This in turn can activate the anti-apoptotic NFκB pathway (Kelliher *et al.*, 1998; Tada *et al.*, 2001) (Figure 4).

1.5 The Role of Rho Proteins in Apoptosis and Metastasis

Ceramides have regulatory functions in several cellular processes, including growth, differentiation and apoptosis. Thon *et al.* described a caspase-independent mode of apoptosis in several cell lines, which is induced by tumor necrosis factor (TNF) and mediated by ceramide. They found that cells deficient for acid sphingomyelinase were protected from this form of apoptosis. Previous work from our lab showed that cells with a knock down of *Dlc-2* RhoGAP function have a defect in their ceramide signaling

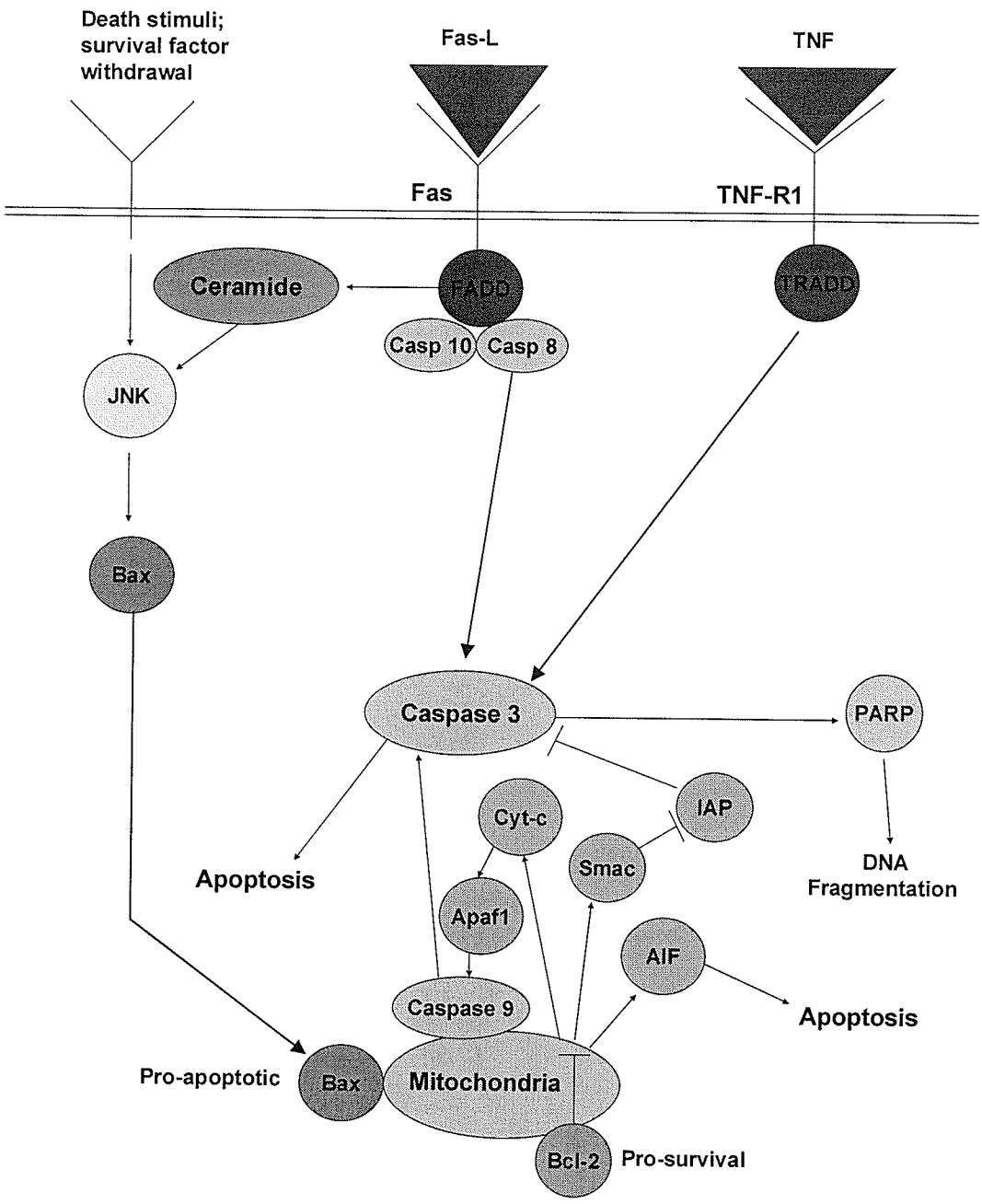

Figure 4. Apoptosis pathways.

Adapted from: Cell Signaling Technology. http://www.cellsignal.com/pathways/apoptosis-signaling.jsp.

pathway due to over-expression of Rho. This resulted in a reduction of phosphatidylglycerolphosphate (PGP) synthase induction after ceramide addition. These cells also showed a resistance to ceramide induced cell death and a decrease in apoptosis (Hatch *et al.*, unpublished results). Rho family members have been shown to activate apoptosis from Fas and cytotoxic T lymphocyte derived granzymes (Subauste *et al.*, 1999). In 1998, Esteve *et al.* reported that Rho induced apoptosis in several cell systems including human erythroleukemia K562 and murine NIH3T3 fibroblasts. They indicated that the generation of ceramides mediates Rho-dependent apoptosis, and that it is dramatically reduced by ectopic expression of *Bcl-2*.

There is also evidence however, of Rho-mediated inhibition of apoptosis. Phosphatidylinositol 3 (PI3) kinase and protein kinase C (PKC) have been identified as effectors of Rho (Zhang *et al.*, 1993; Gomez *et al.*, 1997). A 1997 paper by Gomez *et al.* suggested that constitutively active Rho proteins may prevent apoptosis by indirectly stimulating the activity of the pro-survival *Bcl-2* gene via PI3, PKC and IL-2 signaling pathways. Rho is also involved in the interleukin-2 (IL-2) signaling pathway, which has been shown to activate *Bcl-2* gene expression (Miyazaki *et al.*, 1995). In addition, RhoA has been shown to be required for cell survival in human endothelial cells. Inhibiting Rho activation in these cells decreased levels of the anti-apoptotic Bcl-2 and Mcl-1 proteins, and enhanced expression of pro-apoptotic family member, Bid. The same study also showed that inhibiting the function of Rho proteins promoted apoptosis via the caspase-9 and -3 pathway (Hippenstiel *et al.*, 2002). Bobak *et al.* also demonstrated a role for Rho proteins in cellular survival. Their studies showed that inactivation of Rho

by ADP-ribosylation increased apoptosis in rat aortic smooth muscle cells. The effect of Rho proteins on apoptosis is therefore more complicated than simply promoting or inhibiting the cellular death process.

Rho proteins also appear to have conflicting roles in the metastatic process. Simpson *et al.* found that one explanation may lie in the specific isoform of Rho that is involved. They used RNAi in a breast cancer cell line to knock down function of either the RhoA or RhoC isoform. Based on the experiments they conducted, they concluded that the RhoA isoform inhibits metastatic behavior, while RhoC enhances it. As the only significant difference in sequence between the two lies in the carboxy termini, it stands to reason that these sequences must be responsible for the contradicting behaviors, although the mechanism for this has yet to be elucidated. This may have potential for novel treatments as downregulation of RhoC may impede metastatic behavior.

Thus, there is evidence indicating that Rho proteins, and hence RhoGAPs, play a role in apoptotic and metastatic pathways. These pathways represent potential targets for novel therapies in the treatment of various diseases, including cancer.

1.6 Topoisomerases and Etoposide

In this study, the topoisomerase II inhibitor, etoposide, was used to induce apoptosis. Topoisomerases are enzymes responsible for creating nicks in DNA strands in order to facilitate the unwinding of DNA that is required for basic processes such as replication

and transcription. There are two major types of topoisomerases: DNA topoisomerase I, which causes single-strand breaks, and DNA topoisomerase II, responsible for cleaving double-stranded DNA (Hande, 1998). Topoisomerase II was first identified in 1976 by Gellert *et al.*, in their paper reporting DNA gyrase as an energy-dependent enzyme capable of converting relaxed DNA to the supercoiled form. They identified functions for this enzyme in DNA replication and recombination.

There are several inhibitors of topoisomerase II available, one of which is the podophyllotoxin, etoposide. It was the first inhibitor of this enzyme to be recognized and developed for the treatment of cancer. Isolated from the Podophyllum plant, podophyllotoxins have been used for medicinal purposes for centuries by various cultures. It was established as an inhibitor of mitosis in 1946, but clinical evaluation proved that podophyllin was highly toxic. In the 1950's, work began to isolate derivatives with lower toxicity that could be used as anti-cancer agents. Subsequently, 4'-demethylepipodophyllin benzylidene glucoside (DEPBG) was found to be effective in the treatment of leukemia. An analogue of DEPBG, etoposide, was developed in 1966 and showed an increase in anti-tumor effect. The drug was FDA approved in 1983 for treatment of a variety of cancers, including acute myeloid leukemia (AML), lymphoma, lung cancer and breast cancer (Hande, 1998).

In spite of the fact that etoposide was recognized as an anti-tumor agent, its mechanism of action remained unclear until 1984, when several laboratories identified DNA topoisomerase II as its target (Hande, 1998). Etoposide induces DNA strand breaks by

increasing the concentration of topoisomerase cleavage complexes within the cell, rather than inhibiting enzyme action. Transient strand breaks are converted to permanent ones that cannot be repaired by cellular machinery. This results in chromosomal aberrations, translocations and other defects that ultimately result in death by apoptosis. Given that topoisomerases are only required during specific points in the cell cycle, timing of etoposide treatment is critical, and studies have found that prolonged exposure to low doses of drug provide the maximum benefit (Hande, 1998). Berger *et al.* propose that the cytotoxic effects of etoposide are actually attributable to nonhomologous recombination events that result in the elimination of essential gene functions. These events are initiated by the cleavage complexes formed during drug treatment.

Etoposide is also known to function as a lipid antioxidant, and is capable of inducing apoptosis in HL-60 cells by causing them to undergo oxidative stress. The phenyl ring of etoposide allows this compound to act as a scavenger of free radicals, preventing their interaction with lipids. The oxidation of PS is important for the externalization of this phospholipid during the apoptotic process and the subsequent removal of cellular debris by macrophages. The ability of etoposide to prevent the proper oxidation of PS may contribute to its toxic effects, as the apoptotic remnants are not properly phagocytosed (Tyurina *et al.*, 2004).

1.7 Etoposide and Ceramide

The sphingolipid, ceramide, appears to play a role in both cell survival and apoptosis. Ceramide can be formed by the breakdown of sphingomyelin in a reaction catalyzed by

sphingomyelinase (SMase), or synthesized de novo within the cell (Pham & Hedley, 2001). Sawada *et al.* proposed that etoposide stimulates p53 to produce oxygen free radicals, resulting in the activation of neutral sphingomyelinase (N-SMase) and subsequent production of ceramide. Increased intracellular levels of ceramide during apoptosis promote the accumulation of reactive oxygen species (ROS) by disrupting the flow of electrons through the electron transport chain (Pham & Hedley, 2001). In neuronal cultures, etoposide treatment was found to increase endogenous levels of ceramide suggesting that high levels of this sphingolipid may contribute to apoptosis (Toman *et al.*, 2002).

There are conflicting reports however, regarding the action of ceramide in different types of primary neuronal cultures. Low doses have been correlated with an increase in survival and differentiation in both spinal motor neurons and cerebellar Purkinje cells, whereas high concentrations promote apoptosis (Furuya *et al.*, 1998; Irie & Hirabayashi, 1998).

Several possible mechanisms have been proposed for etoposide resistance. Chinese hamster ovary cell lines showing a dramatic resistance to the cytotoxic effects of etoposide based on resistance to the cleavage effects of topoisomerase II have been identified (Glisson *et al.*, 1986; Spiridonidis *et al.*, 1989). Spiridonidis *et al.* also recognized, but could not characterize, a second mechanism for resistance that was independent of the inhibition of topoisomerase II. Studies conducted by Luo *et al.* on Chinese hamster V79 cells suggest that changes in phosphorylation can influence resistance by affecting the activity or localization of topoisomerase II, or by promoting

changes in chromatin structure. V79 cells can be cultured as monolayers, or in suspension where they aggregate to form spheroids. Comparison of the two revealed that the outer cells of spheroids showed resistance to etoposide compared to cells grown as monolayers, but that the doubling time, total topoisomerase II activity, and rate of etoposide efflux were similar in cells grown under both conditions. One striking difference was that extracts from cells grown as monolayers showed a minimum 10 fold increase in topoisomerase IIα phosphorylation than extracts from the outer cells of spheroids. The topoisomerase IIα protein exerts its cleavage effects on DNA in the nucleus; phosphorylation of the C-terminus has been shown to play a role in targeting the protein to the nucleus. As such, it is likely that the reduction in phosphorylation of the topoisomerase IIα protein in spheroid cells confers resistance to etoposide by failing to correctly target the protein. Dephosphorylation is also associated with changes to chromatin structure, and it is possible that outer spheroid cells are less susceptible to the effects of etoposide due to differences in chromatin packaging (Luo *et al.*, 1998).

1.8 Functional Genomics Approaches

To allow us to be able to study the effects of knocking down the function of *Dlc-1* or *Dlc-2* in our cell lines, it was necessary to employ functional genomics strategies. Technological advances in the sequencing of DNA and the availability of software for analyzing large amounts of information have led to a revolution in molecular and biological research. In addition, high-throughput assays and the advent of microarray technology are allowing the study of gene function and expression profiles in ways that

were not possible before. Using these techniques, it is now possible to evaluate and compare such things as drug response in the genes of unaffected versus affected tissues, which should lead to the development of novel therapies for the treatment of many diseases, including cancer (Keon *et al.*, 2003).

Initially, functional genomic strategies involved the manipulation of mouse embryonic stem cells, which resulted in abrogating gene function in all cells of homozygously deleted animals. In 1992, Orban *et al.* introduced a site-specific method of deleting genes that would allow for functional studies on specific tissues. This was the introduction of the Cre-lox recombinase method, which allows the researcher to target specific genes in specific tissues and/or at specific times, in order to determine their function. The method is based on the use of Cre recombinase and its recognition of specific DNA sequences, loxP sites. The loxP sites may flank a reporter gene, such as the β-galactosidase (β-gal) gene and a recombination event would result in activation of the reporter. Alternatively, loxP sites can be positioned to flank the gene of interest so that a recombination event would result in deletion of the gene (Orban *et al.*, 1992).

The use of RNA interference (RNAi) is also emerging as a valuable tool for silencing specific genes in an organism. This technique uses double-stranded RNA, homologous to the target gene, to target and destroy specific mRNAs (Keon *et al.*, 2003). RNAi studies involving the nematode, *Caenorhabditis elegans*, have allowed for the generation of large-scale, gene-specific mutations for functional studies of these organisms. Gene

function can then be assigned by studying the phenotype associated with the knock-down of a specific gene (Keon *et al.*, 2003).

1.9 Mutagenesis strategies

Although spontaneous mutations occur in the genome, the frequency of such mutations is extremely low, and they are only useful for detecting phenotypes that are visible to the observer. It is therefore impractical to rely on the occurrence of such mutations for functional studies in genetics.

In the 1930's geneticists began to use x-rays as a means to induce mutations in mice with a higher frequency than those occurring spontaneously. Radiation leads to chromosomal damage, including rearrangements, translocations and deletions, which can provide molecular markers for cloning affected genes. The frequency of these mutations is relatively low when compared to other strategies, and because more than one gene is often affected, functional analysis can be difficult (Stanford *et al.*, 2001). Alternatively, chemical agents, such as chlorambucil, can be used to generate point mutations or small deletions. This has the advantage of achieving higher mutation frequency, and can be useful for gene mapping, but functional analysis is still problematic because multiple genes may be affected (Stanford *et al.*, 2001). To overcome some of these drawbacks, targeted mutagenesis strategies have been developed. By using homologous recombination in embryonic stem (ES) cells, the function of a single gene can be disrupted leading to a phenotype that can be studied. The difficulty arises however, in

predicting which biological processes may be affected by the disruption. In addition, some mutations are embryonic lethal, making it impossible to study their effects on an animal. The advent of conditional recombinase systems has helped to overcome some of these problems by allowing gene disruptions to be restricted to certain tissues and expressed at specific times during development (Stanford *et al.*, 2001).

Another strategy for developing somatic cell mutants is retroviral insertional mutagenesis. First described in 1976, this method can be used to determine the location of the gene associated with a recessive phenotype. Vectors can be designed to trap enhancers, promoters or genes. Regardless of the type, gene trap vectors contain a reporter gene and a selectable marker, so that clones with a disruption of an expressed gene as a result of viral integration can be identified (Hubbard *et al.*, 1993; Stanford *et al.*, 2001). Gene trapping vectors can be used to generate a library of clones containing a provirus in most expressed genes. Those clones that have a loss of function mutation resulting in a phenotype can then be selected and the targeted gene can be identified and characterized. Typically between 5×10^6 and 5×10^8 integration events are required for retroviral disruption of all cellular genes. Gene trap selection however, offers the advantage of increasing the proportion of cells with virus-induced mutations by 100- to 1000-fold as compared to cells containing unselected proviruses. Given that only 1×10^4 to 2×10^4 genes are normally expressed in a cell, a library consisting of 1×10^5 gene trap clones is large enough to contain a disruption in all readily targeted genes (Hicks *et al.*, 1995).

1.10 Basics of Gene Trapping

In addition to the features noted above, some gene trap vectors contain a splice acceptor site directly upstream of the reporter gene. The neo selection cassette allows for selection of any clones that have successfully incorporated the vector (Stanford *et al.*, 2001). ES cells incorporating the vector can easily be identified and implanted into host embryos to generate mutant mice (Lako and Hole, 2000). Ideally, insertion occurs in an intron and transcriptional activation of the construct by means of an endogenous promoter results in the formation of a fusion transcript. Gene expression can be tracked via the reporter gene, typically β-geo. This fusion transcript also provides a template so that the flanking sequences can be PCR amplified and the gene identified. Gene trapping is highly successful, the biggest drawback being that in some cases alternative splicing may occur resulting in lower transcription levels (Stanford *et al.*, 2001).

By including recombination sites (ie. loxP) in the vectors, gene trapping can be used in conjunction with recombinase-mediated techniques to allow for additional modifications to be made to trapped genes. It is therefore possible to use this technique to 'knock-in' additional transgenic sequences whose expression is driven by the endogenous promoter. Such constructs can be used for a variety of purposes, including labeling or immortalizing cells, increasing the usefulness of the technique. Currently, large-scale mutagenesis projects are underway using gene trapping to generate libraries of mutagenized ES cells that will be available to the scientific community for functional studies (Stanford *et al.*, 2001).

1.11 The U3NeoSV1 Promoter Trap

Towards the goal of understanding the genetic control of apoptosis, our lab employed retroviral mutagenesis to rescue cells from drug-induced apoptosis and identify the genes involved. This was accomplished using the U3NeoSV1 provirus (obtained from Dr. Earl Ruley – Vanderbilt University).

The U3NeoSV1 provirus was created to facilitate the generation of a library of mutant ES cell clones. Each clone in the library contains a single gene mutated by the insertion of the viral vector. The construct contains BamHI and EcoRI restriction sites, which allow for isolation and cloning of both 5' and 3' flanking sequences. The construct also contains pBR322 origin of replication (ori) and Ampicillin resistance gene (Amp), as well as a promoterless neomycin (G418; neo) selection cassette cloned into the U3 long terminal repeat (LTR) region (Figure 5). Viral integration occurs randomly throughout the genome, the neo resistance cassette ensures that only integrations within an expressed gene will be selected (Hicks *et al.*, 1997). The virus must integrate within 500 nucleotides of a cellular promoter in order for the G418 drug resistance to be active, or be spliced from a nearby exon into the 3' splice acceptor site in the neo gene. These integrations typically result in the inactivation of the targeted gene. Primers specific for the Neo gene can then be used to amplify unique DNA sequences flanking the insertion enabling identification of the disrupted gene. These DNA sequences are known as 'promoter-proximal sequence tags' or PSTs (Hicks *et al.*, 1997).

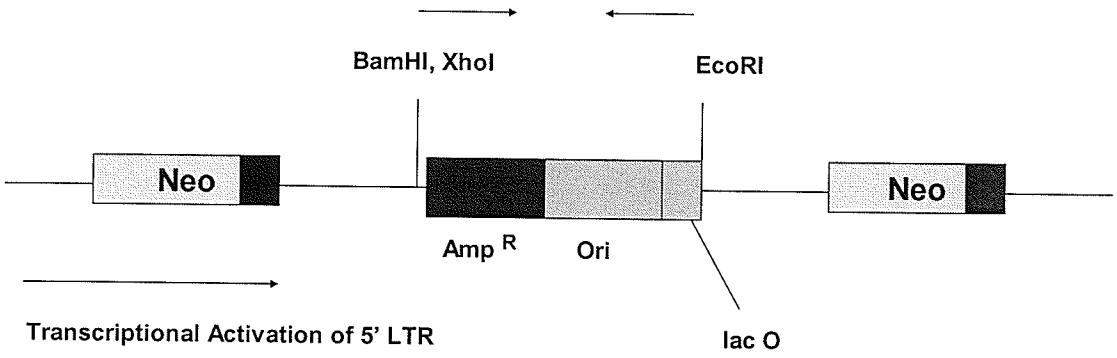

Figure 5. The U3NeoSV1 promoter-trap retrovirus.

Adapted from: Hicks, G.G., Shi, E-G., Chen, J., Roshon, M., Williamson, D., Scherer, C. and Ruley, H.E. 1995. Retrovirus Gene Traps. *Methods Enzymol.* **254**: 263-75.

Over half of the targeted ES cells are capable of generating germ-line mutations, which should allow the characterization of most of the genes expressed in these cells. This provides the potential for functional studies to be conducted without necessarily pinpointing the genomic location of the gene (Hicks *et al.*, 1997).

1.12 Chinese Hamster Ovary Cells – an Ideal Modeling System

The CHO K1 cell line was chosen for use in these experiments because it is functionally hemizygous at approximately 20% of the loci and has a constant diploid chromosome number of 22. Because of this, one mutational event may be sufficient to result in the loss of autosomal gene function. For those genes that are functionally diploid, the second allele is often lost due to recombination or deletion before selection for resistance to apoptosis. Most other lab cell lines are aneuploid or polyploid, and are therefore not suitable for loss of gene function experiments due to the presence of multiple alleles (Hubbard *et al.*, 1994).

CHO cells have been used to identify recessive mutations in somatic cells affecting many different biochemical processes. For example, mutant CHO cells with glycosylation defects conferring resistance to the cytotoxic effects of wheat germ agglutinin have been used to study lectin sensitivity in plants (Stanley, 1981)

1.13 Prior Progress and Results in the Creation of Etoposide-Resistant Cell Lines

Previous work in our lab used promoter trap retroviral mutagenesis to identify genes involved in drug response using a CHO K1 cell line. A library of CHO Cl22 cells was established in which transcriptionally active genes were disrupted using the pU3NeoSV1 retrovirus. Cl22 cells expressing the ecotropic retrovirus receptor gene from a transfected plasmid were used as the host cell for infection, and as the control. These cells show sensitivity to etoposide-induced apoptosis. To ensure a single viral integration per cell, infection was carried out at a virus/cell ratio of 1:20. G418 resistant cells were isolated and approximately 5 X 10^4 CHO K1 clones on 200 plates were collected. This is approximately equal to 2.5 times the number of genes estimated to be transcriptionally active per cell, which increased the likelihood of finding genes that were important for apoptosis. Fifty pools were frozen as a stock of mutants from which to select cells with disrupted apoptosis genes. Cells were then plated in the presence of different apoptosis inducing drugs at concentrations that give greater than 3 logs of kill to ensure little or no cell survival, thereby reducing the background. The E91 cell line showed resistance to the chemotherapeutic drug, etoposide, and defects in ceramide signaling. Sequencing conducted by Yuan Gu revealed that the promoter trap retrovirus had inserted into the *Dlc-2* RhoGAP gene of this cell line (Figure 6). These cells showed an increase in Rho activity as well as morphological changes (Hatch et al., 2007 submitted).

Additional cell lines, RSC1 and RSC6, were created by Yuan Gu, using pSUPER (OligoEngine) vector-mediated short hairpin RNA interference (shRNAi) to target the

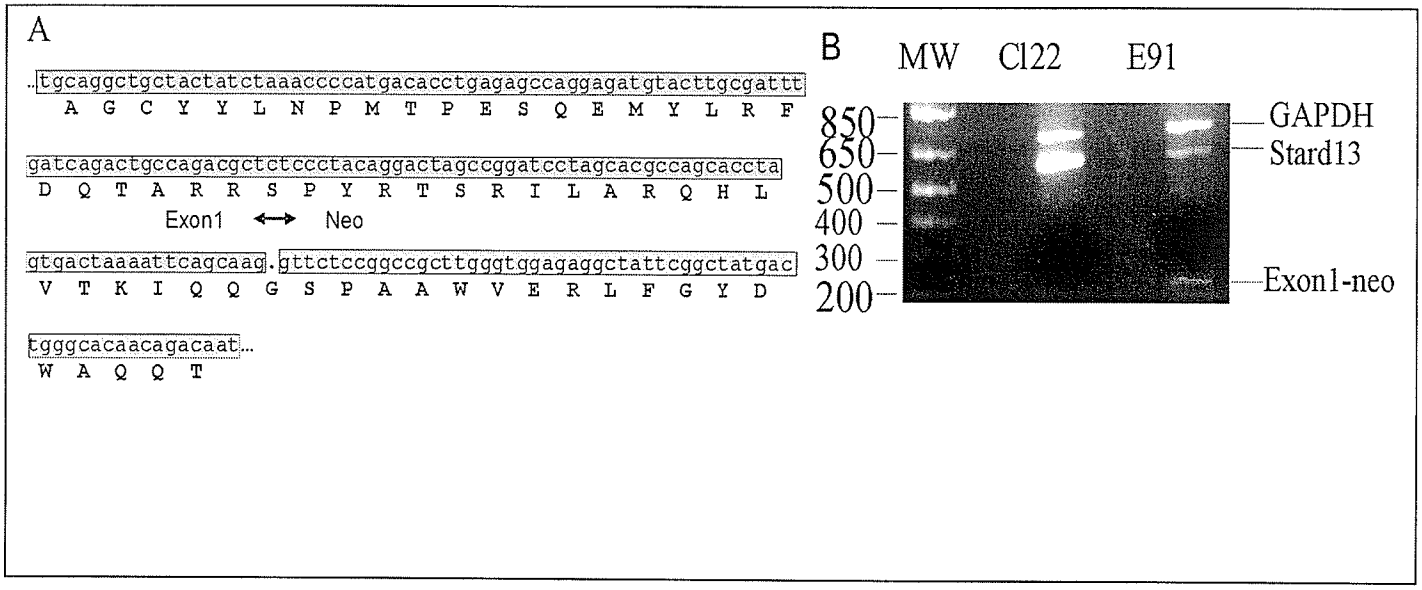

Data from Yuan Gu

Figure 6. Fusion of exon 1 of *Dlc-2* (*Stard13*) gene into the cryptic *Neo* 3' Splice Site. A) cDNA sequence of fusion transcript. The cDNA sequence was generated by 5'RACE and sequenced using Neo A and Stard13 specific primers. Amino acid single letter codes are shown and the Stard13 exon one sequences of the fusion protein and Neo coding sequences. The arrows indicate the location of 1 spliced transcript that uses the Neo 3' SS and the Stard13 exon 1 and Neo boundaries. B) Multiplex RT-PCR of RNA from CHO-K1 Cl22 and E91 cell lines. RT-PCR was performed using primers for *Stard13* exon 1-5, *Neo* gene and *GAPDH* in the same reaction. MW = molecular weight marker.

Dlc-2 transcript and observe the effects of gene knock down on etoposide induced resistance to apoptosis. These cell lines showed down regulation of the *Dlc-2* transcript as compared to the control cell line, RhoGapMT2, which contains the *Dlc-2* sequence mutated at 3 positions and ligated into the pSUPER vector backbone, with no knockdown of the gene transcript (Figure 7).

In addition, he created the Dlc1 and Dlc2 cell lines using a commercially available shRNAi vector, pSM2c (Open Biosystems). These cell lines targeted the *Dlc-1* and *Dlc-2* transcripts respectively. Both CHO K1 and a human non-small cell lung carcinoma cell line were transfected with this vector.

1.14 Transgenic Mouse Basics

In 1961, Tarkowski reported experiments in which two eggs obtained from different donor mice were fused together to form one embryo. He removed the zona pellucida from embryos at the 8-cell stage, combined them and placed them in culture. After 16 hours, the conjoined eggs had combined to form a single morula, and the majority of these developed into early blastocysts after 24 hours. These blastocysts were then transplanted into pseudopregnant females. Although these experiments generated chimeric pups that were morphologically normal, the mortality rate was unexplainably high.

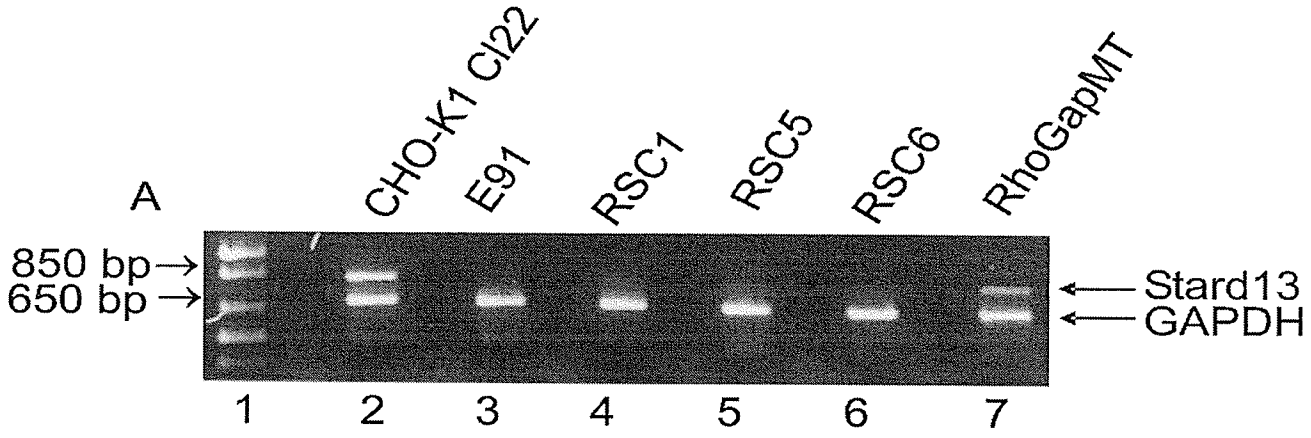

Data from Yuan Gu

Figure 7. Multiplex RT-PCR of cell lines expressing shRNAi plasmids. Multiplex RT-PCR was carried out using primers for *Dlc-2* and *GAPDH* cDNAs. Lane 1: Molecular weight marker; lane 2: CHO-K1 Cl22 cell line; lane 3: E91; lane 4: RSC1; lane 5: RSC5; lane 6: RSC6; lane 7: RhoGapMT. Cell lines RSC1 & 6 contain the pSuper plasmid expressing *Dlc-2* shRNAi. Cell line RSC6 contains the pSuper.neo+GFP plasmid expressing *Dlc-2* shRNAi. RhoGapMt contains pSuper expressing a mutated *Dlc-2* shRNAi.

Then, in 1968, Gardner reported a new method for generating chimeric mice. He separated donor blastocysts into cells, injected these cells into recipient blastocysts, and then implanted them into pseudopregnant females. The donor cells contained a color marker and a chromosomal translocation to facilitate detection of chimerism. His experiments resulted in the production of live-born chimeric offspring, providing evidence that foreign cells injected into blastocysts could be incorporated into the embryo proper.

Gordon and Ruddle coined the term 'transgenic' in 1981 to describe mice they had generated after pronuclear injection of DNA sequences into fertilized oocytes. They were able to demonstrate, not only that injected sequences were detectable in the host genome, but also that the foreign DNA could be transmitted through the germline into offspring. The same year, several other groups reported similar results from their microinjection studies. Human β-globin, herpes simplex virus thymidine kinase (HSV TK) and rabbit β-globin DNA sequences were successfully incorporated into the mouse genome and transferred to progeny (Wagner *et al.*, 1981; Constantini & Lacy, 1981). Although injection of higher numbers of plasmids increased the efficiency of transformation, it was found that this had a negative impact on the survival rate of injected embryos. Injecting 1000 copies was found to have a 50-70 percent embryo survival rate, with approximately 1 in 30 future offspring retaining transferred sequences. Increasing the plasmid copy number to 30,000 lowered the embryo survival rate to 30-50 percent, however 1 in 15 of the progeny retained the foreign DNA (Gordon & Ruddle, 1981).

Another method for creating transgenic mice was described in 1993. In this study, mice were grown from cell culture using early passage ES cells. They combined these ES cells with developmentally deficient tetraploid embryos so that the ES cells would overtake all tissues where they were able to differentiate, forcing the tetraploid derived cells to the extraembryonic tissues. Although the ES cell-tetraploid aggregates developed normally, they died at or around birth. A new ES cell line was developed that was able to sustain viable pups at early passage number, however many of the aggregates did not survive to term and as a result this was not deemed to be a feasible method of generating transgenic mice (Nagy *et al.*, 1993).

Thus, there are two distinct techniques for the generation of transgenic mice, each with their own advantages and disadvantages. Blastocyst injection has been the principal method for developing chimeras, however it is costly, both in terms of time and equipment, as these manipulations require extensive expertise to carry out successfully. The aggregation method has also been deemed effective, in fact equivalent percentages of germline chimerism have been achieved using both techniques, however it is much less expensive, and less specialized (Wood *et al.*, 1993).

1.15 Prior Progress and Results in the Generation of *Dlc-1* Knock Out Mice

Durkin *et al.*, 2005, used a targeting vector to knock out exon 5 of the mouse *Dlc-1* gene. This also generated a frame shift mutation causing a premature stop codon, which resulted in a truncated protein. They found mice heterozygous for the deletion to be

phenotypically normal, however the homozygous null condition was embryonic lethal around day 10.5. They noted several abnormalities in these embryos, including defects in the brain, heart, neural tube and placenta.

For our study, knock out mice were generated using XE082 ES cells (Bay Genomics) from the 129Sv2 strain crossed to a C57Bl/6 background. The gene trap vector used to generate the ES cells was pGT1lxf (Bay Genomics) (Figure 8). This vector contains a β-galactosidase (X-gal) reporter construct fused to a G418 (neo) selection cassette (β-geo), flanked by long terminal repeat (LTR) sequences. In this ES cell line, the gene trap retrovirus inserted into intron 1-2, resulting in a spliced exon 1-β-geo fusion transcript, producing a truncated *Dlc-1* exon 1-β-geo fusion protein. Currently the mice have been backcrossed for three generations onto the C57Bl/6 mouse strain.

1.16 Rationale and Approach of the Current Study

The purpose of this study is two-fold. First, to determine the effects of knocking out the RhoGAP function of two tumor suppressor genes, *Dlc-1* and *Dlc-2*, on programmed cell death induced by the drug etoposide. Second, to see whether knocking out gene function will affect gene expression, phenotype and/or tumorigenesis in *Dlc-1* deficient mice.

Given that Rho proteins have effects on such a variety of important cellular processes and that the RhoGAP genes, *Dlc-1* and *Dlc-2*, have been shown to be tumor suppressors, we hypothesize that disrupting the RhoGAP function of these genes will result in an increase

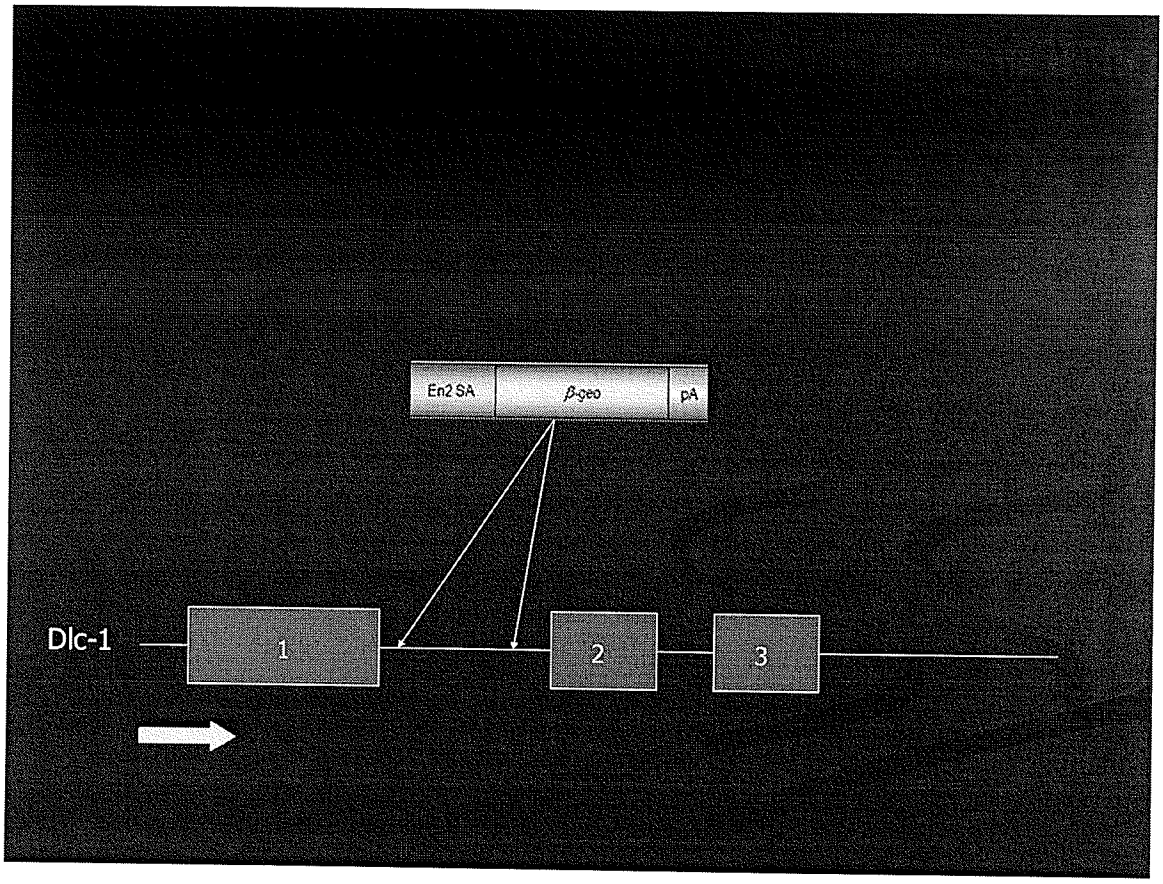

Figure 8. Insertion of the gene trapping vector, pGT1lxf, into intron 1-2 of the *Dlc-1* gene.

in Rho expression leading to reduced apoptosis and increased drug resistance in affected cell lines. We expect to see an increase in the formation of stress fibres in cells with reduced RhoGAP expression, as well as a propensity for cellular aggregation. With respect to the knock out mice, we hypothesize that there may be an increase in the formation of spontaneous tumors, and that the homozygous null condition will be embryonic lethal.

To this end, apoptosis and cell survival assays were conducted on CHO K1 cell lines that have a disruption of either *Dlc-1* or *Dlc-2* function as a result of retroviral mutagenesis or RNA interference (RNAi). Apoptosis was analyzed using flow cytometry, and cell survival was measured using crystal violet colony and MTT assays.

A second goal was to study what effects knocking out *Dlc-1* function has on phenotype and tumorigenesis in mice. This ongoing study is being accomplished by studying gene expression patterns in wild type, heterozygous and homozygous null embryos. Tissues from wild type and heterozygous embryos are being studied at time points E10.5, E12.5 and E14.5, while homozygous deleted embryos are being harvested at E9.5 and E10.5 to elucidate the effects of gene deletion on embryonic development and phenotype. Adult mice are being observed for the formation of spontaneous tumors to determine whether there is an increased incidence of tumor development in heterozygous versus wild type mice.

CHAPTER 2 – EXPERIMENTAL PROCEDURES

2.1 Cell Culture Conditions

All cells were cultured in a humidified incubator with 5% CO_2 at 37°C. The CHO K1 cell lines, ie. Cl22, E91, RhoMT2, RSC1 and RSC6 and Dlc1 cell lines were grown in Ham F-12 medium (Invitrogen), supplemented with 3.7 g/l of sodium bicarbonate, 100 μg/ml streptomycin, 100 U/ml penicillin G and 5% fetal bovine serum. The human NSCLC cell lines, ie. H460, H460 non-silencing, and Dlc2 were grown in alpha-Minimal Essential Medium (α-MEM) (Invitrogen) containing 3.7 g/l of sodium bicarbonate, 100 μg/ml of streptomycin, 100 U/ml penicillin G and 10% fetal bovine serum.

2.2 Examination of Cellular Morphology

Twenty thousand cells were grown overnight on coverslips in 2.0 ml of medium in a 6 well plate. Cells were gently rinsed with 1 X phosphate buffered saline (PBS) and fixed with 2% paraformaldehyde (PFA) for 15 minutes at room temperature. Cells were rinsed again with 1 X PBS and permeabilized with 0.2% Triton-X-100 in PBS for 15 minutes. The cells were then blocked with 3% BSA (bovine serum albumin) in PBS for 30 minutes. Eighty μl of 0.1 μg/ml phalloidin-tetramethylrhodamine B isothiocyanate (TRITC) was placed on a piece of parafilm, and the coverslip was placed on top, cells side down. The coverslips were then incubated for 30 minutes in a humidified chamber at room temperature, then returned to the 6 well plate and rinsed with 1 X PBS. After

removing the PBS, 1.0 ml of diluted Hoechst stain was added, and incubation was continued for five minutes. The stain was removed, and coverslips were washed three times in 1 X phosphate buffered saline-Tween 20 (0.1%) (PBS-T), followed by a rinse in 1 X PBS. A drop of Crystal/Mount was placed on a slide, the coverslip was removed from the plate using forceps, the excess PBS was drained off, and the coverslip was placed on the drop, cells side down. The Crystal/Mount (Biomedia Corp) was allowed to harden, and coverslips were sealed with clear nail polish and imaged on an Olympus IX81 confocal microscope using a 40X objective at 3X zoom and at a resolution of 0.1 X 0.1. The number of pixels per picture was 1024 X 1024. The images were captured using an Olympus camera and processed using Fluoview software. Cellular morphology was examined twice for each cell line, once with no treatment, and once after treatment with 25 μM etoposide (SIGMA) (stock solution 50 mM) for 24 hours.

2.3 Examination of Etoposide Resistance Using the Crystal Violet Colony Assay

One thousand cells were seeded, in triplicate, on 6 well plates in 2.0 ml of medium. Cells were allowed to adhere overnight then treated the next day with etoposide freshly prepared in DMSO (dimethyl sulfoxide). After aspirating the media, individual wells were treated as follows: one well control, untreated (0), one well control, treated with DMSO, one well treated with each of 50 nM, 100 nM, 500 nM and 1.0 μM etoposide in media. After 48 hours, the medium containing the drug was removed and each well was washed with 1.0 ml of 1 X PBS. Two ml of the appropriate medium was added per well, and cells were allowed to recover until controls became confluent (approximately one

week). The media was changed every two days. After one week, the media was removed, each well was washed with 1.0 ml of 1 X PBS, and 1.0 ml of 0.5% aqueous crystal violet stain was added. Plates were then incubated for one hour at 37°C with 5% CO_2. The crystal violet stain was removed by aspiration and the plates were rinsed gently in two changes of ddH_2O. The plates were allowed to dry overnight and then 1.0 ml of 0.1% acetic acid in 50% ethanol was added to dissolve the stain. Two hundred µl from each well was transferred into 96 well plates, in triplicate, and the absorbance was read on Spectramax 190 plate reader at a wavelength of 538 nM. SOFTmax Pro 3.1.2 software was used to assemble the data into chart form.

2.4 Examination of Etoposide Resistance Using the MTT Assay

Cells were seeded in 96 well plates at 2 X 10^2, 3 X 10^2, 4 X 10^2 and 5 X 10^2 cells per well, in triplicate, for each concentration of vehicle (DMSO) and etoposide. The total volume of medium per well was 200 µl. Etoposide concentrations used were 0, 500 nM, 1.0 µM, 5.0 µM, 10.0 µM and 25.0 µM with the same volumes of DMSO used as vehicle controls. The cells were allowed to adhere overnight at 37°C in 5% CO_2. The next day the media was removed by flicking the plates over absorbent pads, and the cells were treated with the appropriate concentration of etoposide or and equivalent volume of vehicle. After 48 hours, the etoposide was removed and each well was washed with 200 µl of 1 X PBS, which was then replaced with 200 µl of medium. Plates were incubated until the controls became confluent (for at least 4 logs of growth), approximately one week. At this time, 10 µl of 5 mg/ml 1-(4,5-dimethylthiazol-2-yl)-3,5-diphenylformazan

(MTT) in PBS (Sigma-Aldrich) was added per well and plates were incubated for three hours to allow the formation of formazan crystals. The plates were spun on a Beckman Coulter Allegra 25R centrifuge at 2000 rpm for 10 minutes to sediment the crystals. The media was then removed and the crystals were dissolved in 200 µl of DMSO by shaking on a Dynatech Minishaker. Optical density (OD) readings were taken on a Spectramax 190 at a wavelength of 538 nM, and the data was assembled into chart form using SOFTmax Pro 3.1.2 software.

2.5 FACS Analysis of Apoptosis in Response to Etoposide Treatment

1 X 10^5 cells were seeded on 6 well plates for 1, 12 and 24 hour time points. 5 X 10^4 cells were seeded for 48 and 96 hour time points. All wells contained 2.0 ml of the appropriate medium for the cell line. The cells were allowed to adhere for 24 hours and drugged the next day as follows: one well control, untreated, one well control, treated with 1.0 µl of DMSO, one well treated with 1.0 µM etoposide, one well with 5.0 µM etoposide and one well with 25.0 µM etoposide. At the appropriate time, the medium from each well was transferred to a 5 ml Falcon tube (BD Falcon), on ice. One ml of 10 mM ethylene diamine tetra-acetic acid (EDTA) in PBS was added to each well and the plates were incubated for 8 minutes. Cells were released by tapping the plate and the EDTA solution was transferred to the Falcon tubes. Each well was washed with 500 µl of 1X PBS, which was also added to the tubes. The tubes were spun for 5 minutes at 2000 rpm at room temperature in a Damon-IEC DPR-6000 centrifuge. The liquid was aspirated and the pellets were resuspended in 250 µl of 1X binding buffer. One µl of

AnnexinV-FITC (fluorescein isothiocyanate) and 0.5 µl of 7 amino-actinomycin-D (7AAD) were added to each tube and the tubes were incubated for 15 minutes in the dark at room temperature. Cells were sorted on a flow cytometer (Becton Dickinson FACSCalibur) as per the manufacturer's specifications. For the 96 hour time point, the etoposide was removed after 48 hours, the plates were washed with 1.0 ml 1 X PBS and 2.0 ml of fresh medium was added per well. The cells were allowed to recover for an additional 48 hours at 37°C with 5% CO_2 before readings were taken.

2.6 Statistical Analysis of Results

The results of the cellular assays were statistically analyzed using the Generalized Linear Model (GLM) procedure, least squares method. The analysis was conducted by Mrs. Mary Cheang, M. Math (Stat.), consultant of the Biostatistical Consulting Unit, Community Health Services Department.

2.7 Characterization of *Dlc-1* Deficient Mouse Embryos

2.7.1 Extraction of Genomic DNA

Approximately 0.5 cm was cut from the end of the tail of each mouse between 21 and 28 days of age, and each clipping was placed into a labeled Eppendorf tube. 0.6 ml of STE lysis buffer [(0.1 M NaCl, 10 mM Tris (pH 8.0), 1 mM EDTA (pH 8.0)), 0.1 mg/ml Proteinase K (20 mg/ml stock), 0.1 mg/ml RNase A (10 mg/ml stock) and 0.5% SDS] was added to each tube, and the tubes were shaken overnight at 55°C in a thermomixer.

An equal volume of 1:1 phenol (pH 8.0):chloroform/isoamyl alcohol (24:1) was then added, mixed by inverting the tubes, and spun for two minutes. The supernatant (approximately 0.5 ml) was transferred to a fresh tube, and an equal volume of chloroform/isoamyl alcohol (24:1) was added; tubes were mixed by inverting and layers were separated by a two minute spin. The supernatant (approximately 0.4 ml) was again transferred to a fresh tube. One ml of absolute ethanol was added to precipitate the DNA, the tubes were inverted to mix, and the DNA was collected by centrifugation for two minutes. The liquid was poured off and tubes were inverted to dry. The pellets were resuspended in 0.1 ml of TE (pH 8.0) by incubating at 65°C for approximately 1 hour.

2.7.2 Genotyping of Tail DNA Using PCR

2.7.2.1 Primer Sequences

Primer Name	Primer Target	Primer Sequence 5'→ 3'
NeoGSP1	U3NeoSV1 Neomycin Resistance Gene	GGA TAC TTT CTC GGC AGG AGC AAG GTG A
NeoGSP2	U3NeoSV1 Neomycin Resistance Gene	TTG GGT GGA GAG GAG AGG CTA TTC GGC TAT GAC
GSP1CHGAPDH		GAA GTC GCA GGA GAC AAC CTG GTC CT
GSP2CHGAPDH		TGG CAA GTT CAA AGG CAC AGT CAA GG

2.7.2.2 PCR, Electrophoresis and Visualization

Five µl of genomic DNA was added to 5.0 µl of 10X reaction buffer (TaKaRa Biomedicals), 10mM final concentration of dNTP mixture (TaKaRa Biomedicals), 5 units/µl (0.5 ul) *TaKaRa Taq* (TaKaRa Biomedicals), with 30 pmols each of NeoGSP1 and NeoGSP2 primers (Qiagen) and 10 pmols each of GSP1CHGAPDH and GSP2CHGAPDH primers (Invitrogen), and brought to a final volume of 50 µl. The samples were heated to 94°C for 2 minutes, followed by 35 cycles of 94°C for 30 seconds, 54°C for 2 minutes and 72°C for 2 minutes. The final extension was at 72°C for 10 minutes. 15 µl of the PCR product was separated on a 1% agarose gel containing ethidium bromide (0.2 µg/ml), in 1 X TAE buffer (40mM Tris, 20mM acetic acid, 1mM EDTA) (Figure 9).

2.7.3 Standard X-gal Staining for Whole Mount Embryos up to E14.5

Embryos were dissected at embryonic days 9.5 and 10.5 and placed into one well of a 24 well plate. They were rinsed, 3 X 5 minutes in ice cold PBS and fixed for one hour in 4% PFA in PBS on ice. They were rinsed twice for 10 minutes in PBS, and then incubated for 15 minutes in permeabilization solution (100 µl of 1M $MgCl_2$, 500 µl 1% Na Deoxycholate, 100 µl 10% NP40, 2.5 ml 20X PBS, brought to 50 ml with ddH_2O) on ice. The solution was aspirated, and fresh permeabiliztion solution was added for a further 15 minutes at room temperature. The permeabilization solution was aspirated and enough

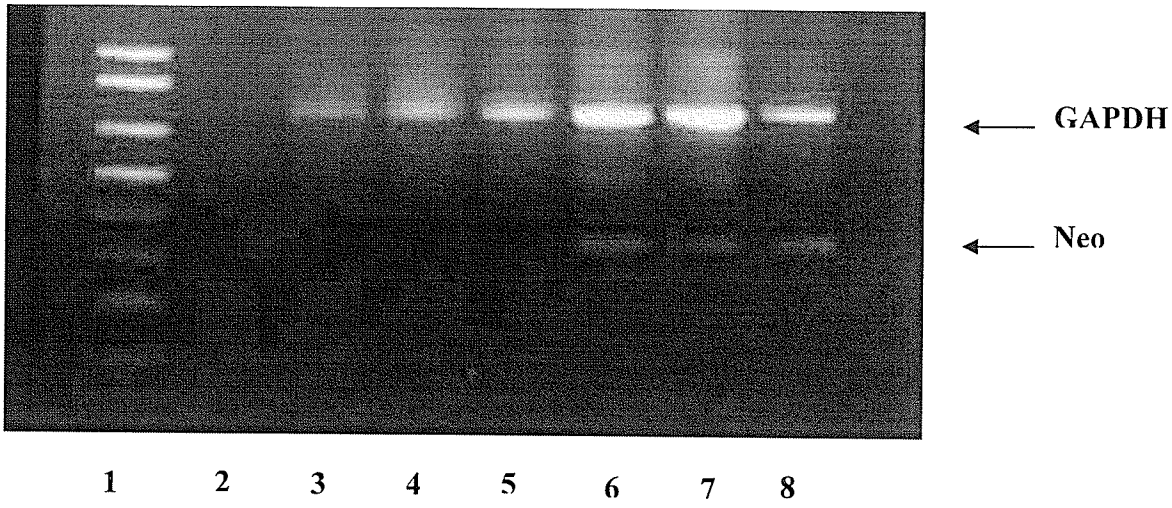

Figure 9. Agarose gel electrophoresis of PCR amplified tail DNA for genotyping. GAPDH serves as a control for the PCR. Neo band indicates a positive result for the insertion of the viral vector. Lane 1: 1kb Plus DNA ladder. Lane 2: negative control. Lanes 3-5: indicate wild type pups as they are negative for the insertion. Lanes 6-8: indicate heterozygous pups as they are positive for the insertion.

freshly made X-gal staining solution (0.2 ml X-gal dissolved at 50 mg/ml in DMSO, 0.5 ml 20X PBS, 0.25 ml 200 mM $K_3Fe(CN)_6$, 0.25 ml 200 mM $K_4Fe(CN)_6$, 0.2 ml 100 mM $MgCl_2$, 0.2 ml 10% NP40, brought to 10 ml with ddH_2O) was added to cover the embryos. They were incubated overnight at 30°C (temperature is critical to limit endogenous staining at 37°C). The next day, they were rinsed, 3 X 10 minutes in 1 X PBS. Fixation was done overnight in 4% PFA in PBS at 4°C. Embryos were again rinsed, 3 X 10 minutes in PBS and then photographed or processed for cryosectioning.

2.7.4 Processing Embryos for Cryosectioning

The PBS was removed, 10% sucrose in PBS was added to cover each embryo and the embryos were incubated overnight at 4°C. The following day the 10% sucrose/PBS was replaced with 20% sucrose/PBS and embryos were incubated again overnight at 4°C. The 20% sucrose/PBS was then replaced with 30% sucrose/PBS and a third overnight incubation at 4°C was done. Each embryo was placed in a tissue embedding mold, covered with Tissue Tek medium and frozen by slowly lowering into 2-methyl-butane on dry ice. They were wrapped in aluminum foil and stored at -80°C until ready to section on the cryostat.

2.7.5 Tissue Sectioning

Tissue sectioning was performed on a Leica CM3050S cryostat at 14°C and a thickness of 10.0 μM. Sections were placed on slides and imaged using a Zeiss Axiovision

microscope at 20X magnification. Photographs were taken with a Zeiss Axiocam MMRC camera and processed using Axiovision 4.5 software.

CHAPTER 3 – RESULTS

3.1 Overview

The following section describes the results of the analysis of cell lines studied during the course of this project. As previously stated, the E91 cell line contains a promoter trap retrovirus inserted into the *Dlc-2* RhoGAP gene, and the Cl22 cells, which express the ecotropic retrovirus receptor gene from a transfected plasmid, served as the control for this cell line. The RhoGapMT2 cell line expresses a short hairpin RNAi vector (shRNAi) against the *Dlc-2* sequence that is mutated at three positions and ligated into the pSUPER vector backbone. This line serves as a control for the shRNAi expressing lines RSC1, RSC6 and Dlc1 cell lines. The RSC1 and RSC6 cell lines were created using pSUPER vector-mediated short hairpin RNA interference to target the Dlc-2 transcript. The Dlc1 cell line used a commercially available shRNAi vector, pSM2c, to target the Dlc-1 transcript in CHO K1 cells. The pSM2c vector was also transfected into a human non-small cell carcinoma cell line, H460, targeted against the Dlc-2 transcript, giving the Dlc2 cell line. The H460 cells were used as a control for this cell line throughout most of the project. However, recently the H460ns cell line was developed, which contains the pSM2c vector with a scrambled, non-silencing shRNAi. While this control was unavailable for the experimental studies, morphological pictures were taken for comparison purposes.

The purpose of the project was to determine whether disruption of a RhoGAP gene, *Dlc-1* or *Dlc-2*, was sufficient to confer resistance to the chemotherapeutic drug etoposide, and what effects if any, disruption of the *Dlc-1* gene would have on mouse development. In addition, the *Dlc-1* knock out mice were observed for the possibility of spontaneous tumor formation. Observations of heterozygous and homozygous null mouse tissues and embryos are also included.

3.2 Morphological Changes in E91, RSC1, RSC6, Dlc1 and Dlc2 Cell Lines

Because of the known effects of Rho on the cytoskeleton, it was important to observe the differences between the knock down cell lines. The experimental cell lines E91, RSC1, RSC6, Dlc1 and Dlc2, and the control cell lines Cl22, RhoMT2, H460 and H460ns, were stained with the nuclear stain, Hoechst, and the actin cytoskeleton stain phalloidin-TRITC.

The cell lines containing a disruption of the RhoGAP gene, *Dlc-1* or *Dlc-2*, showed several distinct morphological changes. In particular, the E91 cell line, which contains a retroviral integration into the *Dlc-2* RhoGAP gene, showed a marked increase in the formation of stress fibres in all cells examined as compared to the control Cl22 cells, in which the stress fibres are only slightly visible with darkest staining around the periphery of the cells. This increase in stress fibre formation resulted in a dramatic increase in the size of E91 cells, and they appeared more rounded than Cl22 cells which have an angular, irregular shape (Figure 10).

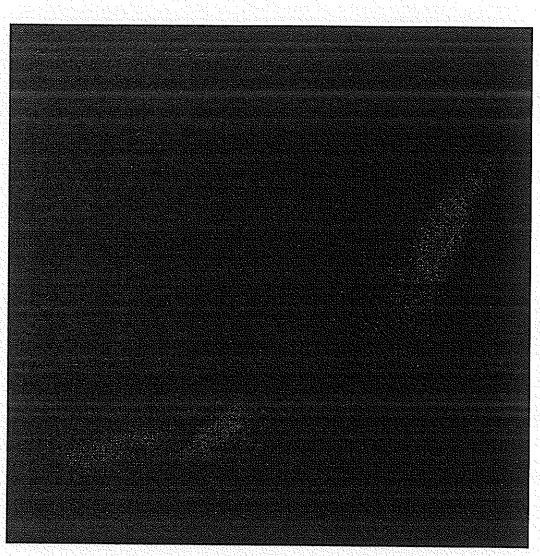

A

B

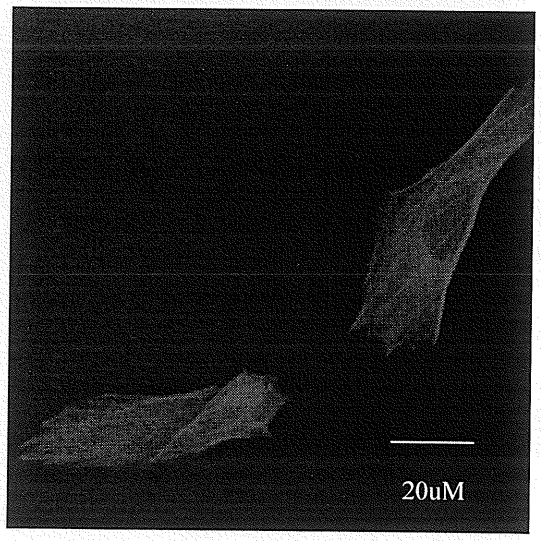

C

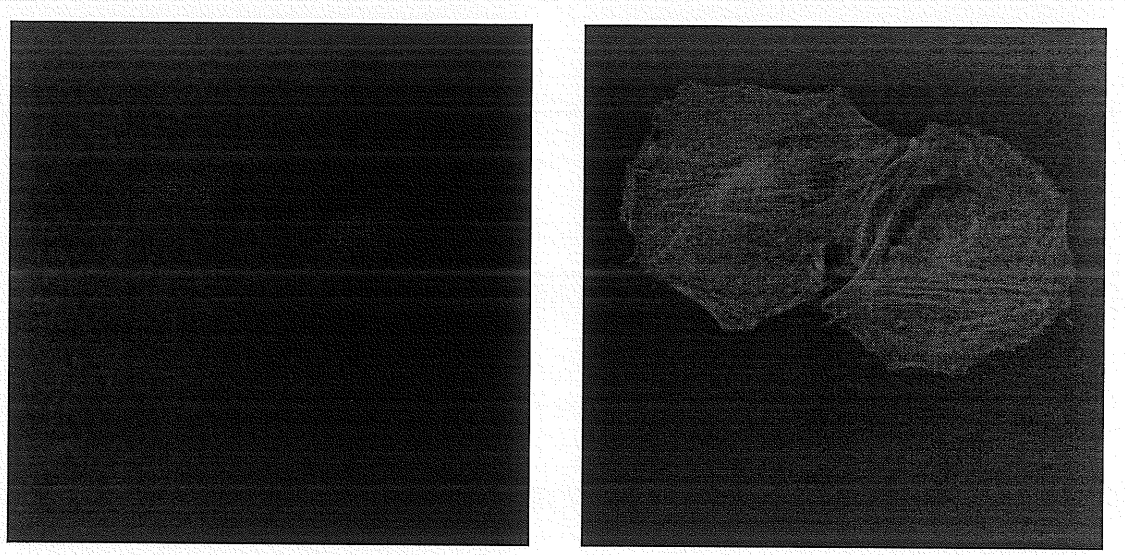

D

E

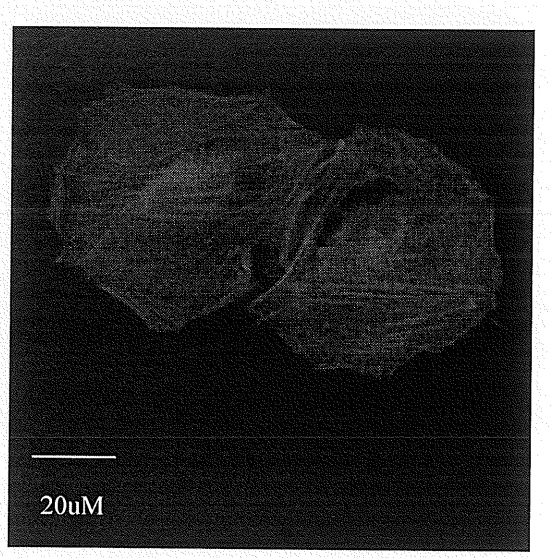

F

Figure 10. Cellular morphologies. Images were taken on a confocal microscope at 40X magnification, 3X zoom, and at a resolution of 1024 X 1024. A. Cl22 stained with Hoechst. B. Cl22 stained with phalloidin. C. Overlay of Cl22 images. D. E91 stained with Hoechst. E. E91 stained with phalloidin. F. Overlay of E91 images.

The cell lines expressing a shRNAi against the *Dlc-2* RhoGAP gene (RSC1 and RSC6) were compared against the RhoGapMT2 control, which expresses a mutant shRNAi. In the RSC1 cells, the nucleus of the vast majority of cells appeared as a black hole when the phalloidin staining was viewed. Almost all cells were round in shape but had irregular edges. The RSC6 cells, on the other hand, were quite angular. Both knock down cell types showed a high proportion of aggregated cells, approximately 80% for RSC1 and 95% for RSC6. The stress fibres were very visible and highly organized, although more so in the RSC6 cells, and the nuclei appeared very round and uniform. This is evident in Figure 11d-i, where multiple nuclei are visible in what would otherwise look like one cell. They also appeared to be much larger than the control RhoGapMT2 cells, which are very like the Cl22 cells. This similarity between the control cell lines is not surprising, given that the mutant shRNAi in the RhoGapMT2 cells is not expected to cause any changes. The Dlc1 knockdown cells appeared slightly larger than the control with the same irregular shape, but had a more pronounced and enlarged nucleus that showed heavy actin staining. The stress fibres were visible in approximately 10% of the cells examined and did not appear as highly organized as in the RSC1 and RSC6 cell lines. This may be due to the heavy nuclear staining which may overshadow the staining of fibres (Figure 11).

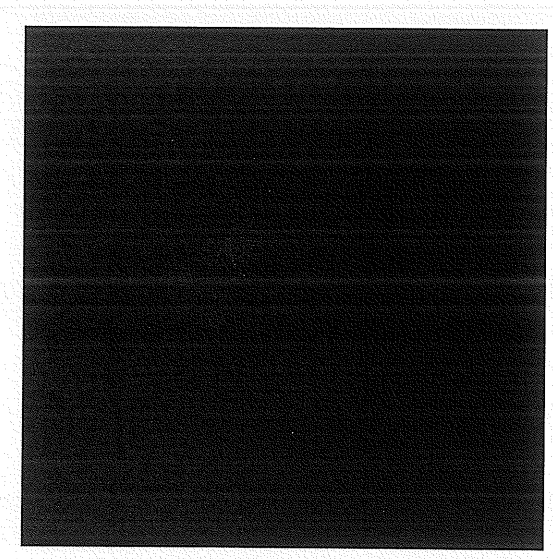

A

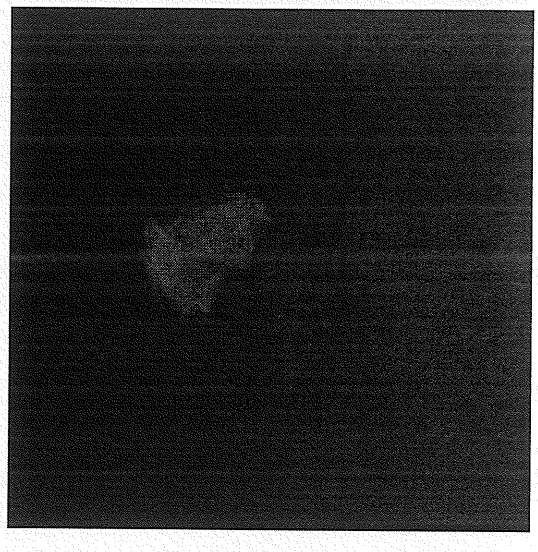

B

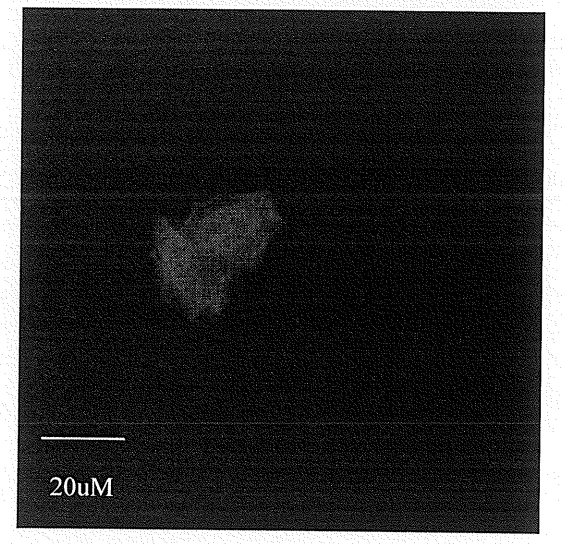

C

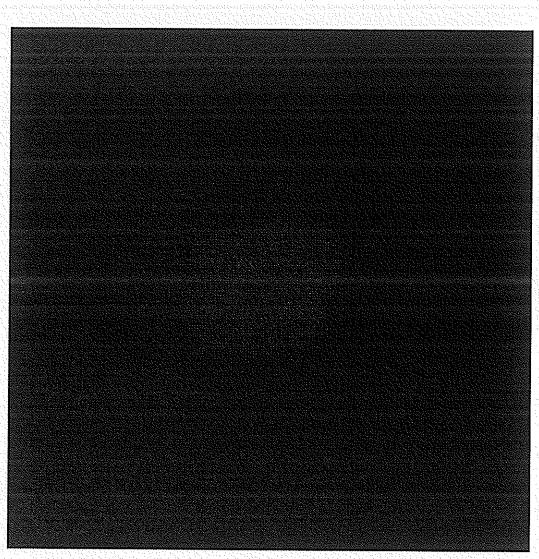

D

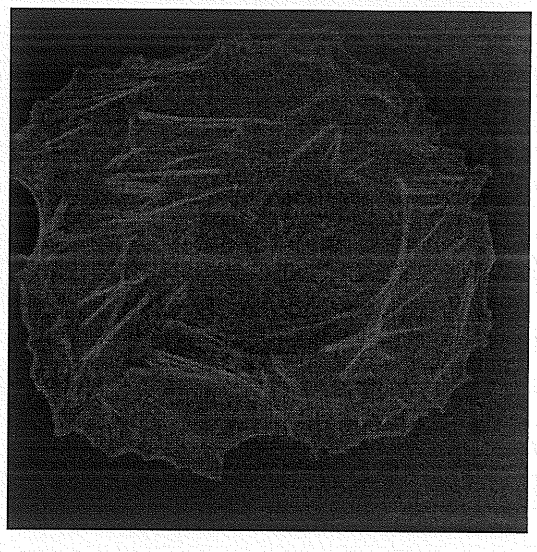

E

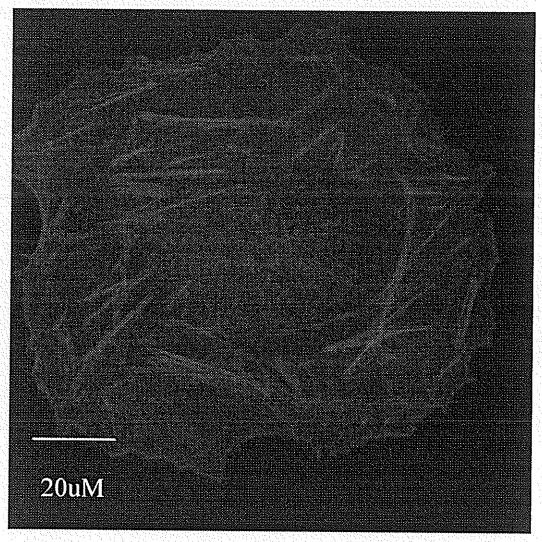

F

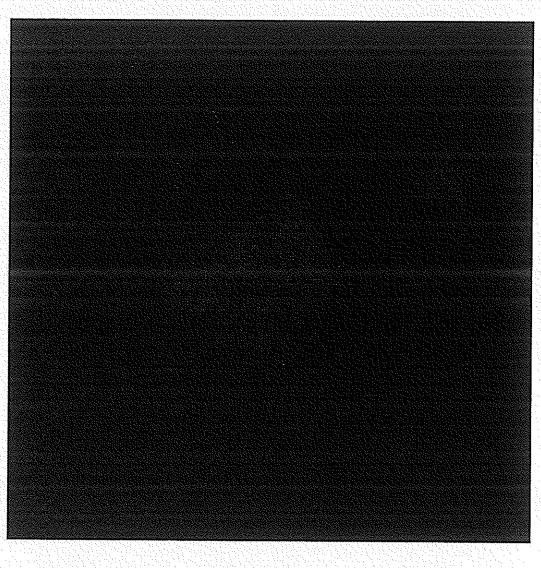

G

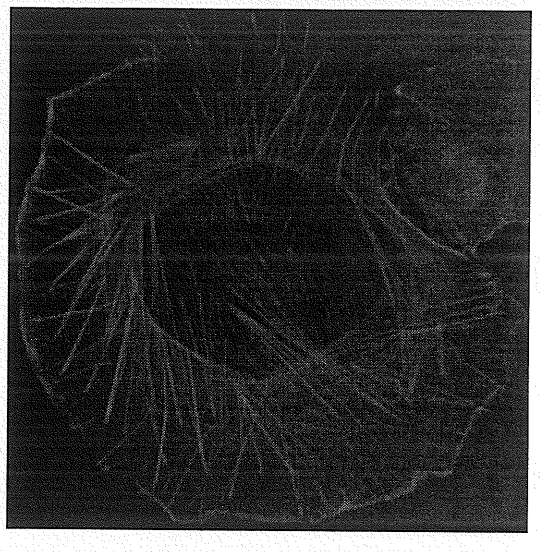

H

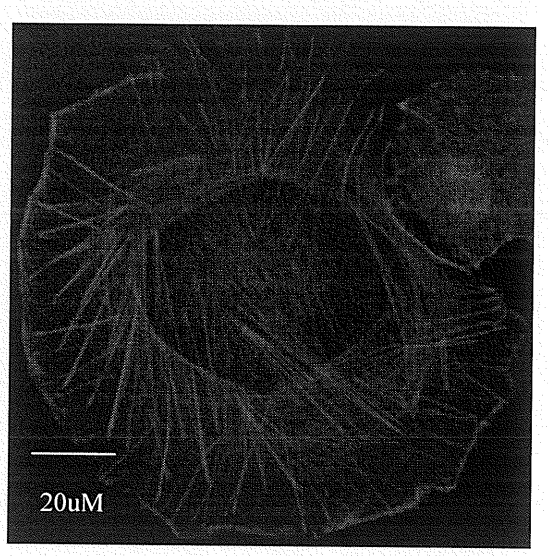

I

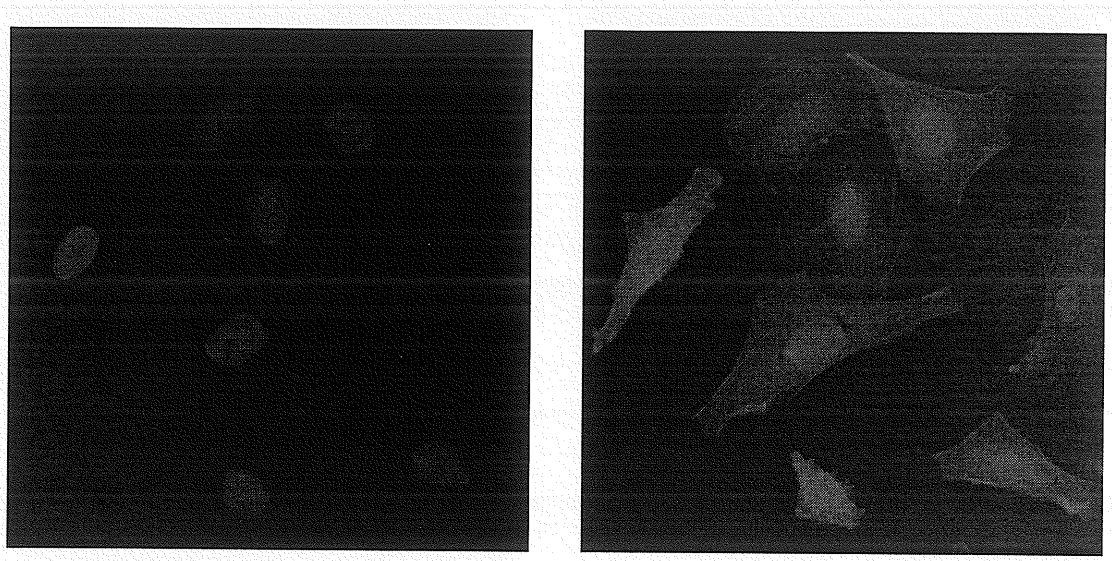

J K

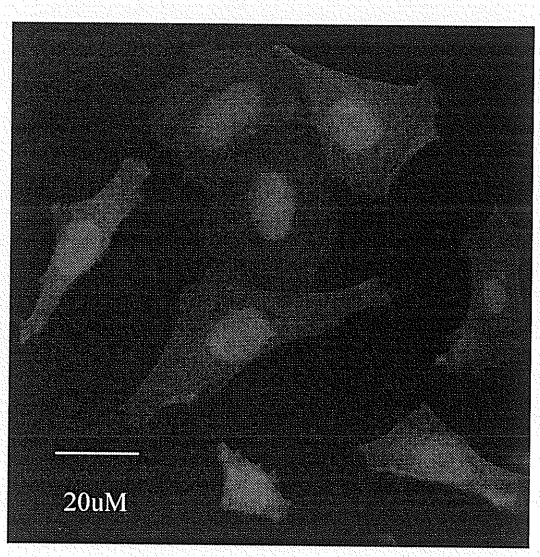

L

Figure 11. Cellular morphologies. Images were taken on a confocal microscope at 40X magnification, 3X zoom, and at a resolution of 1024 X 1024. A. RhoGapMT2 stained with Hoechst. B. RhoGapMT2 stained with phalloidin. C. Overlay of RhoGapMT2 images. D. RSC1 stained with Hoechst. E. RSC1 stained with phalloidin. F. Overlay of RSC1 images. G. RSC6 stained with Hoechst. H. RSC6 stained with phalloidin. I. Overlay of RSC6 images. J. Dlc1 stained with Hoechst. K. Dlc1 stained with phalloidin. L. Overlay of Dlc1 images.

Hoechst staining of the H460 lung carcinoma and Dlc2 cell lines revealed similar nuclei between both cell types, round and uniform. The H460 cells were virtually all clustered and approximately 90% of the cells showed hair-like projections (visible under the microscope). The Dlc2 cells also showed hair-like projections, but appeared to be reduced in size and less clustered. Phalloidin staining showed very concentrated staining of the nuclei of the Dlc2 cells, similar to the Dlc1 cell line. The stress fibres were also not as obvious in the Dlc2 cells as compared to the H460, which again may be due to the heavy fluorescence emanating from the nuclei. A second control was established near the end of this project. This control, H460 non-silencing (H460ns), contains the pSM2c vector with a scrambled, non-silencing shRNAi in H460 cells. While the control was not available early enough to conduct all the experiments with it, the cellular morphology experiments were done. These cells showed virtually no phalloidin staining outside the nucleus, but exhibited the same heavy staining in the nucleus as the Dlc1 and Dlc2 cell lines did (Figure 12).

The cell lines were also stained after being treated with 25 μM of etoposide for 24 hours. The Cl22 cells showed condensed, highly staining nuclei, and several contained multiple nuclei. The treated cells appeared slightly larger than the untreated ones, with blebbing around the outside edges. Approximately 30% of the cells examined showed signs of apoptosis. Treated E91 cells showed little morphological difference from untreated ones (Figure 13).

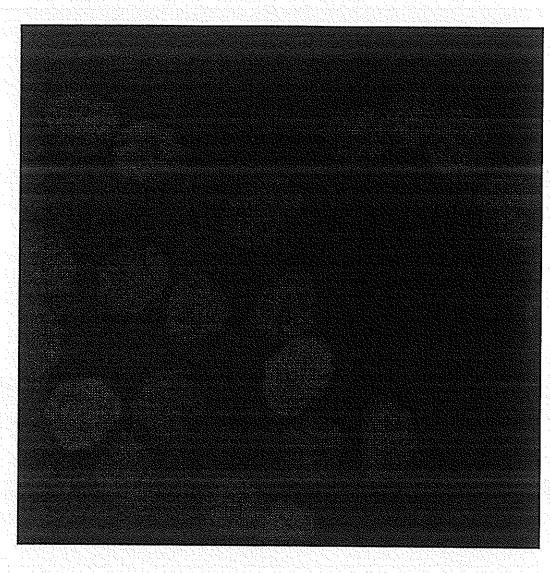

A

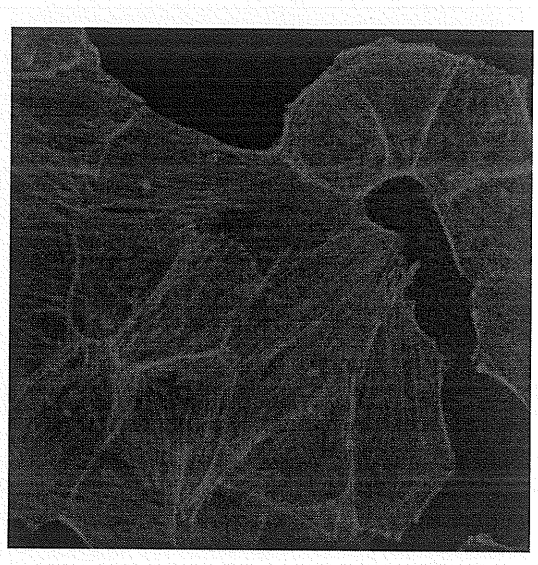

B

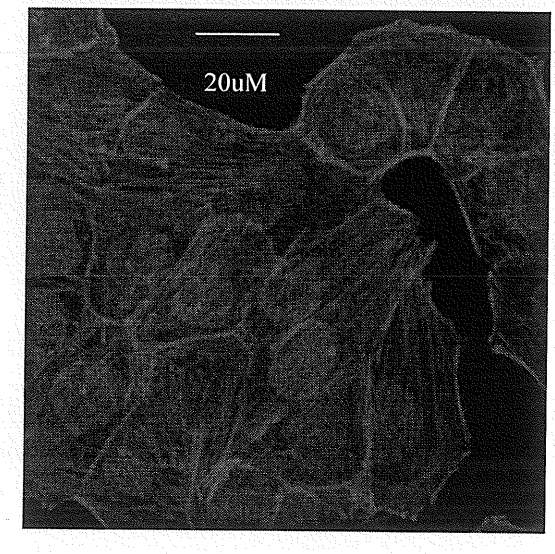

C

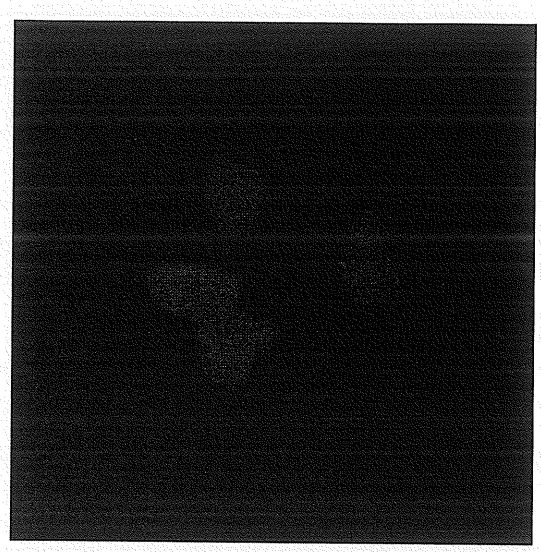

D

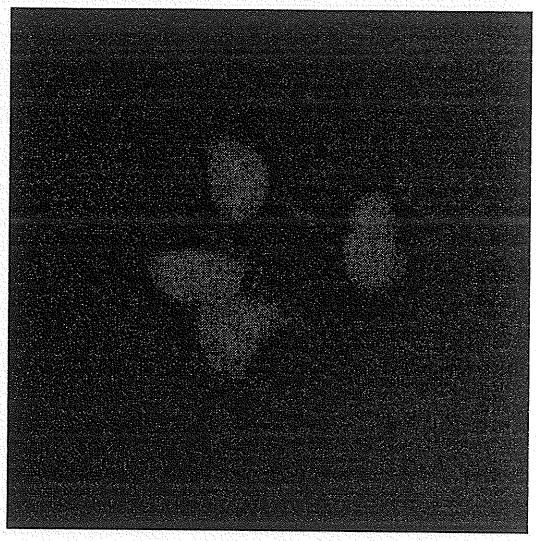

E

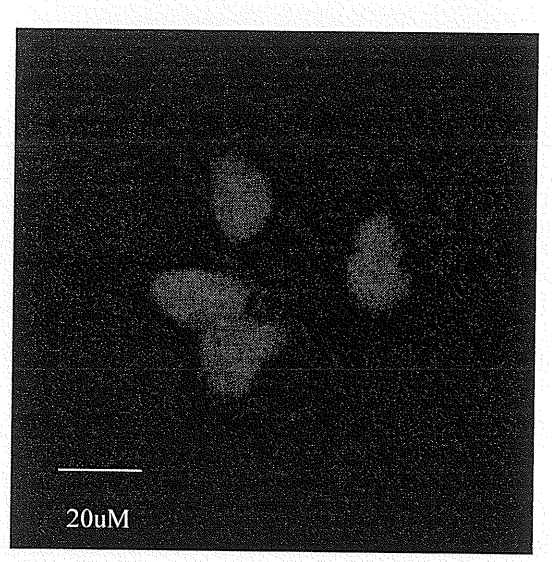

F

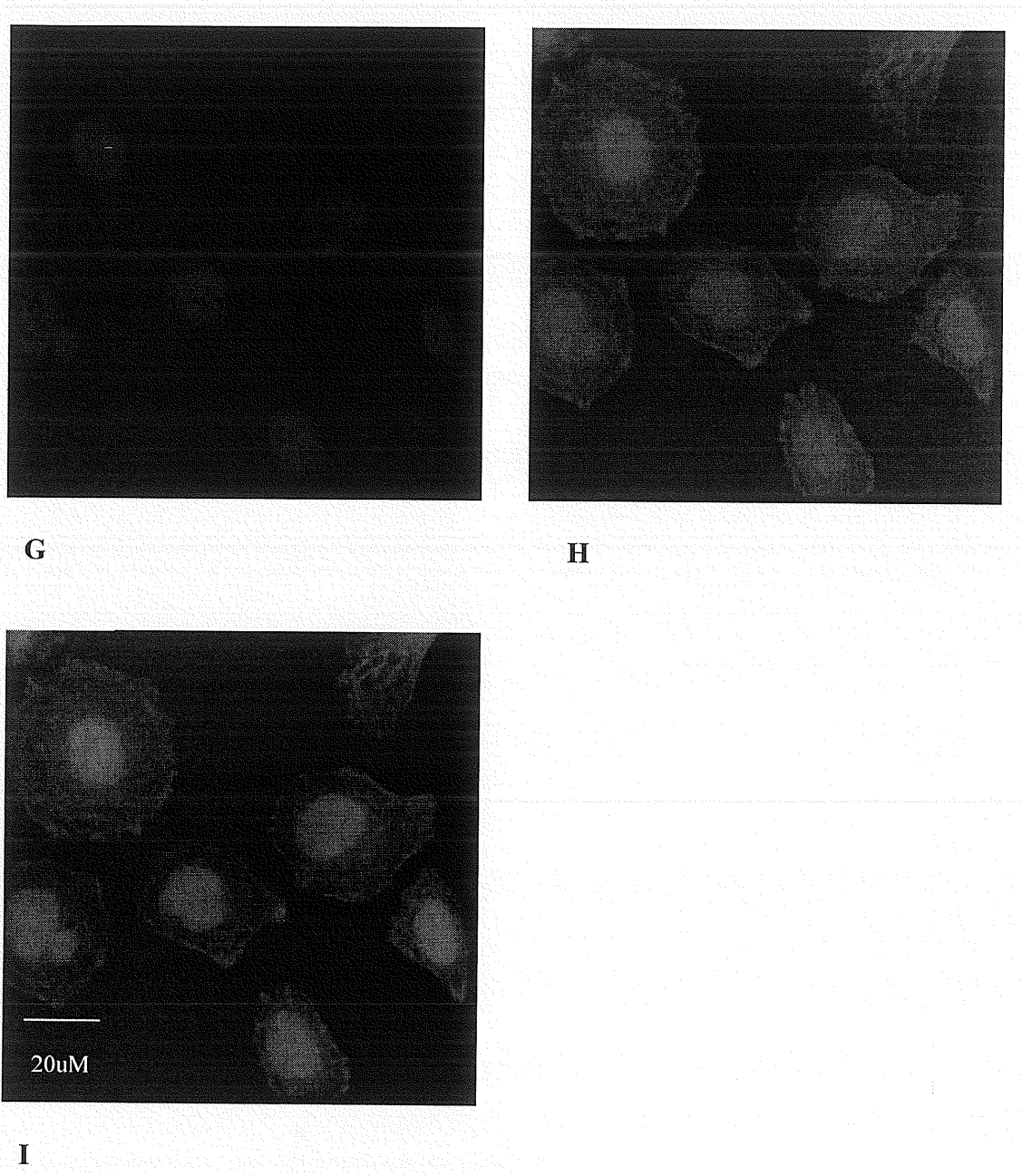

Figure 12. Cellular morphologies. Images were taken on a confocal microscope at 40X magnification, 3X zoom, and at a resolution of 1024 X 1024. A. H460 stained with Hoechst. B. H460 stained with phalloidin. C. Overlay of H460 images. D. H460 with non-silencing siRNA stained with Hoechst. E. H460 with non-silencing siRNA stained with phalloidin. F. Overlay of H460 with non-silencing siRNA images. G. Dlc2 stained with Hoechst. H. Dlc2 stained with phalloidin. I. Overlay of Dlc2 images.

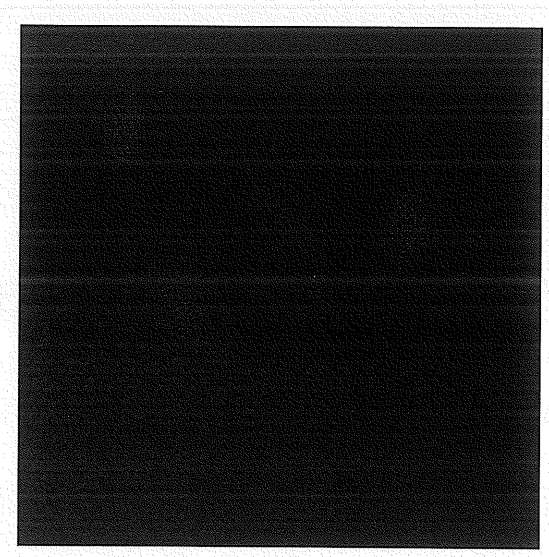

A

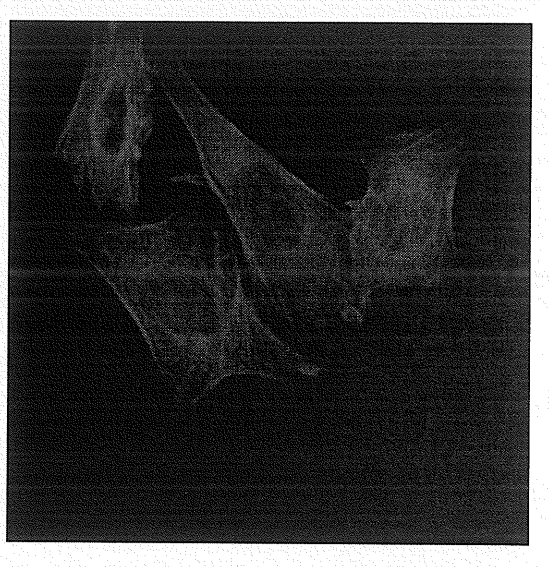

B

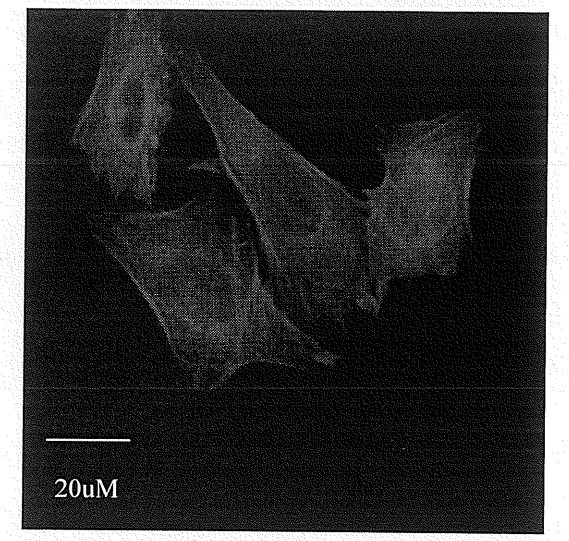

C

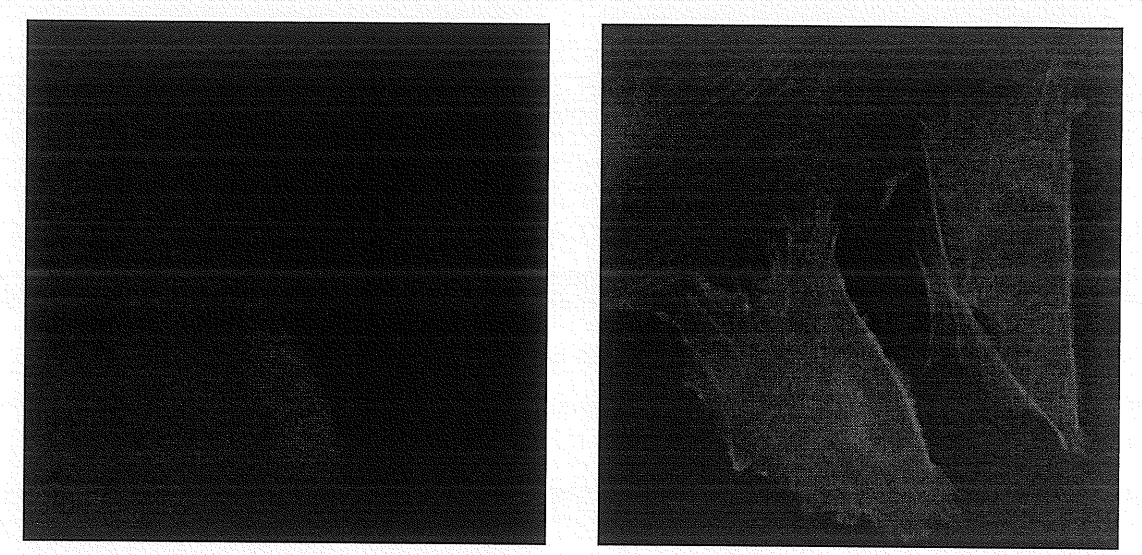

D

E

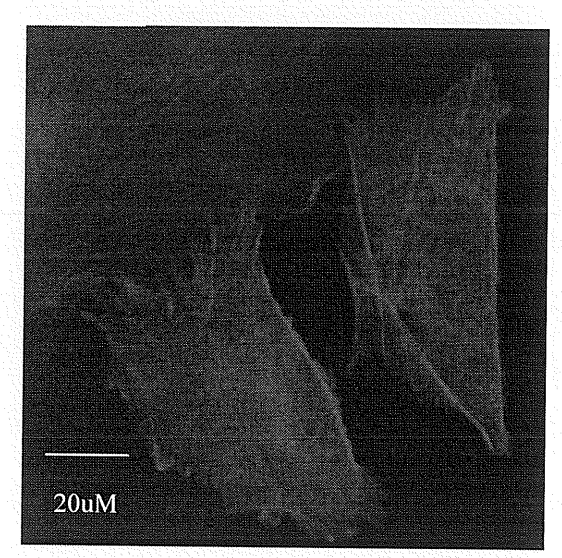

F

Figure 13. Cellular morphologies. Cells were treated with 25 μM etoposide for 24 hours. Images were taken on a confocal microscope at 40X magnification, 3X zoom, and at a resolution of 1024 X 1024. A. Cl22 stained with Hoechst. B. Cl22 stained with phalloidin. C. Overlay of Cl22 images. D. E91 stained with Hoechst. E. E91 stained with phalloidin. F. Overlay of E91 images.

RhoGapMT2 cells after treatment appeared more rounded and enlarged with nuclear condensation in approximately 40% of cells observed. The stress fibres were not as visible, and actin staining appeared less organized with blebbing on the outer edges of about 50% of the cells. The RSC1 and RSC6 cells were also more rounded and less uniform in shape, and did not appear to be as aggregated as the untreated cells. Otherwise there was little change in the appearance of these cells, and few were apoptotic. The Dlc1 cells appeared to have a reduction in phalloidin staining of the nucleus in about 95% of cells when treated with etoposide, and correspondingly these cells showed an increase in stress fibre staining (Figure 14).

The H460 cells, while they did not show an overall increase in size, did appear to have enlarged nuclei as shown by the Hoechst staining. The hair-like projections were no longer visible, and cells were much less clustered after treatment. Likewise, the Dlc2 cells did not show an overall size difference, but the phalloidin staining was more concentrated on the outer edges of the cells after treatment and they also exhibited loss of the hair-like protrusions. The H460ns and Dlc2 cells no longer showed the phalloidin staining of the nucleus after being treated with etoposide, but did have punctuate staining around the cell periphery. The H460ns cells appeared to be much smaller than either the H460 or Dlc2 cells (Figure 15).

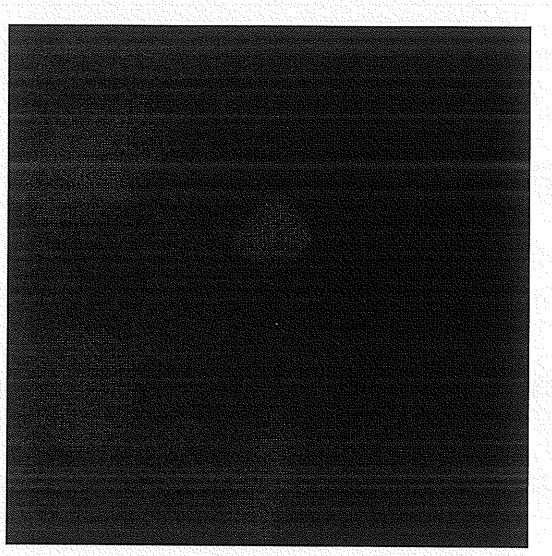

A

B

C

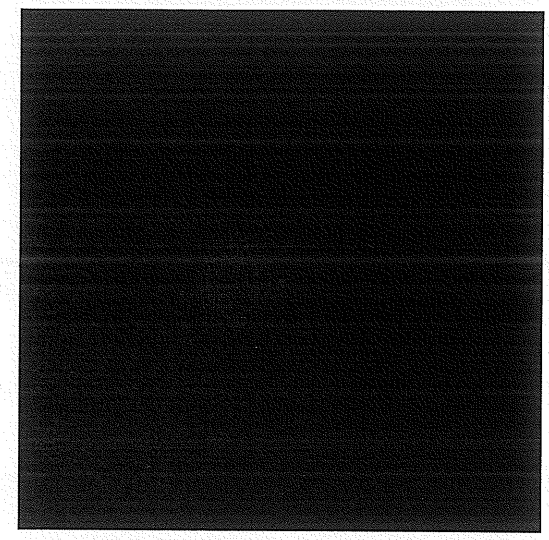

D

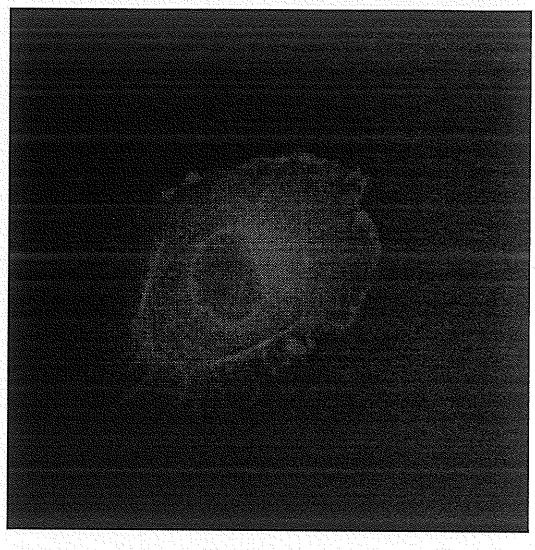

E

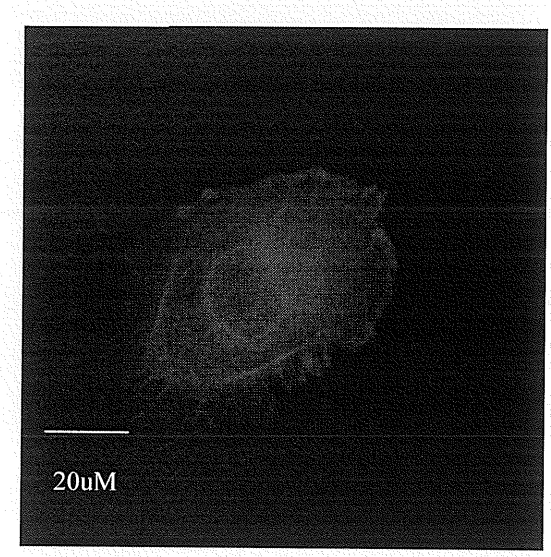

F

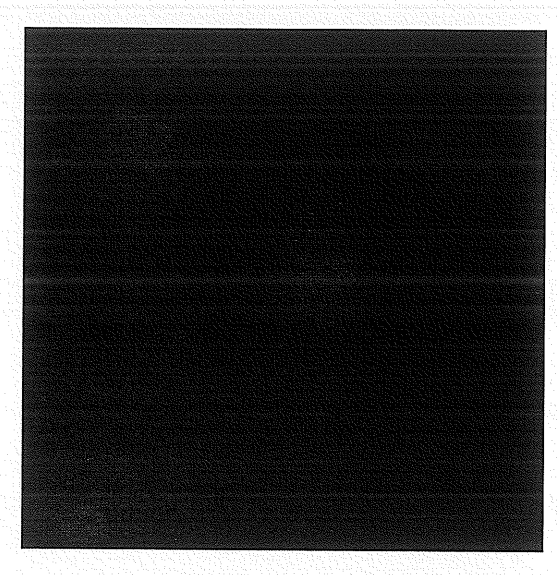

G

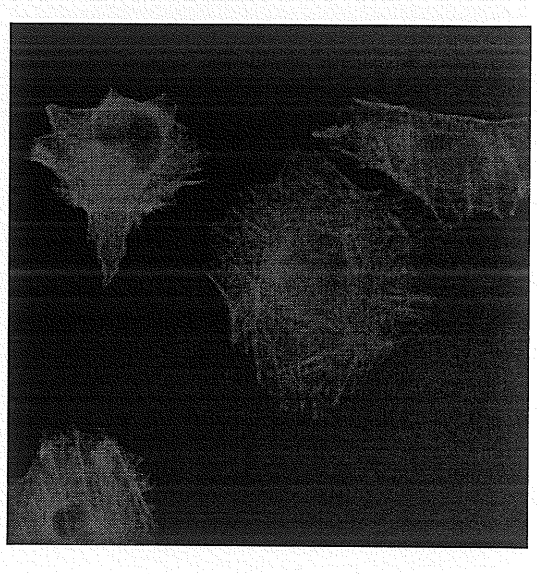

H

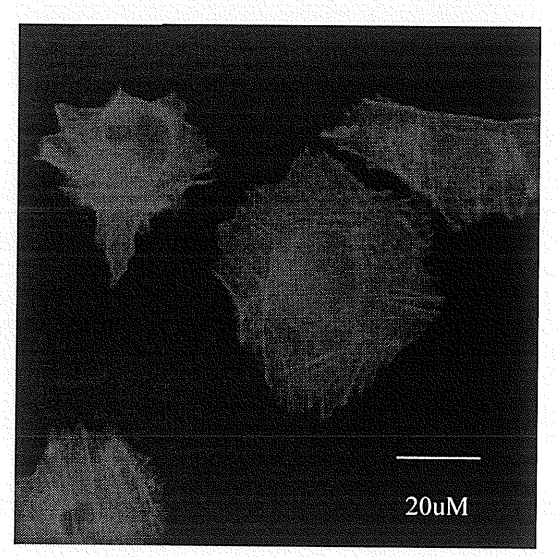

I

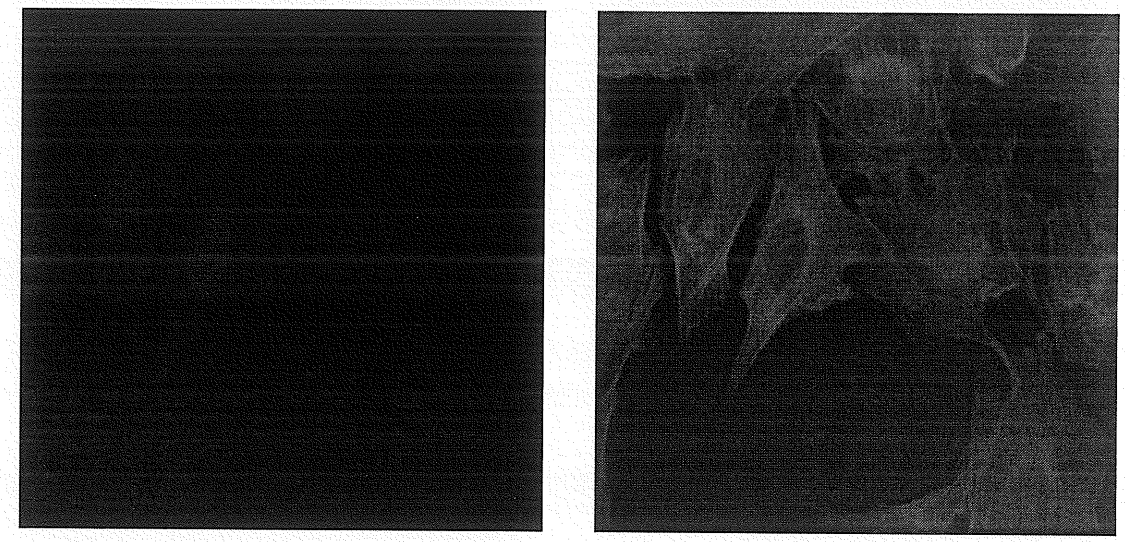

J

K

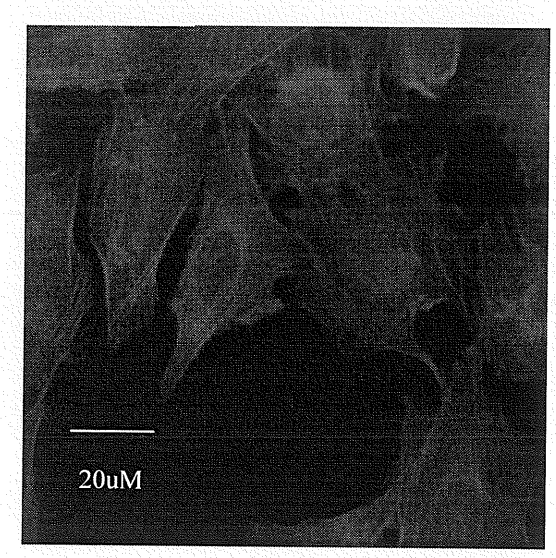

L

Figure 14. Cellular morphologies. Cells were treated with 25 μM etoposide for 24 hours. Images were taken on a confocal microscope at 40X magnification, 3X zoom, and at a resolution of 1024 X 1024. A. RhoGapMT2 stained with Hoechst. B. RhoGapMT2 stained with phalloidin. C. Overlay of RhoGapMT2 images. D. RSC1 stained with Hoechst. E. RSC1 stained with phalloidin. F. Overlay of RSC1 images. G. RSC6 stained with Hoechst. H. RSC6 stained with phalloidin. I. Overlay of RSC6 images. J. Dlc1 stained with Hoechst. K. Dlc1 stained with phalloidin. L. Overlay of Dlc1 images.

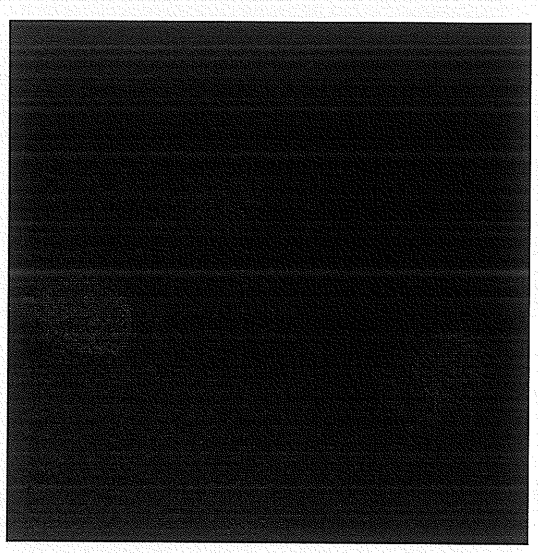

A

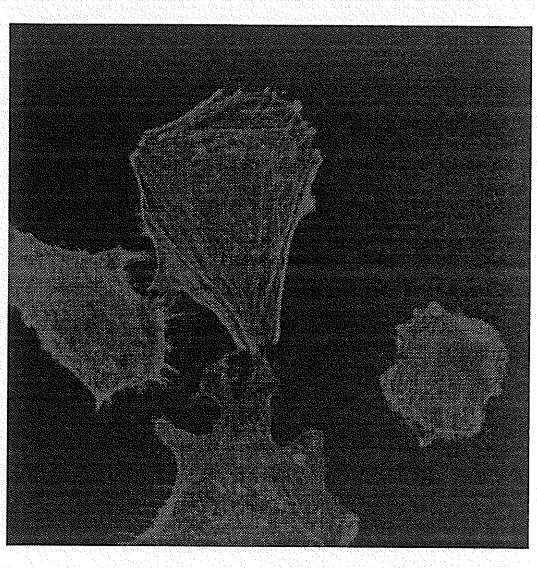

B

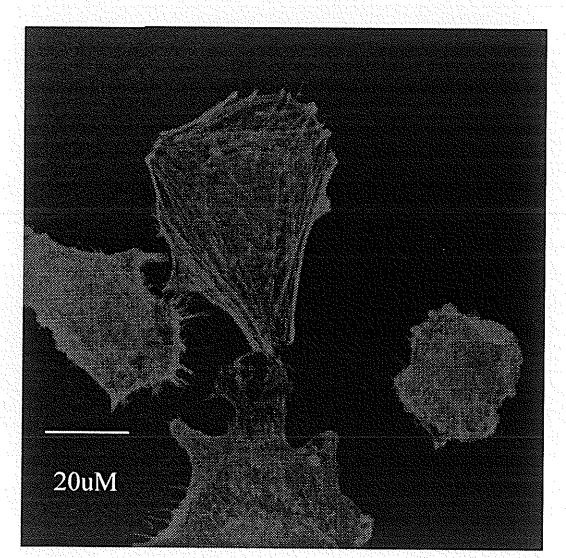

C

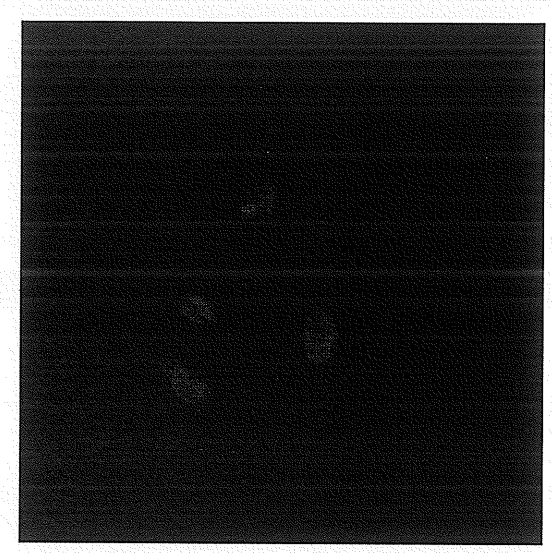

D

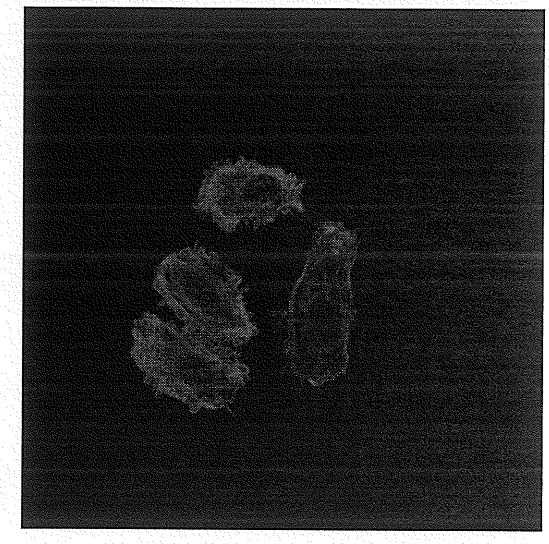

E

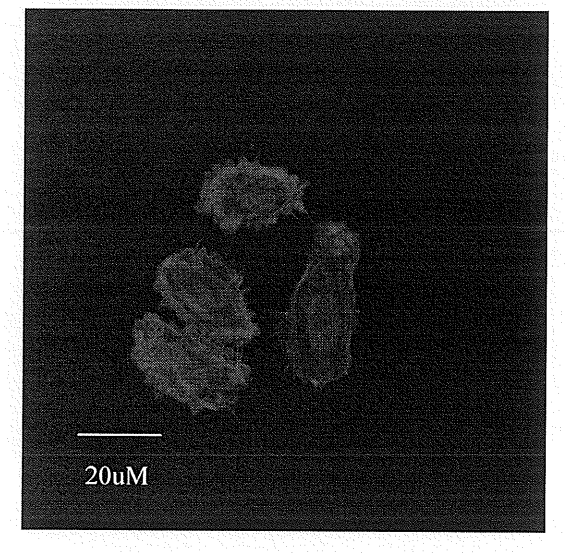

F

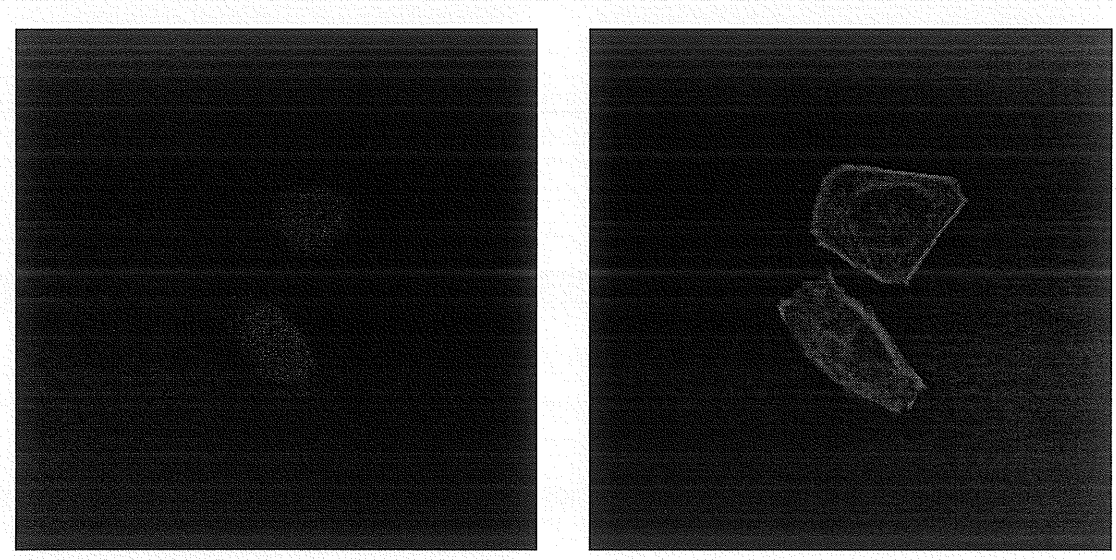

G

H

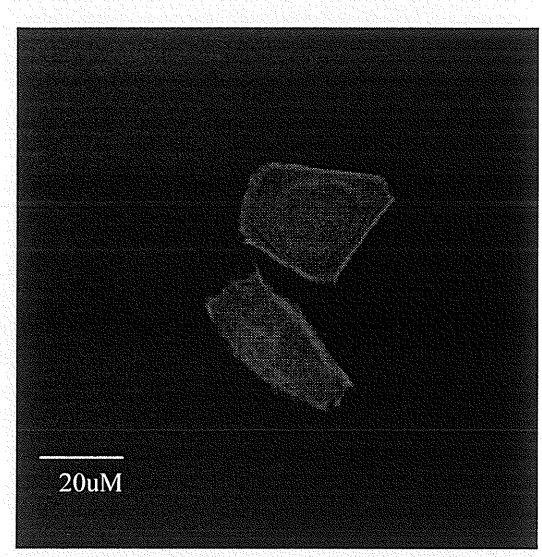

I

Figure 15. Cellular morphologies. Cells were treated with 25 μM etoposide for 24 hours. Images were taken on a confocal microscope at 40X magnification, 3X zoom, and at a resolution of 1024 X 1024. A. H460 stained with Hoechst. B. H460 stained with phalloidin. C. Overlay of H460 images. D. H460 with non-silencing siRNA stained with Hoechst. E. H460 with non-silencing siRNA stained with phalloidin. F. Overlay of H460 with non-silencing siRNA images. G. Dlc2 stained with Hoechst. H. Dlc2 stained with phalloidin. I. Overlay of Dlc2 images.

3.3 Results of Cell Survival Analyses

3.3.1 Results of Crystal Violet Colony Assays

We wanted to determine whether loss of *Dlc-1* or *Dlc-2* function would have an effect on cell survival after etoposide treatment. To investigate this, crystal violet colony assays were conducted. These assays showed an increase in cell survival in the E91 cell line as compared to the parental CHO Cl22 cell line. As expected, there were no significant differences between the controls, which were treated with DMSO only. E91 cells treated with 50 nM and 100 nM concentrations showed a statistically significant difference compared to Cl22 cells (p-value < 0.0001 as determined by the least squares method), while cells treated with 500 nM of etoposide showed a significant difference (p-value $<$ 0.01). At 1.0 μM, although the E91 cells did show more survival than Cl22, the difference did not reach statistical significance (Figure 16A).

When the RNAi control cell line, RhoGapMT2, was compared to the RSC1, RSC6, Dlc1 and Dlc2 cell lines (the Dlc2 cells used in these experiments were CHO cells and not H460) after treatment with etoposide, again the DMSO controls showed no significant differences. The RSC6 cell line showed significance at p-value < 0.001 for the 50 nM treatment, and < 0.0001 for the 100 nM treatment. Similarly, the Dlc1 cell line showed resistance at these treatment levels. For both concentrations the p-value for this cell line was < 0.005. Neither cell line showed appreciable differences in survival at the 500 nM or 1.0 μM treatment level. No significant differences were seen upon comparing the RhoGapMT2 control with the RSC1 or Dlc2 cell lines (Figure 16B).

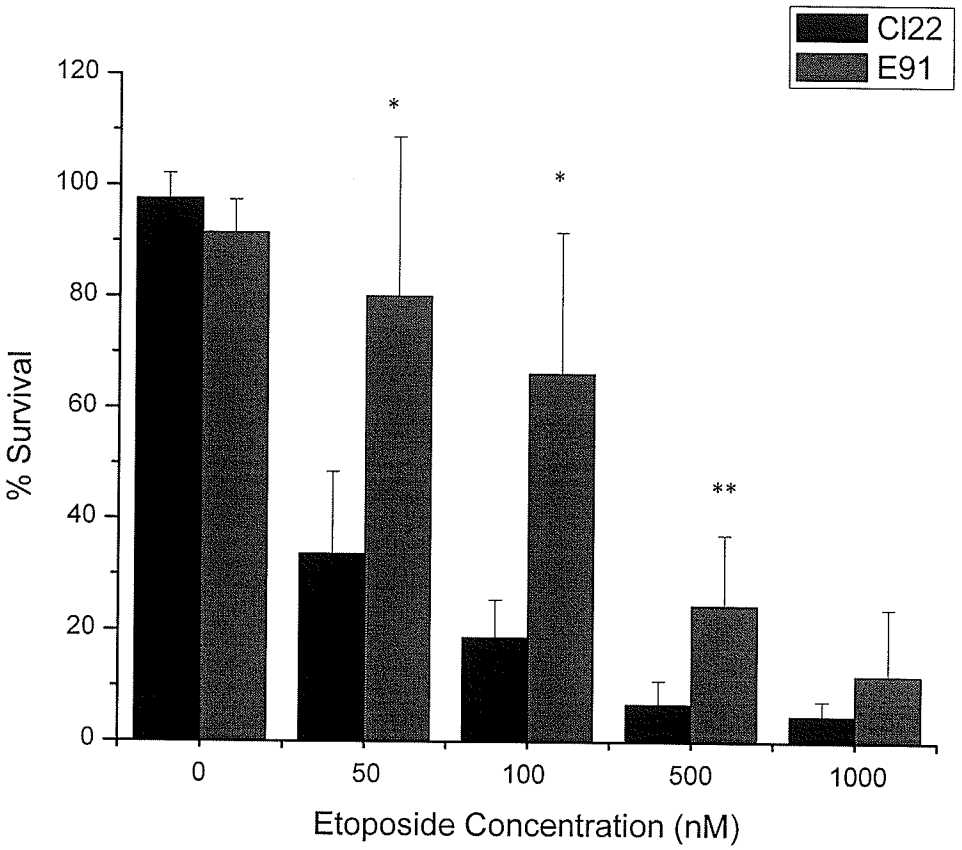
Cl22
E91
120
100
80
60
40
20
0
% Survival
*
*
**
0
50
100
500
1000
Etoposide Concentration (nM)

A

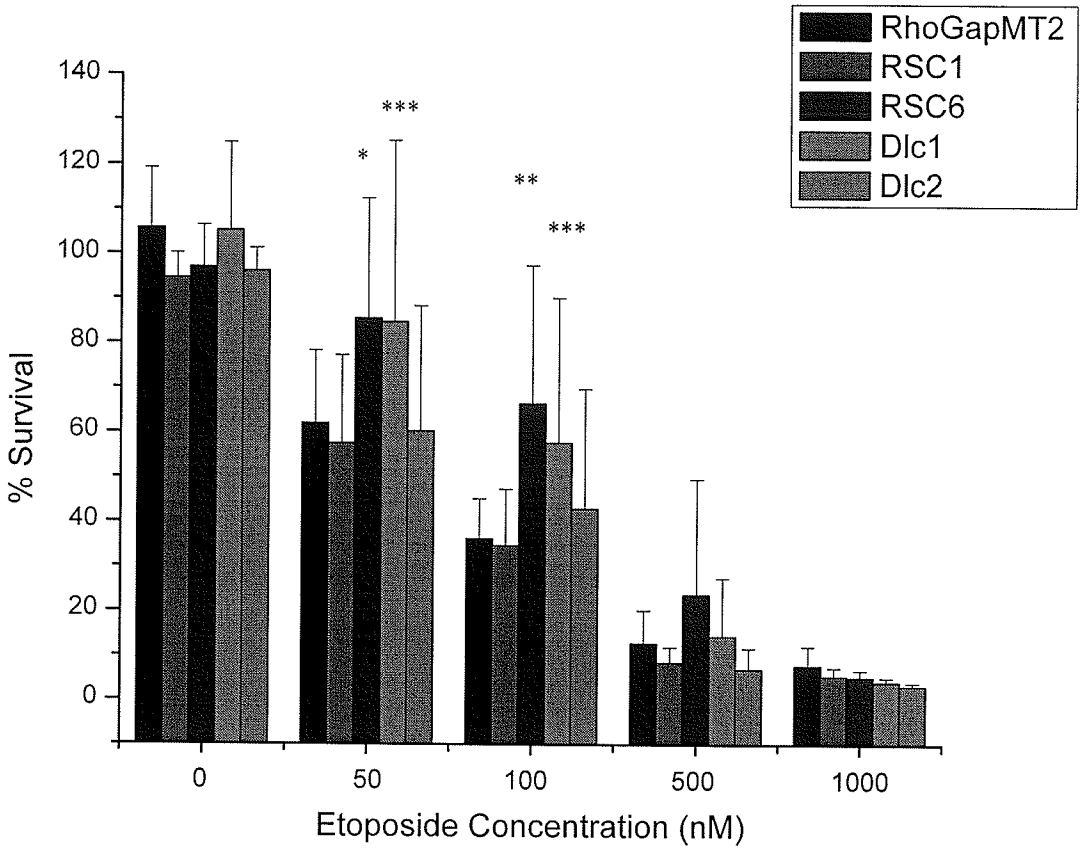

B

Figure 16. Graphs of crystal violet colony assay results. A. Cl22 vs. E91. * p-value < 0.0001, ** p-value < 0.01. B. RhoGapMT2 vs. RSC1, RSC6, Dlc1 and Dlc2. * p-value < 0.001, ** p-value < 0.0001, *** p-value < 0.005. Error bars represent standard error, n = 5.

3.3.2 Results of MTT Assays

We next wanted to determine the viability of cells after etoposide treatment. This was done using the MTT assay which measures the ability of mitochondrial dehydrogenase enzymes in live cells to reduce the yellow MTT to a purple formazan. Comparison of the Cl22 and E91 cell lines by MTT assay, normalized to the DMSO vehicle alone, showed statistically significant differences at all concentrations of etoposide used. At treatment levels of 0.5 μM, 1.0 μM and 5.0 μM the p-value was < 0.0001 using the least squares method. As the drug concentration increased beyond this point, the level of significance decreased. For treatment with both 10 μM and 25 μM, the p-value was 0.05, however at 25 μM concentration the significance was borderline. The Bonferroni correction provides a stricter p-value and is used when multiple tests of statistical significance are conducted on the same data, where 1 in 20 hypothesis-tests will appear significant at $p = .05$ due to chance alone. If the Bonferroni correction is applied to this data, the p-value to determine significance becomes 0.01 and only the 0.5 μM, 1.0 μM and 5.0 μM treatment levels remain statistically significant (Figure 17A). This assay did not show any statistically significant differences for any of the other cell lines studied (Figure 17B and 17C).

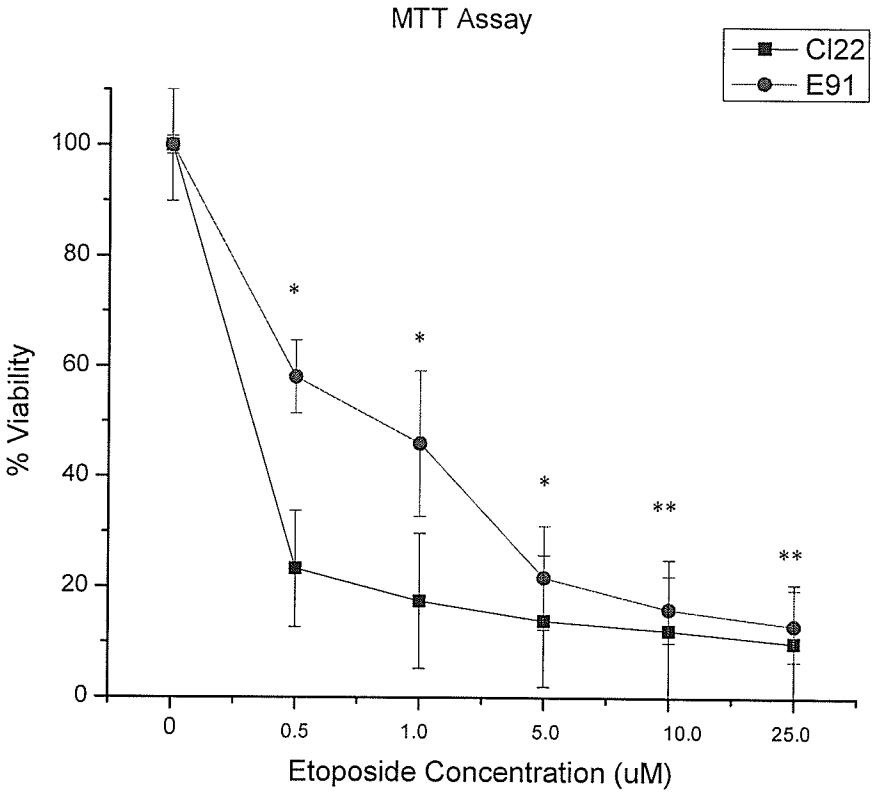
MTT Assay
Cl22
E91
% Viability
100
80
60
40
20
0
*
*
*
**
**
0
0.5
1.0
5.0
10.0
25.0
Etoposide Concentration (uM)

A

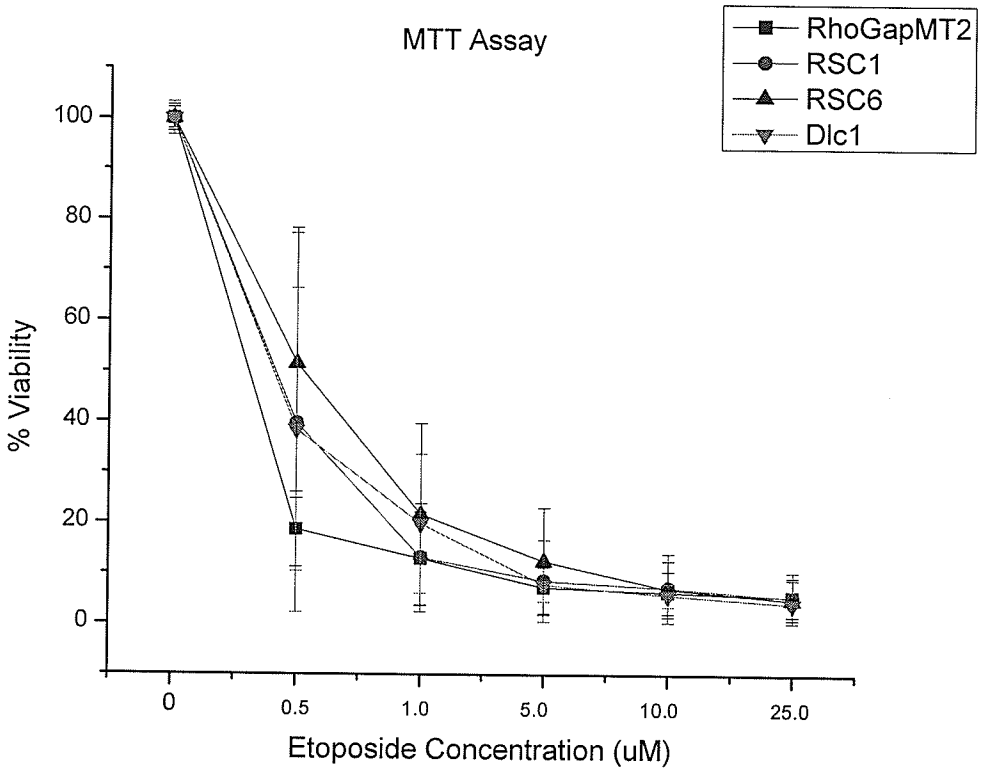
MTT Assay
RhoGapMT2
RSC1
RSC6
Dlc1
% Viability
100
80
60
40
20
0
0
0.5
1.0
5.0
10.0
25.0
Etoposide Concentration (uM)

B

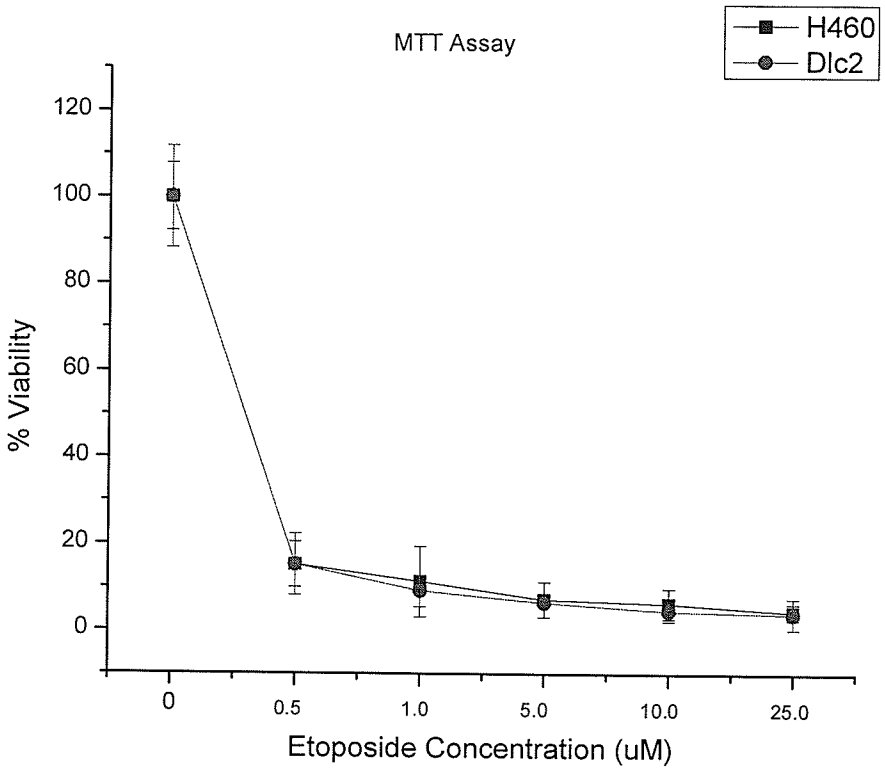

C

Figure 17. Graphs of MTT assay results. A. Cl22 vs. E91. * p-value < 0.0001, ** p-value < 0.05. B. RhoGapMT2 vs. RSC1, RSC6 and Dlc1. No significant differences. C. H460 vs. Dlc2. No significant differences. Error bars represent standard error, n = 5.

3.4 Results of Apoptosis Analyses

3.4.1 Results of Flow Cytometry Analysis

In addition, we wanted to determine if there were any differences in the rates of apoptosis induction in the cell lines. Analysis of the Cl22 and E91 cell lines by FACS showed a significant difference in the levels of apoptosis only at the 96 hour time point for the higher drug concentrations. At the 5.0 μM treatment level, the difference was significant at p-value < 0.0001, while at 25 μM, the p-value was < 0.005 (Figure 18A). No statistically significant differences were observed for any of the other cell lines studied (Figure 18B and Figure 18C).

3.5 Expression of *Dlc-1* in Tissues of Knock Out Mouse

To investigate expression patterns of the *Dlc-1* gene, and what, if any, effects a homozygous deletion would have on embryonic development, whole embryos were dissected and stained at embryonic days 9.5 and 10.5. The E9.5 heterozygous embryo showed high expression in vessels, particularly those in the inter-somite regions. The E9.5 homozygous null embryo showed a definite phenotype, there was evidence of defects in vasculature, the neural tube and the heart (Figure 19). The E10.5 homozygous null embryo also exhibited heart and vasculature defects, as well as growth retardation compared to its heterozygous counterpart (Figure 20). X-gal staining of whole embryo sections at day 10.5 showed ubiquitous expression of the *Dlc-1* gene. Heterozygous embryos showed particularly heavy staining in the notochord and heart (Figure 21 and Figure 22).

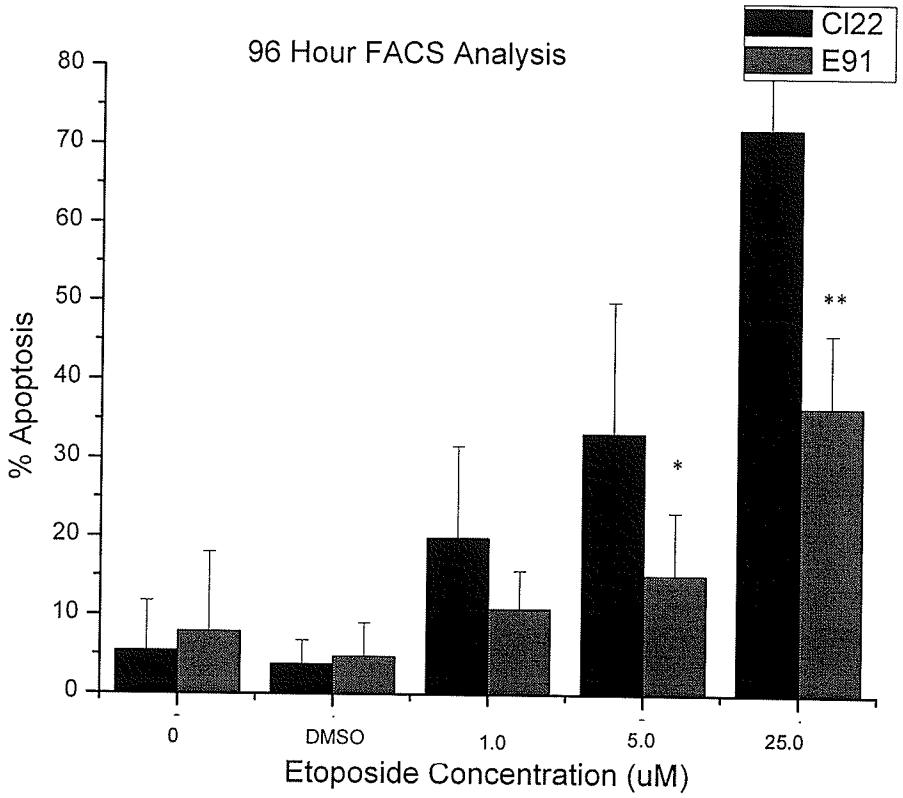
96 Hour FACS Analysis
CI22
E91
% Apoptosis
80
70
60
50
40
30
20
10
0
*
**
0
DMSO
1.0
5.0
25.0
Etoposide Concentration (uM)

A

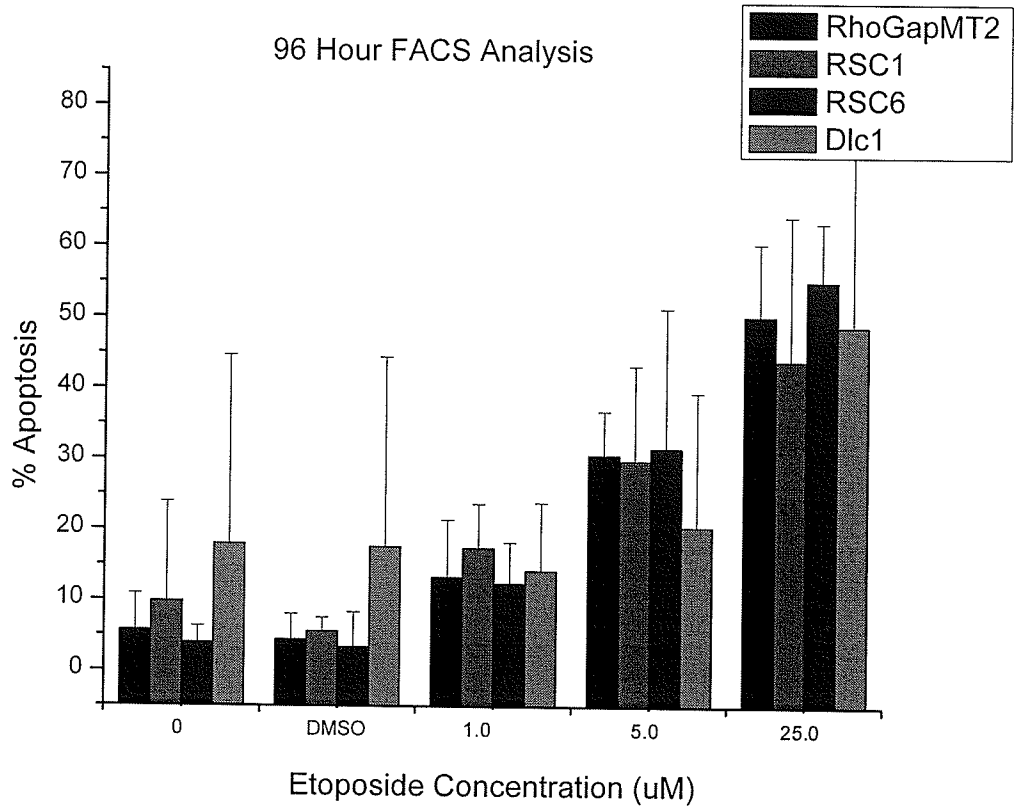
96 Hour FACS Analysis
RhoGapMT2
RSC1
RSC6
Dlc1
% Apoptosis
80
70
60
50
40
30
20
10
0
0
DMSO
1.0
5.0
25.0
Etoposide Concentration (uM)

B

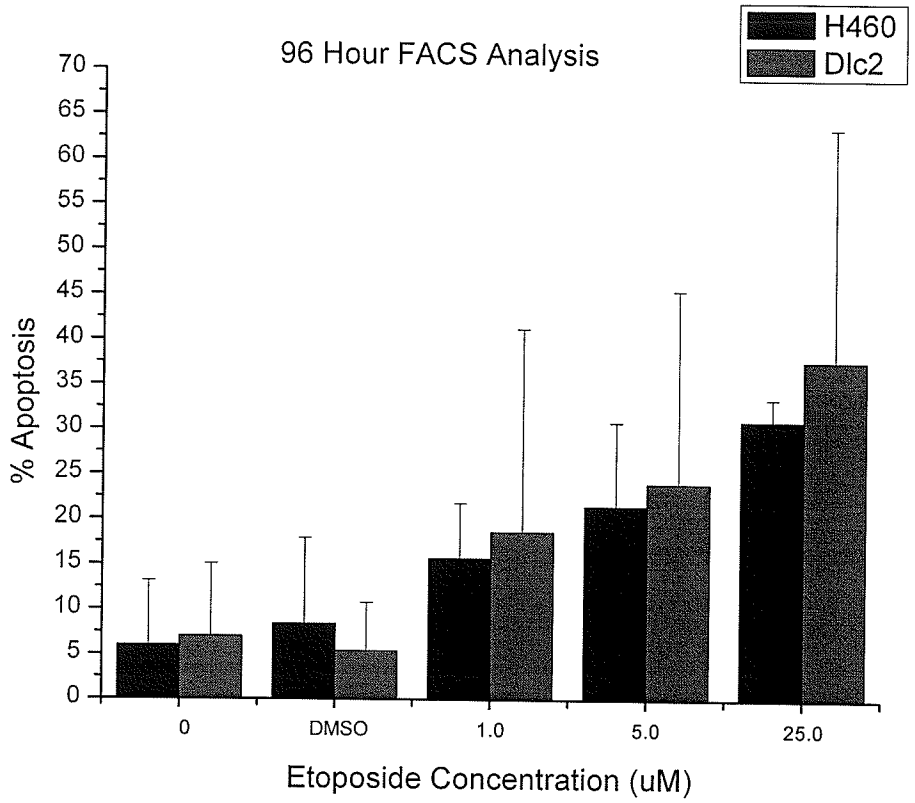

C

Figure 18: Results of 96 hour FACS analysis. A. Cl22 vs. E91. * p-value < 0.0001, ** p-value < 0.005. B. RhoGapMT2 vs. RSC1, RSC6 and Dlc1. No significant differences. C. H460 vs. Dlc2. No significant differences. Error bars represent standard error, n = 5.

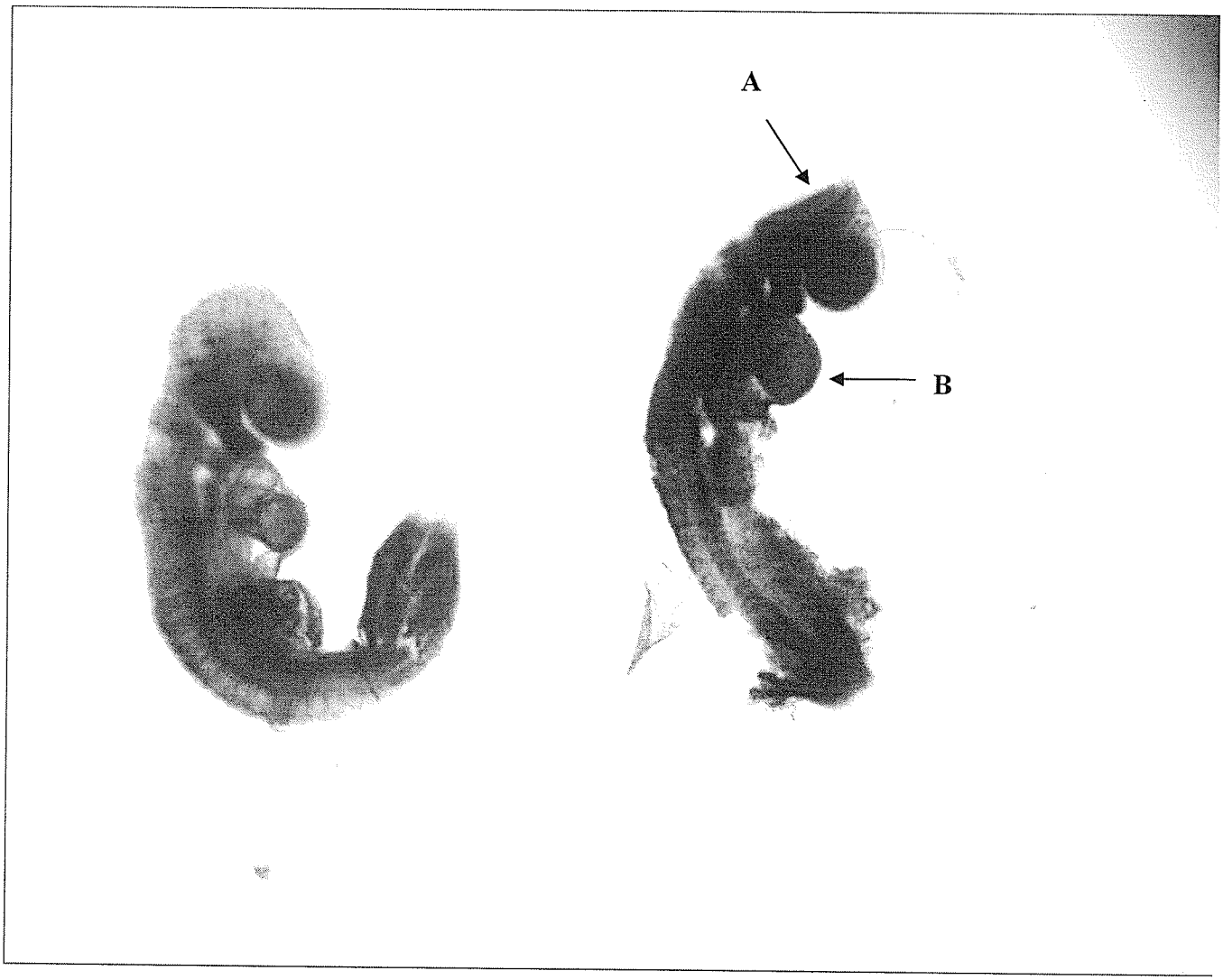

Figure 19. X-gal staining of *Dlc-1* homozygous null and heterozygous embryos at embryonic day 9.5. The null embryo shows defects in vasculature, A. neural tube defects and B. an enlarged heart.

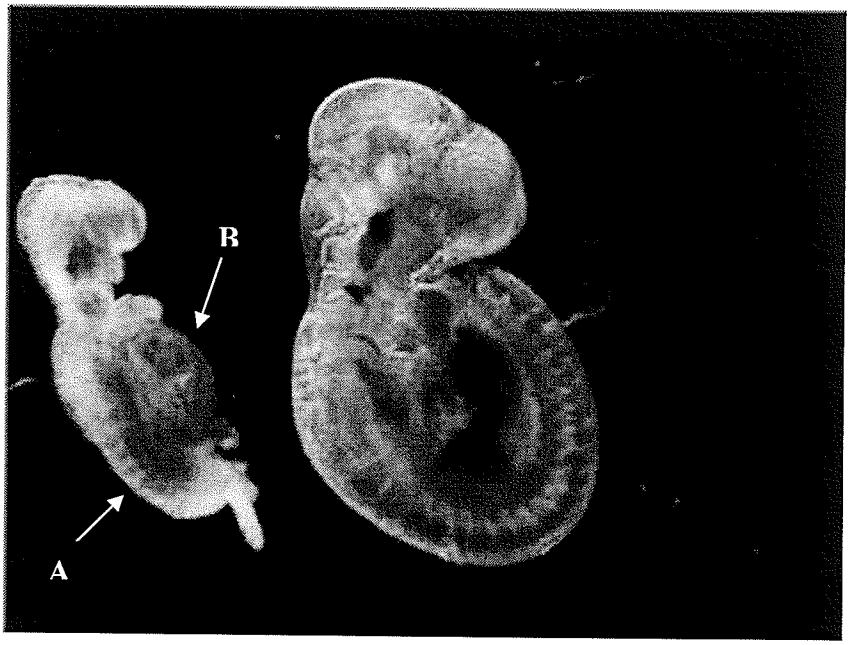

Figure 20. X-gal staining of *Dlc-1* homozygous null and heterozygous embryos at embryonic day 10.5. The null embryo (right) shows growth retardation, A. reduction in somite formation with decreased staining of the vasculature and B. an enlarged heart.

Figure 21. X-gal stained section of heterozygous E10.5, 2.5X magnification. The embryo shows particularly heavy staining in the regions of A. the head, B. the notochord and C. the heart.

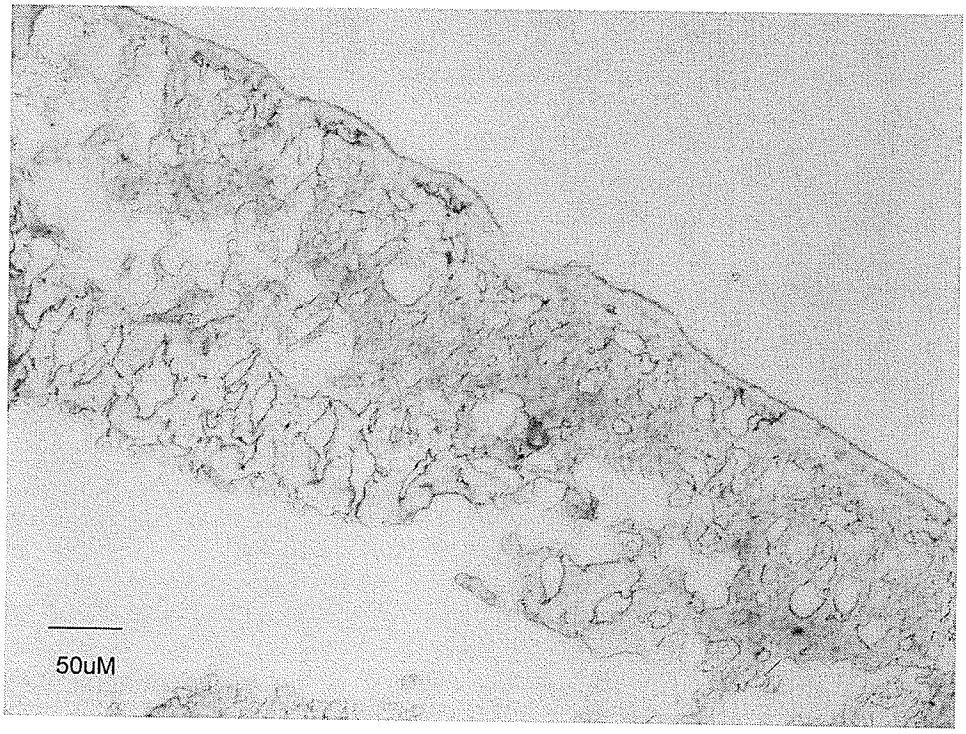

A

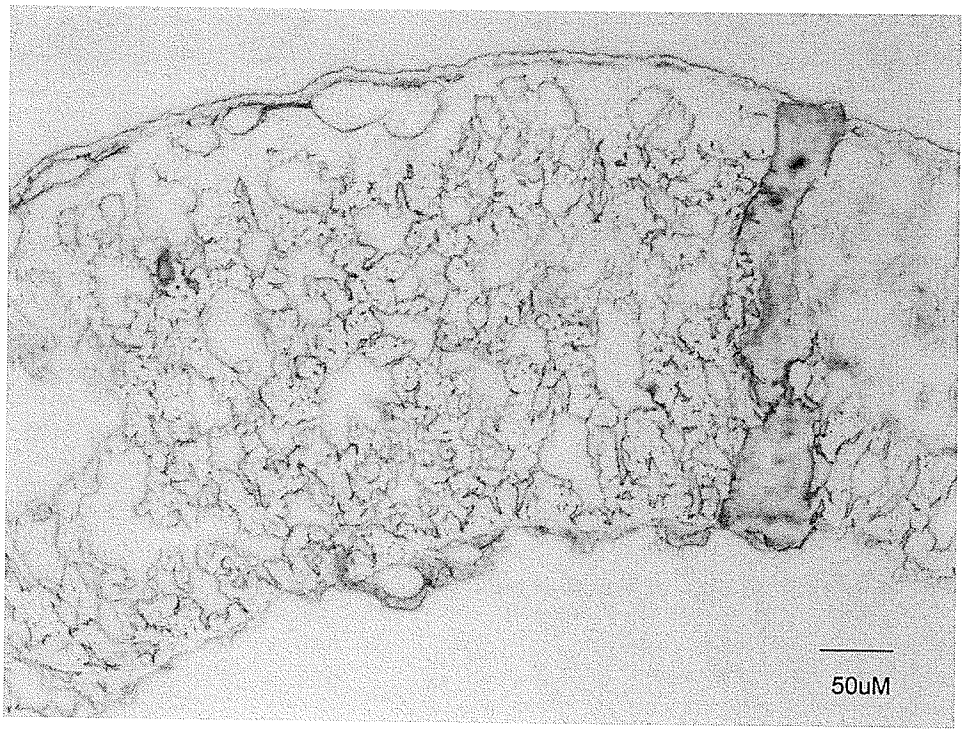

B

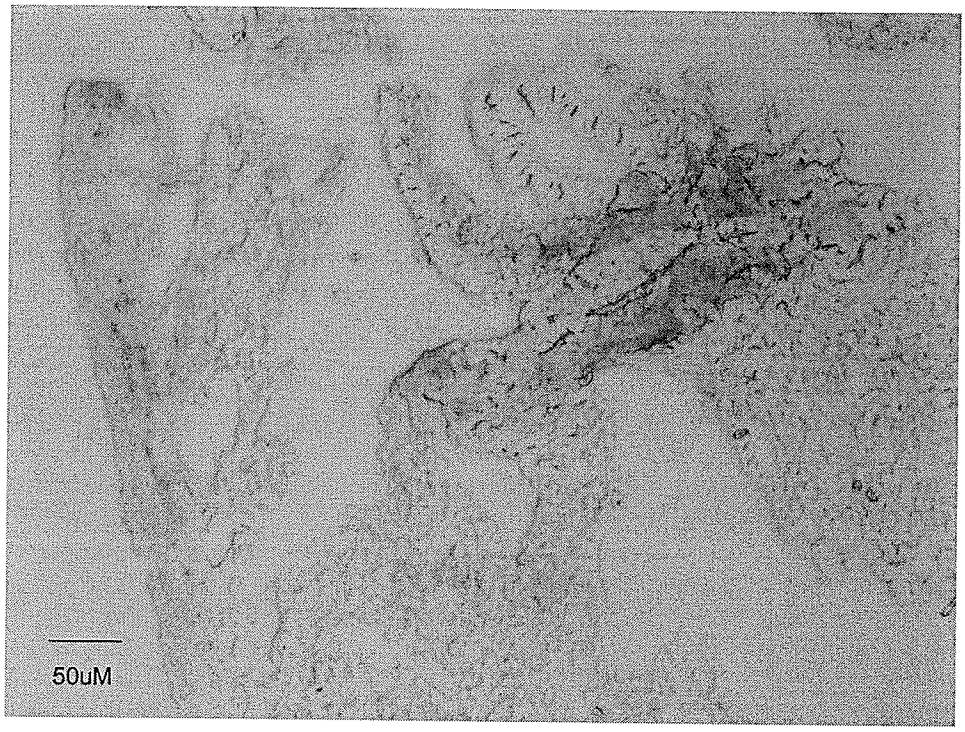

C

Figure 22. X-gal stained sections of heterozygous E10.5 taken at 20X magnification. The embryo shows particularly heavy staining in the regions of A. the head, B. the notochord and C. the heart.

CHAPTER 4 - DISCUSSION

4.1 Introduction

The hypotheses of this project were that down regulation of the *Dlc-1* and *Dlc-2* genes would correlate with an increase in resistance to etoposide induced cell killing and apoptosis, and that knocking down the RhoGAP function of these genes would promote tumorigenesis.

Rho proteins are known to have many important effects on cellular processes; among these are their effects on stress fibre formation, cellular adhesion and cell cycle progression. Active Rho proteins interact with effectors in order to initiate a response. Some of the known effectors of Rho include PI3 kinase, ROCK kinases, lipid kinases, lipases, oxidases and scaffold proteins (Jaffe and Hall, 2002; Moon and Zheng, 2003; Boettner and van Aelst, 2002). The RhoGAP domain of *Dlc-1* and *Dlc-2* enables these tumor suppressor genes to function as regulators of Rho proteins. Disruption of this domain in several cell lines has allowed us to study the consequences of increased Rho activity in cells.

4.2 Observations from Studies of Cell Lines

There are definite morphological changes in the CHO cell lines that contain a disruption of either the *Dlc-1* or *Dlc-2* transcript that would be expected from increased Rho activity

in these cells. These differences in morphology appear to different degrees in different cell lines, and are likely related to the degree of knock down of the affected transcript. For instance, the E91 cells show the lowest expression of *Dlc-2* due to retroviral vector insertion and low expression of the other allele. These cells exhibit a dramatic increase in stress fibre formation as well as being significantly enlarged. They also show an angular, flattened morphology. Similarly, the RSC6 cells show more dramatic stress fibre formation than the RSC1 cells, and correspondingly, the RSC6 cells show a better knockdown of the *Dlc-2* transcript than the RSC1 cells do (see Figure 6). This is not surprising considering the fact that Rho proteins are associated with the formation of actin-myosin filaments, thus an increase in active Rho in cells deficient for RhoGAP would be expected to show enhanced formation of stress fibres. Many of the cells also appear to be multinucleate and may therefore have defects in cytokinesis, which is again not surprising given that Rho proteins play a role in cell division (Glotzer, 2001; Huckaba and Pon, 2002; Villalonga and Ridley, 2006).

One interesting observation was that the Dlc1 and Dlc2 cell lines show heavy actin staining in the nucleus. This appears to be due to the presence of the vector and not the effects of the shRNAi, since the H460 non-silencing control (H460ns), which contains the pSM2c vector with a scrambled shRNAi, also shows this phenomenon. Interestingly, after etoposide treatment this was no longer the case and cell types containing this vector showed the majority of actin staining around the periphery. Because this was observed in the control cells as well as cells containing shRNAi, we decided to examine the vector itself more closely to determine if there were any differences between pSM2c and other

vectors we were using that may be causing this phenomenon. Further investigation of the pSM2c vector revealed the presence of firefly luciferase DNA sequences in the vector backbone, generating a luciferase-neo fusion protein, a feature that was not included on the vector map. Initially, it was thought this may explain the unexpected fluorescence, however a literature search did not reveal any precedence for autofluorescence of these sequences, and because there is no substrate for luciferase in our cells, it is unlikely that this is affecting fluorescence. It is worth noting that in 2006, Goley *et al.* identified the polymerization of nuclear actin as a requirement for viral replication by the baculovirus *Autographa californica* multiple nucleopolyhedrovirus (AcMNPV). In addition, another group found that actin filaments were formed in the nuclei of epithelial cells infected with pseudorabies virus (PRV), and that neurons infected with either PRV or herpes simplex virus type I also exhibited this characteristic (Feierbach *et al.*, 2006). Therefore, the presence of actin in the nucleus is not unique. It is possible that the hairpin microRNA is knocking down proteins that affect actin polymerization, or that some type of off-target effect is playing a role. This however is speculation at this point, and further investigation is required.

My experimental results showed dramatic changes to the actin cytoskeleton in cells with a disruption of *Dlc-1* gene activity. The Dlc-1 protein has been found to localize to caveolae (Ullmannova and Popescu, 2006; Yam *et al.* 2006). These invaginations in the plasma membrane are rich in proteins and lipids, including sphingolipids, and have been shown to function in signal transduction (Anderson, 1998). Yam *et al.* identified a caveolin-1 binding motif on both the Dlc-1 and tensin2 proteins, and showed that the

Dlc1-tensin2 complex causes cytoskeletal rearrangements via interaction with RhoGTPases. Interestingly, tensin2 is highly expressed in liver, and perhaps functions to target *Dlc-1* to the caveolae where its RhoGAP domain can exert its regulatory effects on Rho proteins (Yam *et al.*, 2006). In addition, a study by Liao *et al.* identified the tensin family member C-terminal tensin like (cten) as a binding partner for *Dlc-1*. The interaction occurs through the SH2 binding domain of cten, which binds to a critical tyrosine residue on *Dlc-1*. When the cten-Dlc-1 interaction is disrupted, it results in aberrant localization of the Dlc-1 protein and a corresponding loss of its tumor suppressor activity. This further supports the hypothesis that disruption of this domain and the subsequent increase in Rho expression plays a role in tumorigenesis. The fact that effector proteins of RhoGTPases include lipases and lipid kinases, and that caveolae are rich in sphingolipids, suggests a role for the START domain of *Dlc-1* in this context. Perhaps inactivation of *Dlc-1* affects the activity or transport of RhoGTPases via the lack of lipid binding by the START domain.

There is evidence to support the observations that CHO cells underexpressing *Dlc-2* appear to be more angular in shape with an increase in stress fibre formation than cells with the functional protein. *Dlc-2* has been found to localize primarily to the cytoplasm, where overexpression was shown to induce morphological changes. These changes included a reduction in the formation of stress fibres that resulted in the cells appearing rounded with protrusions, rather than angular and spindle shaped. Mutation analysis confirmed that these alterations were due to the function of the RhoGAP domain (Leung *et al.*, 2005). *Dlc-2* was more recently shown to localize to mitochondria, in the vicinity

of lipid droplets. This targeting was found to occur via the START domain, which is not surprising given that this domain functions in the binding and transport of lipids. This finding suggests that *Dlc-2* may be involved in the transport of mitochondrial lipids (Ng *et al.*, 2006).

With respect to the analysis by flow cytometry, the only area where there was any statistical significance was at the 96 hour time point, at 5.0 μM and 25.0 μM concentrations in the analysis between Cl22 and E91 cells. There are several factors that likely played a role in the outcome of this apoptosis assay. In some cases there was a high background level, that is, there was a high proportion of cell death in the untreated controls, in spite of the fact that precautions were taken to reduce cell damage during the experimental process. This may have been caused in the later time points by untreated cells becoming confluent, thus inducing apoptosis due to starvation. These background levels could not be adjusted for during statistical analysis, and therefore may have skewed the results. This may be due to the fact that upon removal of the drug, and given the additional 48 hours of recovery time, the E91 cells that remained viable were able to proliferate, whereas the Cl22 cells were unable to recover and continued to die. At the 1.0 μM concentration perhaps not enough damage was induced to prevent the Cl22 cells from recovering once the drug was removed.

The mechanism of action of etoposide must also be considered, as it may be relevant to the fact that significant differences in apoptosis were not detected at the earlier time points as expected. The phenyl ring of etoposide has the ability to act as a scavenger of

free radicals. This characteristic of etoposide gives it lipid antioxidant properties that prevent the oxidation of PS, which is required for its externalization to the outer membrane of the cell (Tyurina *et al.*, 2004). If drug treatment prevented the externalization of this phospholipid, it would be unable to bind to AnnexinV-FITC and would therefore be undetectable by flow cytometry until much later when the amount of cellular damage becomes significant enough to leave the cells permeable to the dye. Alternatively, it is possible that the cells were dying by another mechanism, such as mitotic catastrophe, or that the time points used were insufficient to detect the onset and early stages of apoptosis, as the process occurs rapidly.

In addition, the E91 cells may have been able to recover at the 96 hour time point due to the fact that they have defects in the induction of PGP synthase by C2-ceramide signaling, conferring resistance to ceramide induced cell death (Hatch *et al.*, unpublished results). Ceramides regulate many cellular processes, including growth, differentiation and Rho-dependent apoptosis (Esteve *et al.*, 1998). Etoposide treatment has been found to increase endogenous levels of ceramide, contributing to apoptosis (Toman *et al.*, 2002). This could also explain why the E91 cells showed statistically significant growth in the colony assay experiments as compared to the Cl22 control cells.

The effects of ceramide also have implications for the results of the MTT assay. This assay relies on the ability of active mitochondrial dehydrogenases to cleave the pale yellow tetrazolium salt converting it to an insoluble purple formazan, which can then be measured by spectrophotometry. Etoposide has been found to increase endogenous

levels of ceramide (Toman *et al.*, 2002), which in turn promotes the accumulation of ROS by disrupting the flow of electrons through the electron transport chain (Pham & Hedley, 2001). Disruption of the electron transport chain may impair the ability of dehydrogenases to cleave the MTT, thereby affecting the results of the assay. Because the E91 cells have a defect in ceramide signaling, they may be protected from this effect as the flow of electrons through the electron transport chain remains stable and dehydrogenases are able to cleave the MTT. The Cl22 cells however, would be susceptible to the accumulation of ceramide and consequently would not survive to the end of the experiment.

Another possible explanation as to why little or no differences were observed in the cell viability and apoptosis analyses may have to do with the fact that a role for Rho proteins has also been identified in cell survival. This may be dependent on the particular isoform of the protein that is expressed. RhoA was shown to be required for survival in human endothelial cells and inhibiting its function promoted apoptosis (Hippenstiel *et al.*, 2002) therefore an increase in RhoA activity would lead to increased survival. The RhoGAP domain of both the *Dlc-1* and *Dlc-2* genes has been shown to be specific for RhoA (Wong *et al.*, 2003). Therefore, downregulation of the function of these genes would increase the activity of RhoA, and presumably promote cell viability. There has also been some evidence that *Dlc-1* and *Dlc-2* proteins are able to cooperate with each other to suppress tumor cell growth (Ullmannova and Popescu, 2006). A compensatory role between these two genes is another potential explanation for the lack of resistance to apoptosis observed in our cell lines.

Another phenomenon that must be considered is the incidence of off-target effects in cell lines that were created using shRNAi. The fact that the RhoGapMT2 cell line shows some reduction in expression of the *Dlc-2* transcript compared with the Cl22 control cells indicates that the presence of the shRNAi may be affecting gene expression in an unexpected manner (see Figure 6). In addition, there is a faint 850 bp band visible for the RSC1 cell line, indicating that the knock down of the gene transcript is not as efficient for these cells as it is for the RSC6 cell line (see Figure 6). It is possible that some non-specific binding occurred with other complementary sequences that may have affected these cell lines and the corresponding results. In addition, the presence of firefly luciferase DNA appears to have had an effect on the cell lines that contain the pSM2c vector, although the mechanism by which this is occurring remains to be elucidated. There have been reports of undesirable effects of siRNAs, including their ability to affect the translation of unintended targets, even if there is only partial sequence similarity. In addition, the interferon response has been shown to be initiated by siRNAs constructed by plasmids or viral vectors expressing shRNA (Jackson and Linsley, 2004).

4.3 Characterization of the *Dlc-1* Knock Out Mouse

This study of *Dlc-1* deficient mice incorporated a disruption to exon 1 of the gene, generating an exon 1-βgeo fusion transcript that resulted in a truncated peptide. The heterozygous embryos showed heavy staining in the head and tail regions, as well as the heart. Staining of whole embryo sections revealed ubiquitous expression, with

particularly intense staining in the regions of the heart, liver, neural tube and brain. The E9.5 homozygous deleted embryo showed neural tube defects and an enlarged heart in addition to a deficiency in the formation of vessels. This was particularly evident in the inter-somite regions. These defects in vascularization may be what lead to embryonic lethality. The E10.5 homozygous deleted embryo showed similar defects in the heart and vasculature, in addition to growth retardation. This correlates well with the findings of Durkin *et al.* from their 2005 paper, in which they generated a *Dlc-1* knock out incorporating a disruption of exon 5. They reported that the heterozygous mice were phenotypically normal and that the *Dlc-1* transcript in these animals was widely expressed, especially in the heart, liver and lungs. Homozygous deletion of the gene was found to be embryonic lethal at around day 10.5 and these embryos showed defects in the brain, heart, neural tube and placenta (Durkin *et al.*, 2005).

Alternative splicing of the *Dlc-1* gene leads to the production of two major transcripts, approximately 5.5 and 6.5 kb, and one minor transcript of approximately 7.5 kb (Durkin *et al.*, 2002). This group determined that the major transcripts were expressed in many tissues, including brain, heart, liver, kidney and lung, and that the minor transcript was expressed in the heart. Recent work in our laboratory employed RT-PCR using primers specific for each exon 1 to determine the individual expression patterns. The results indicated that the 6.5 kb transcript is only expressed in the brain and placenta and that the 5.5 kb transcript is expressed in various tissues (Golam Sabbir, personal communication). The disruption we generated was integrated into the intron for the 5.5 kb splice variant. This downstream insertion should knock out all the splice variants, however this will

have to be experimentally determined to rule out the possibility of a functional protein being produced by the larger transcript splicing around the vector. This may therefore affect the severity of the phenotype in *Dlc-1*$^{-/-}$ mice.

As previously mentioned, Ullmannova and Popescu have suggested that the Dlc genes may cooperate in their ability to suppress tumorigenic growth. Although this may occur in the adult animal, it does not appear to be the case during embryonic development as the homozygous null condition is lethal. Possibly the genes are expressed at different times in development which may make it impossible for one to effectively compensate for the loss of the other.

4.4 Future Directions

There remains a variety of avenues that could be pursued with respect to this project. In terms of cell lines, Cl22 and E91 cells expressing a dominant-negative Rho transcript have been created. The cell survival and apoptosis assays performed during the course of this project could be repeated with these cell lines and compared with the data presented here. In addition, as previously mentioned, Shannon Neumann has now established a control H460 cell line which expresses a scrambled shRNAi ligated into the pSM2c vector. This would serve as a better control for the Dlc2 cells than the H460 cell line used here, and my experiments could be repeated with this control. However, due to the fact that no appreciable differences were noted between the H460 and Dlc2 cell lines, any

differences detected using the new control could be attributed to the effects of the shRNAi and one would have to be cautious when interpreting these results.

Other than the differences noted in the RSC6 and Dlc1 results from the colony assay experiments, the RNAi cell lines tested throughout this project showed no significant differences when compared to control cell lines, however it may be useful to quantify the mRNA expression of these cell lines using RT-PCR to determine whether this may in fact be due to insufficient knock down of the transcript. It may also be informative to check levels of the *Dlc-2* transcript in *Dlc-1* deficient cells, and vice versa, and compare these levels with expression levels of the control to determine if there is compensation by one gene for loss of the other. Because the E91 cell line appears to have the lowest level of *Dlc-2* gene expression of the cell lines described in this study, this may be the most informative group of cells to study in future experiments. Another option would be to study stem cells derived from the *Dlc-1* knock out mice. Experiments could be conducted to determine the level of Rho activity and whether or not these cells show resistance to etoposide induced apoptosis. Due to the fact that etoposide treatment may be interfering with AnnexinV-FITC binding, it may be better quantitate apoptosis by examining caspase 3 activation or PARP cleavage, or perhaps using the TUNEL assay rather than flow cytometry.

Additional studies may include determining the methylation status of the *Dlc-1* and *Dlc-2* transcripts in our cell lines. Hypermethylation of the *Dlc-1* CpG island is one modification that may be responsible for inactivating the gene. Cells exhibiting an

increase in methylation could be treated with DNA methyltranserferase inhibitor to determine if function can be restored, and what effects this may have on cells.

It may also be informative to determine the phosphorylation status of the topoisomerase IIα protein in our cell lines, as decreased phosphorylation has been shown to correlate with susceptibility to the drug (Luo *et al.*, 1998). Perhaps some of our RNAi cell lines have a change in phosphorylation status compared to controls that may contribute to their sensitivity to etoposide induced cell death in spite of the knock down of RhoGAP function.

It will be interesting to further characterize the function of the *Dlc-1* gene in the formation of spontaneous tumors and metastases in our mice. An ES cell line now exists for the creation of *Dlc-2* deficient mice, and we are currently in the process of developing a *Dlc-2* knock out. This will be a conditional knock out which will allow gene activity to be disrupted in a time and tissue specific manner, which will circumvent the problem of embryonic lethality. This will allow observation of the effects of gene ablation in the adult organism. It would also be interesting to study the expression patterns of the *Dlc-2* gene in adult tissues to see if there is any correlation in expression with the *Dlc-1* transcript. Perhaps we could investigate whether there is an upregulation of the *Dlc-2* transcript in *Dlc-1* deficient mice, and vice versa to attempt to elucidate any cooperative effects between the two genes.

Given that the experiments integrating RNAi into cell lines showed few statistical differences, it may be prudent to test gene disruptions generated using this technique through microinjection directly into mice, rather than testing cells in culture. siRNA can be incorporated directly into the animal to allow specific tissues to be targeted and studied with respect to gene expression and tumor formation (Schiffelers *et al.*, 2004). One way to accomplish this is through hydrodynamic tail vein (HTV) delivery, a process in which siRNA in a large quantity of physiological fluid is injected into the tail vein. This is a very effective method for delivering nucleic acids to the liver in particular, although expression can be detected in all major organs (Herweijer and Wolff, 2007). Hydrodynamic limb vein (HLV) delivery is a comparable technique that can be used to target skeletal muscle (Herweijer and Wolff, 2007). siRNA to specifically target tumors can also be engineered and delivered through intravenous injection. Tumors are selectively targeted by complexing the siRNA with peptide ligands flanked by amino acid sequences that are specific for the integrins expressed on endothelial cells in the blood vessels of the tumor (Schiffelers *et al.*, 2004). This group was able to show that siRNA could inhibit gene expression in a sequence-specific manner, resulting in a decrease in the growth of the tumor. Likewise, intraperitoneal injection of anti-TNFα siRNA was shown to have a protective effect on mice subjected to a lethal dose of lipopolysaccharide (LPS) (Sorensen *et al.*, 2003). A similar method has been used to target vascular endothelial growth factor (VEGF) in choroidal neovascularization (CNV). In this study, intravitreal injection was used to administer VEGF siRNA into monkeys and shown to reduce the growth of laser-induced CNV. This has implications for the treatment of patients with age-related macular degeneration (AMD) (Tolentino *et al.*, 2004). These strategies may

help to overcome some of the off target effects of RNAi that may be interfering in the cell culture experiments. In addition, it may be useful to use a recombinant adenovirus expressing *Dlc-1* in mouse tumors to determine what, if any, effects this has on tumor growth and apoptosis.

RhoGAP genes are implicated in several critical biological processes that have direct consequences for tumor formation and growth, including cell cycle progression, gene expression and metastasis. Given that the *Dlc-1* and *Dlc-2* genes are found deleted in such a wide variety of tumors, targeting RhoGAP genes in general, and the *Dlc* family in particular, may provide an opportunity to develop novel therapies in the treatment of cancer and other diseases.

CHAPTER 5 - LITERATURE CITED

Anderson RG (1998). The caveolae membrane system. Annu Rev Biochem **67**: 199-225.

Bezabeh T, Mowat MRA, Jarolim L, Greenberg AH, Smith ICP (2001). Detection of drug-induced apoptosis and necrosis in human cervical carcinoma cells using ^{1}H NMR spectroscopy. Cell Death Differ **8**: 219-24.

Bobak D, Moorman J, Guanzon A, Gilmer L and Hahn C (1997). Inactivation of the small GTPase Rho disrupts cellular attachment and induces adhesion-dependent and adhesion-independent apoptosis. Oncogene **15**: 2179-89.

Boettner B, van Aelst L (2002). The role of Rho GTPases in disease development. Gene **286** (2): 155-74.

Brandao MM, Silva-Brandao KL, Costa FF, Saad STO (2006). Phylogenetic analysis of RhoGAP domain-containing proteins. Geno Prot Bioinfo **4** (3): 182-88.

Buja LM, Eigenbrodt ML, Eigenbrodt EH (1993). Apoptosis and necrosis basic types and mechanisms of cell death. Arch Pathol Lab Med **117**: 1208-14.

Chamond RR, Anon JC, Aguilar CM and Pasadas FG (1999). Apoptosis and disease. Alergol Inmunol Clin **14** (6): 367-74.

Ching YP, Wong CM, Chan SF, Leung T, Ng D, Jin DY and Ng I (2003). Deleted in liver cancer (DLC) 2 encodes a RhoGAP protein with growth suppressor function and is underexpressed in hepatocellular carcinoma. J Biol Chem **278** (12): 10824-30.

Costantini F and Lacy E (1981). Introduction of a rabbit β-globin gene into the mouse germ line. Nature **294**: 92-4.

Darzynkiewicz Z, Juan G, Li X, Gorczyca W, Murakami T, Traganos F (1997). Cytometry in Cell Necrobiology: Analysis of Apoptosis and Accidental Cell Death (Necrosis). Cytometry **27**: 1-20.

Daugas E, Nochy D, Ravagnan L, Loeffler M, Susin SA, Zamzami N and Kroemer G (2000). Apoptosis-inducing factor (AIF): a ubiquitous mitochondrial oxidoreductase involved in apoptosis. FEBS Lett **476**: 118-23.

Deveraux QL, Roy N, Stennicke HR, van Arsdale T, Zhou Q, Srinivasula SM, Alnemri ES, Salvesen GS and Reed JC (1998). IAPs block apoptosis events induced by caspase-8 and cytochrome c by direct inhibition of distinct caspases. EMBO J **17**: 2215-23.

Diekmann D, *et al.* (1991). Bcr encodes a GTPase-activating protein for p21rac. Nature **351**: 400-22.

Dive C, Gregory CD, Phipps DJ, Evans DL, Milner AE and Wyllie AH (1992). Analysis and discrimination of necrosis and apoptosis (programmed cell death) by multiparameter flow cytometry. Biochim Biophys Acta **1133**: 275-85.

Du C, Fang M, Li Y, Li L and Wang X (2000). Smac, a mitochondrial protein that promotes cytochrome c-dependent caspase activation by eliminating IAP inhibition. Cell **102**: 33-42.

Duriez PJ, Shah GM (1997). Cleavage of poly(ADP-ribose)polymerase: a sensitive parameter to study cell death. Biochem Cell Biol **75**: 337-49

Durkin ME, Yuan BZ, Thorgeirsson SS, Popescu NC (2002). Gene structure, tissue expression, and linkage mapping of the mouse DLC-1 gene (Arhgap7). Gene **288**: 119-27.

Durkin ME, Avner MR, Huh C, Yuan B, Thorgeirsson SS and Popescu NC (2005). DLC-1, a Rho GTPase-activating protein with tumor suppressor function, is essential for embryonic development. FEBS Lett **579**: 1191-6.

Durkin ME, Ullmannova V, Guan M and Popescu NC (2007). Deleted in liver cancer 3 (DLC-3), a novel Rho GTPase-activating protein, is down regulated in cancer and inhibits tumor cell growth. Oncogene (http://www.nature.com/onc/journal/v26/n31/abs/1210244a.html).

Esteve P, Embade N, Perona R, Jimenez B, del Peso L, Leon J, Arends M, Miki T and Lacal JC (1998). Rho-regulated signals induce apoptosis *in vitro* and *in vivo* by a p53-independent, but Bcl2 dependent pathway. Oncogene **17**: 1855-69.

Feierbach B, Piccinotti S, Bisher M, Denk W and Enquist LW (2006). Alpha-Herpesvirus infection induces the formation of nuclear actin filaments. PLoS Pathog **2** (8): 763-76.

Flaherty KM, McKay DB, Kabsch W and Holmes KC (1991). Similarity of the three-dimensional structures of actin and the ATPase fragment of a 70-kDa heat shock cognate protein. Proc Natl Acad Sci **88**: 5041-5.

Gardner RL (1968). Mouse chimaeras obtained by the injection of cells into the blastocyst. Nature **220**: 596-7.

Gavrieli Y, Sherman Y and Ben-Sasson SA (1992). Identification of programmed cell death in situ via specific labeling of nuclear DNA fragmentation. J Biol Chem **119** (3): 493-501.

Gellert M, Mizuuchi K, O'Dea MH and Nash HA (1976). DNA gyrase: an enzyme that introduces superhelical turns into DNA. Proc Natl Acad Sci **73** (11): 3872-76.

Glisson B, Gupta R, Smallwood-Kentro S and Ross W (1986). Characterization of acquired epipodophyllotoxin resistance in a Chinese hamster ovary cell line: loss of drug-stimulated DNA cleavage activity. Cancer Res **46**: 1934-8.

Glotzer M (2001). Animal cell cytokinesis. Annu. Rev. Cell Dev. Biol. **17**: 351-86.
Goley ED, Ohkawa T, Mancuso J, Woodruff JB, D'Alessio JA, Cande WZ, Volkman LE and Welch MD (2006). Dynamic nuclear actin assembly by Arp2/3 complex and a baculovirus WASP-like protein. Science **314**: 464-7.

Gomez J, Garcia A, Borlado L, Bonay P, Martinez C, Silva A, Fresno M, Carrera A, Eicher-Streiber C and Rebollo A (1997). IL-2 signaling controls actin organization through Rho-like protein families phosphatidylinositol 3-kinase and protein kinase C-zeta. J Immunol **158**: 1516.

Gomez J, Martinez C, Giry M, Garcia A and Rebollo A (1997). Rho prevents apoptosis through Bcl-2 expression: implications for interleukin-2 receptor signal transduction. Eur J Immunol **27**: 2793-9.

Goodison S, Yuan J, Sloan D, Kim R, Li C, Popescu NC and Urquidi V (2005). The RhoGAP protein DLC-1 functions as a metastasis suppressor in breast cancer cells. Cancer Res **65** (14): 6042-53.

Gordon JW and Ruddle FH (1981). Integration and stable germ line transmission of genes injected into mouse pronuclei. Science **214**: 1244-6.

Green DR and Kroemer G (2004). The pathophysiology of mitochondrial cell death. Science **305**: 626-29.

Guan M, Zhou X, Soulitzis N, Spandidos DA and Popescu NC (2006). Aberrant methylation and deacetylation of *Deleted in Liver Cancer-1* gene in prostate cancer: potential clinical applications. Clin Cancer Res **12** (5): 1412-19.

Hande KR (1998). Etoposide:four decades of development of a topoisomerase II inhibitor. Eur J Cancer **10**: 1514-21.

Hegde R, Srinivasula SM, Zhang Z, Wassell R, Mukattash R, Cilenti L, DuBois G, Lazebnik Y, Zervos AS, Fernandes-Alnemri T and Alnemri ES (2002). Identification of Omi/HtrA2 as a mitochondrial apoptotic serine protease that disrupts inhibitor of apoptosis protein-caspase interaction. J Biol Chem **277** (1): 432-8.

Herweijer H and Wolff JA (2007). Gene therapy progress and prospects: hydrodynamic gene delivery. Gene Ther **14**: 99-107.

Hicks GG, Shi E, Chen J, Roshon M, Williamson D, Scherer C and Ruley HE (1995). Retrovirus gene traps. Methods Enzymol **254**: 263-75.

Hippenstiel S, Schmeck B, N'Guessan P, Seybold J, Krull M, Preissner K, Eichel-Streiber CV and Suttorp N (2002). Rho protein inactivation induced apoptosis of cultured human endothelial cells. Am J Physiol Lung Cell Mol Physiol **283**: L830-8.

Hu S, Vincenz C, Ni J, Gentz R and Dixit VM (1997). I-FLICE, a novel inhibitor of tumor necrosis factor recetor-1- and CD-95-induced apoptosis. J Biol Chem **272** (28): 17255-7.

Huckaba TM, Pon LA (2002). Cytokinesis: Rho and formins are the ringleaders. Curr Biol **12**: R813-4.

Hubbard SC, Walls L, Ruley HE, Muchmore EA (1994). Generation of Chinese hamster ovary cell glycosylation mutants by retroviral insertional mutagenesis. J Biol Chem **269** (5): 3717-24.

Jackson AL and Linsley PS (2004). Noise amidst the silence: off-target effects of siRNAs? Trends Genet **20** (11): 521-4.

Jaffe AB and Hall A (2002). Rho GTPases in transformation and metastasis. Adv Cancer Res: 57-80.

Jaffe AB and Hall A (2005). Rho GTPases: biochemistry and biology. Annu Rev Cell Dev Biol **21**: 247-69.

Kam PCA and Ferch NI (2000). Apoptosis: mechanisms and clinical implications. Anaesthesia **55**: 1081-93.

Kelliher MA, Grimm S, Ishida Y, Kuo F, Stanger BZ and Leder P (1998). The death domain kinase RIP mediates the TNF-induced NF-kappaB signal. Immunity **8**: 297-303.

Keon J, Curtis R, Cabrera H and Hargreaves J (2003). A genomics approach to crop pest and disease research. Pest Manag Sci **59**: 143-8.

Kerr JFR, Wyllie AH and Currie AR (1972). Apoptosis: a basic biological phenomenon with wide-ranging implications in tissue kinetics. Br J Cancer **26**: 239-57.

Kerr JFR, Winterford CM and Harmon BV (1994). Apoptosis: its significance in cancer and cancer therapy. Cancer **73**: 2013-26.

Kim TY, Johg H, Song S, Dimtchev A, Jeong S, Lee J, Kim T, Kim N, Jung M, and Bang Y (2003). Transcriptional silencing of the DLC-1 tumor suppressor gene by epigenetic mechanism in gastric cancer cells. Oncogene **22**: 3943-51.

Kim TY, Lee JW, Kim H, Jong H, Kim T, Jung M, Bang Y (2007). DLC-1, a GTPase-activating protein for Rho, is associated with cell proliferation, morphology, and migration in human hepatocellular carcinoma. Biochem Biophys Res Commun **21**: 72-7.

Lako M and Hole N (2000). Searching the unknown with gene trapping. Expert Rev Mol Med (http://www.ermm.cbcu.cam.ak.uk/00001824h.html).

Leung T, Ching Y, Yam J, Wong C, Yau T, Jin D and Ng I (2005). Deleted in liver cancer 2 (DLC2) suppresses cell transformation by means of inhibition of RhoA activity. Proc Natl Acad Sci **102** (42): 15207-12.

Li H, Fung K, Jin D, Chung SSM, Ching, Y, Ng, IO, Sze K, Ko BCB and Sun H (2007). Solution structures, dynamics, and lipid-binding of the sterile α-motif domain of the deleted in liver cancer 2. Proteins: Structure, Function, and Bioinformatics **67**: 1154-66.

Liao Y, Si L, deVere White RW and Lo S (2007). The phosphotyrosine-independent interaction of DLC-1 and the SH2 domain of cten regulates focal adhesion and growth suppression activity of DLC-1. J Biol Chem **176** (1): 43-9.

Luo C, Johnston PJ, MacPhail SH, Banath JP, Oloumi A and Olive PL (1998). Cell fusion studies to examine the mechanism for etoposide resistance in Chinese hamster V79 spheroids. Exp Cell Res **243**: 282-9.

Majno G and Joris I (1995). Apoptosis, oncosis, and necrosis: An overview of cell death. Am J Pathol **146**: 3-15.

Miyazaki T, Liu ZJ, Kawahara A, Minami Y, Yamada K, Tsujimoto Y, Barsoumian EL, Perlmutter RM and Taniguchi T (1995). Three distinct IL-2 signaling pathways mediated by *bcl-2*, *c-myc*, and *lck* cooperate in hematopoietic cell proliferation. Cell **81**: 223.

Moon SY and Zheng Y (2003). Rho GTPase-activating proteins in cell regulation. Trends Cell Biol **13** (1): 13-22.

Nagy A, Rossant J, Nagy R, Abramow-Newerly W and Roder JC (1993). Derivation of completely cell culture-derived mice from early-passage embryonic stem cells. Proc Natl Acad Sci USA **90**: 8424-8.

Ng DC, Chan S, Kok KH, Yam J, Ching Y, Ng IO and Jin D (2006). Mitochondrial targeting of growth suppressor protein DLC2 through the START domain. FEBS Lett **580**: 191-8.

Orban PC, Chui D, and Marth JD (1992). Tissue- and site-specific DNA recombination in transgenic mice. Proc Natl Acad Sci **89**: 6861-5.

Orth K, Chinnaiyan AM, Garg M, Froelich CJ and Dixit VM (1996). The CED-3/ICE-like protease Mch2 is activated during apoptosis and cleaves the death substrate lamin A. J Biol Chem **271**: 16443-6.

Osipovich AB, White-Grindley EK, Hicks GG, Roshon MJ, Shaffer C, Moore JH and Ruley HE (2004). Activation of cryptic 3' splice sites within introns of cellular genes following gene entrapment. Nucleic Acids Res **32** (9): 2912-24.

Park SW, Durkin ME, Thorgeirsson SS and Popescu NC (2003). DNA variants of DLC-1, a candidate tumor suppressor gene in human hepatocellular carcinoma. Int J Oncol **23**: 133-37.

Pham N and Hedley DW (2001). Respiratory chain-generated oxidative stress following treatment of leukemic blasts with DNA-damaging agents. Exp Cell Res **264**: 345-52.

Ponting CP, Aravind L (1999). START: a lipid-binding domain in StAR, HD-ZIP and signaling proteins. Prot Seq Motifs **24**: 130-32.

Qian X, Li G, Asmussen HK, Asnaghi L, Vass WC, Braverman R, Yamada KM, Popescu NC, Papageorge AG and Lowy DR (2007). Oncogenic inhibition by a deleted in liver cancer gene requires cooperation between tensin binding and Rho-specific GTPase-activating protein activities. Proc Natl Acad Sci **104** (21): 9012-7.

Sakahira H, Enari M, Nagata S (1998). Cleavage of CAD inhibitor in CAD activation and DNA degradation during apoptosis. Nature **391**: 96-9.

Sawada M, Nakashima S, Kiyono T, Nakagawa M, Yamada J, Yamakawa H, Banno Y, Shinoda J, Nishimura Y, Nozawa Y and Sakai N (2001) p53 regulates ceramide formation by neutral sphingomyelinase through reactive oxygen species in human glioma cells. Oncogene **20** (11): 1368-78.

Scaffidi C, Fulda S, Srinivasan A, Friesen C, Li F, Tomaselli KJ, Debatin KM, Krammer PH and Peter ME (1998). Two CD95 (APO-1/Fas) signaling pathways. EMBO J **17** (6): 1675-87.

Schiffelers RM, Ansari A, Xu J, Zhou Q, Tang Q, Storm G, Molema G, Lu PY, Scaria PV and Woodle MC (2004). Cancer siRNA therapy by tumor selective delivery with ligand-targeted sterically stabilized nanoparticle. Nucleic Acids Res **32** (19): e149.

Schmid I, Krall WJ, Uittenbogaart CH, Braun J and Giorgi JV (1992). Dead cell discrimination with 7-amino-actinomycin D in combination with dual color immunofluorescence in single laser flow cytometry. Cytometry **13**:204-8.

Schultz J, Ponting CP, Hofmann K, Bork P (1997). SAM as a protein interaction domain involved in developmental regulation. Prot Sci **6**: 249-53.

Simpson KJ, Dugan AS and Mercurio AM (2004). Functional analysis of the contribution of RhoA and RhoC GTPases to invasive breast carcinoma. Cancer Res **64**: 8694-701.

Sorensen DR, Leirdal M and Sioud M (2003). Gene silencing by systemic delivery of synthetic siRNAs in adult mice. J Mol Biol **327**: 761-6.

Spiridonidis CA, Chatterjee S, Petzold SJ and Berger NA (1989). Topoisomerase II-dependent and –independent mechanisms of etoposide resistance in Chinese hamster cell lines. Cancer Res **49**: 644-50.

Stanford, WL, Cohn, JB and Cordes SP (2001). Gene-trap mutagenesis: past, present and beyond. Nat Rev Genet **2**: 756-68.

Stanley, P (1981). Selection of specific wheat germ agglutinin-resistant (Wga^R) phenotypes from Chinese hamster ovary cell populations containing numerous lec^R genotypes. Mol Cell Biol 1 (8): 687-96.

Subauste MC, von Herrath M, Benard V, Chamberlain CE, Chuang T, Chu K, Bokoch GM and Hahn KM (1999). Rho family proteins modulate rapid apoptosis induced by cytotoxic T lymphocytes and Fas. J Biol Chem **275** (13): 9725-33.

Susin SA, Lorenzo HK, Zamzami N, Marzo I, Snow BE, Brothers GM, Mangion J, Jacotot E, Costantini P, Loeffler M, Larochette N, Goodlett DR, Aebersold R, Ssiderovski DP, Penninger JM and Kroemer G (1999). Molecular characterization of mitochondrial apoptosis-inducing factor. Nature **397**: 441-5.

Tada K, Okazaki T, Sakon S, Kobarai T, Kurosawa K, Yamaoka S, Hashimoto H, Mak TW, Yagita H, Okumura K, Yeh W-C and Nakano (2001). Critical roles of TRAF2 and TRAF5 in tumor necrois factor induced NF-kappaB activation and protection from cell death. J Biol Chem **276**: 36530-4.

Tarkowski AK (1961). Mouse chimeras developed from fused eggs. Nature **190**: 857-60.

Thon L, Mohlig H, Mathieu S, Lange A, Bulanova E, Winoto-Morbach S, Schutze S, Bulfone-Paus S and Adam D (2005). Ceramide mediates caspase-independent programmed cell death. FASEB J **19**: 1945-56.

Tikoo A, Czekay S, Viars C, White S, Heath JK, Arden K and Maruta H (2000). P190-A, a human tumor suppressor gene, maps to the chromosomal region 19q13.3 that is reportedly deleted in some gliomas. Gene **257**: 23-31.

Tolentino MJ, Brucker AJ, Fosnot J, Ying G, Wu I, Malik G, Wan S and Reich SJ (2004). Intravitreal injection of vascular endothelial growth factor small interfering RNA

inhibits growth and leakage in a nonhuman primate, laser-induced model of choroidal neovascularization. Retina **24**: 132-8.

Toman RF, Movsesyan V, Murthy SK, Milstien S, Spiegel S and Faden AI (2002). Ceramide-induced cell death in primary neuronal cultures: upregulation of ceramide levels during neuronal apoptosis. J Neurosci Res **68**: 323-30.

Tyurina YY, Serinkan FB, Tyurin VA, Kini V, Yalowich JC, Schroit AJ, Fadeel B and Kagan VE (2004). Lipid antioxidant, etoposide, inhibits phosphatidylserine externalization and macrophage clearance of apoptotic cells by preventing phosphatidylserine oxidation. J Biol Chem **279** (7): 6056-64.

Ullmannova V and Popescu NC (2006). Expression profile of the tumor suppressor genes DLC-1 and DLC-2 in solid tumors. Int J Oncol **29**: 1127-32.

Vermeulen K, Van Bockstaele DR and Berneman ZN (2005). Apoptosis: mechanisms and relevance in cancer. Ann Hematol **84**: 627-39.

Villalonga P and Ridley AJ (2006). Rho GTPases and cell cycle control. Growth Factors **24**(3): 159-64.

Wagner EF, Stewart TA and Mintz B (1981). The human β-globin gene and a functional viral thymidine kinase gene in developing mice. Proc Natl Acad Sci **78** (8): 5016-20.

Wong C, Lee JM, Ching Y, Jin D, Ng IO (2003). Genetic and epigenetic alterations of *DLC-1* gene in hepatocellular carcinoma. Cancer Res **63**: 7646-51.

Wood SA, Allen ND, Rossant J, Auerbach A and Nagy A (1993). Non-injection methods for the production of embryonic stem cell-embryo chimaeras. Nature **365**: 87-9.

Wyllie AH, Kerr JFR and Currie AR (1980). Cell death: the significance of apoptosis. Int Rev Cytol **68**: 251-306.

Yam JWP, Ko F, Chan CY, Jin DY and Ng I (2006). Interaction of Deleted in Liver Cancer 1 with Tensin2 in caveolae and implications in tumor suppression. Cancer Res **66** (17): 8367-72.

Yuan BZ, Miller MJ, Keck CL, Zimonjic DB, Thorgeirsson SS, and Popescu NC (1998). Cloning, characterization and chromosomal localization of a gene frequently deleted in human liver cancer (*DLC-1*) homologous to rat RhoGAP. Cancer Res **58**: 2196-99.

Yuan BZ, Durkin ME, Popescu NC (2003). Promoter hypermethylation of *DLC-1*, a candidate tumor suppressor gene, in several common human cancers. Cancer Genet Cytogenet **140**: 113-17.

Zhang J, King WG, Dillon S, Hall A, Feig L and Rittenhouse SE (1993). Activation of platelet phosphatidylinositide 3-kinase requires the small GTP-binding protein Rho. J Biol Chem **268**: 22251.

Zhou X, Thorgeirsson SS and Popescu NC (2004). Restoration of DLC-1 gene expression induces apoptosis and inhibits both cell growth and tumorigenicity in human hepatocellular carcinoma cells. Oncogene **23**: 1308-13.